



**NATIONAL AND KAPODISTRIAN UNIVERSITY OF ATHENS**

**SCHOOL OF SCIENCES**

**DEPARTMENT OF CHEMISTRY**

**DEPARTMENTAL POSTGRADUATE PROGRAMME IN "CHEMISTRY"  
SPECIALIZATION "ANALYTICAL CHEMISTRY"**

**MASTER THESIS**

**A study of removal and identification of transformation  
products of niflumic acid during ozonation in aqueous  
solutions using LC-QToF-MS**

**ELENI MILA  
CHEMICAL ENGINEER**

**ATHENS**

**OCTOBER 2016**



## **MASTER THESIS**

A study of removal and identification of transformation products of niflumic acid during ozonation in aqueous solutions using LC-QToF-MS

**ELENI MILA**

**A.M.:** 11401

### **SUPERVISING PROFESSOR:**

Nikolaos Thomaidis, Associate Professor, NKUA

### **THREE-MEMBER EXAMINATION COMMITTEE:**

Anastasios Economou, Professor, NKUA

Michalis Koupparis, Professor, NKUA

Nikolaos Thomaidis, Associate Professor, NKUA

DEFENDING DATE 06/10/2016

## **ΕΡΕΥΝΗΤΙΚΗ ΕΡΓΑΣΙΑ ΔΙΠΛΩΜΑΤΟΣ ΕΙΔΙΚΕΥΣΗΣ**

Μελέτη απομάκρυνσης και ταυτοποίησης των προϊόντων μετατροπής του νιφλουμικού οξέος κατά την οζόνωση υδατικών διαλυμάτων με LC-QToF-MS

**ΕΛΕΝΗ ΜΗΛΑ**

**A.M.: 11401**

### **ΕΠΙΒΛΕΠΩΝ ΚΑΘΗΓΗΤΗΣ:**

Νικόλαος Θωμαΐδης, Αναπληρωτής Καθηγητής ΕΚΠΑ

### **ΤΡΙΜΕΛΗΣ ΕΞΕΤΑΣΤΙΚΗ ΕΠΙΤΡΟΠΗ:**

Αναστάσιος Οικονόμου, Καθηγητής ΕΚΠΑ

Μιχάλης Κουππάρης, Καθηγητής ΕΚΠΑ

Νικόλαος Θωμαΐδης, Αναπληρωτής Καθηγητής ΕΚΠΑ

ΗΜΕΡΟΜΗΝΙΑ ΕΞΕΤΑΣΗΣ 06/10/2016

## ABSTRACT

Ozonation is a promising disinfectant method for the removal of trace organic compounds and especially pharmaceuticals remaining in secondary wastewater treatment effluents. Usually, during oxidation with ozone, pharmaceuticals cannot reach total elimination but they can be transformed to new, structurally-related compounds called transformation products (TPs). Even though some of these products are considered to be more easily biodegradable than their precursors, most of them remain unknown. Thus, their identification is essential not only to provide a comprehensive risk assessment on micropollutants in the environment, but also to design improved removal technologies for persistent trace contaminants.

In this study, ozonation experiments have been set up in order to investigate the efficacy of this technique in the removal of niflumic acid (NA) from aqueous solutions. The influence of different initial ozone concentrations and different pH values on the removal of NA was also tested. TPs have been identified by reversed-phase liquid chromatography quadrupole-time-of-flight mass spectrometry (RPLC-QToF-MS) in both positive and negative electrospray ionization mode. A workflow for suspect and non-target screening has been developed. Structure elucidation of TPs was based on accurate mass, isotopic pattern measurements and interpretation of the acquired MS/MS spectra. The same procedure was also followed for its most abundant TP in order to examine its removal and to identify second generation TPs.

Results indicate the highly reactivity of NA with the molecular ozone. Initial ozone concentration and aqueous solution's pH are proven to be crucial parameters. A total of seventeen TPs have been identified, while the most abundant was confirmed by reference standard (2-aminopyridine-3-carboxylic acid). A probable structure based on diagnostic evidence was proposed for fifteen additional TPs, while a tentative candidate structure is suggested for the last one. The part of NA containing the pyridine-like moiety is proposed to be the active part of the molecule and this assumption was verified during the ozonation of 2-aminopyridine-3-carboxylic acid. Results have shown that this TP has the same behavior as its parent compound during ozonation. Also, three second generation TPs have been detected.

**SUBJECT AREA:** Environmental Analytical Chemistry

**KEYWORDS:** Niflumic acid, ozonation, removal, transformation products,  
RPLC-QToF-MS

## ΠΕΡΙΛΗΨΗ

Η οζόνωση είναι μια πολλά υποσχόμενη τεχνική απολύμανσης που χρησιμοποιείται για την απομάκρυνση των οργανικών ενώσεων που βρίσκονται σε ίχνη και ειδικά των φαρμάκων, τα οποία παραμένουν στα εξερχόμενα λύματα μετά τη δευτεροβάθμια επεξεργασία τους στα κέντρα επεξεργασίας λυμάτων. Συνήθως κατά την οζόνωση οι φαρμακευτικές ουσίες δεν διαλύονται εντελώς αλλά μετατρέπονται σε νέες ενώσεις που έχουν παρόμοια δομή με τις μητρικές και ονομάζονται προϊόντα μετατροπής. Αυτές οι ενώσεις στην πλειοψηφία τους παραμένουν άγνωστες.

Στην παρούσα εργασία, πειράματα οζόνωσης σχεδιάστηκαν με σκοπό τη διερεύνηση της απομάκρυνσης του νιφλουμικού οξέος από υδατικά διαλύματα, εξετάζοντας πώς επηρεάζεται από διαφορετικές αρχικές συγκεντρώσεις όζοντος και διαφορετικές τιμές pH των διαλυμάτων. Τα προϊόντα μετατροπής ταυτοποιήθηκαν με υγρή χρωματογραφία αντίστροφης φάσης συζευγμένη με υβριδικό αναλυτή φασματομετρίας μάζας (reversed-phase liquid chromatography quadrupole-time-of-flight mass spectrometry, RPLC-QToF-MS) σε θετικό και αρνητικό ιοντισμό με ηλεκτροψεκασμό. Για το σκοπό αυτό, αναπτύχθηκε ένα διάγραμμα ροής για ύποπτη και μη-στοχευμένη σάρωση. Η εξαγωγή της δομής των προϊόντων μετασχηματισμού βασίστηκε σε μετρήσεις ακριβούς μάζας και ισοτοπικού προφίλ αλλά και στην κατανόηση των φασμάτων μάζας που λήφθηκαν κατά την ανάλυση. Η ίδια διαδικασία ακολουθήθηκε για το πιο εύθρονο προϊόν μετατροπής του νιφλουμικού οξέος εξετάζοντας την απομάκρυνσή του και την ταυτοποίηση προϊόντων μετασχηματισμού δεύτερης γενιάς.

Τα αποτελέσματα έδειξαν πως το νιφλουμικό οξύ αντιδρά εκλεκτικά με το μοριακό όζον και οι παράμετροι που εξετάστηκαν είναι κρίσιμες για την απομακρυσή του απ τα υδατικά διαλύματα. Παρόμοια συμπεριφορά παρουσίασε και πιο εύθρονο προϊόν μετατροπής του. Συνολικά, ταυτοποιήθηκαν δεκαέφτα προϊόντα μετασχηματισμού πρώτης γενιάς, το ένα ταυτοποιήθηκε πλήρως, σε δεκαπέντε αποδόθηκαν πιθανές δομές και σε ένα αποδόθηκαν υποψήφιες δομές, καθώς ανιχνεύθηκαν και τρία προϊόντα μετασχηματισμού δεύτερης γενιάς.

**ΘΕΜΑΤΙΚΗ ΠΕΡΙΟΧΗ:** Περιβαλλοντική Αναλυτική Χημεία

**ΛΕΞΕΙΣ ΚΛΕΙΔΙΑ:** Νιφλουμικό οξύ, οζόνωση, απομάκρυνση, προϊόντα μετατροπής, RPLC-QToF-MS

## CONTENTS

<b>ABSTRACT</b> .....	<b>5</b>
<b>ΠΕΡΙΛΗΨΗ</b> .....	<b>7</b>
<b>INDEX OF FIGURES</b> .....	<b>13</b>
<b>INDEX OF TABLES</b> .....	<b>18</b>
<b>PREFACE</b> .....	<b>20</b>
<b>CHAPTER 1: PHARMACEUTICALS IN THE ENVIRONMENT</b> .....	<b>21</b>
1.1 Emerging Contaminants (ECs) .....	21
1.2 Occurrence, fate and transformation of pharmaceuticals in the environment .....	22
1.3 Conventional wastewater treatment .....	23
1.3.1 Primary and Secondary treatment .....	24
1.3.2 Disinfection .....	25
1.3.2.1 Chlorination .....	25
1.3.2.2 UV Disinfection .....	25
1.3.2.3 Ozonation .....	26
1.3.2.4 Advanced oxidation processes .....	29
1.4 Nonsteroidal Anti- inflammatory drugs as ECs .....	30
1.4.1 Niflumic Acid (NA).....	31
<b>CHAPTER 2: APPROACHES FOR TPs IDENTIFICATION- LITERATURE REVIEW FOR OCCURRENCE AND TRANSFORMATION OF NONSTEROIDAL ANTIFLAMMATORY DRUGS</b> .....	<b>32</b>
2.1 Introduction.....	32
2.2 Identification of TPs – Analytical approaches .....	33
2.2.1 Target analysis.....	34
2.2.2 Suspect screening.....	34
2.2.3 Non-target screening.....	36

2.2.4 Structure elucidation and identification confidence levels in HR-MS .....	37
2.3 Occurrence of NSAIDs in WWTPs worldwide .....	39
2.4 Occurrence of NSAIDs in WWTPs and surface water in Greece .....	40
2.4.1 Occurrence of Niflumic Acid in WWTPs and surface water in Greece .....	41
2.5 Formation of transformation products of diclofenac and ibuprofen through ozonation and advanced oxidation processes .....	42
<b>CHAPTER 3: SCOPE AND OBJECTIVES.....</b>	<b>47</b>
<b>CHAPTER 4: MATERIALS AND INSTRUMENTATION.....</b>	<b>49</b>
4.1 Reagents, standards and solvents .....	49
4.2 Experimental setup used for the production of ozone stock solution ....	50
4.3 UHPLC-HRMS/MS system and analysis .....	51
<b>CHAPTER 5: STUDY OF REMOVAL AND IDENTIFICATION OF TRANSFORMATION PRODUCTS OF NIFLUMIC ACID DURING OZONATION EXPERIMENTS .....</b>	<b>54</b>
5.1 Removal of niflumic acid during ozonation .....	54
5.1.1 Removal of niflumic acid in pH 7.0 ± 0.2 with different initial ozone concentrations and scavenger .....	54
5.1.2 Removal of niflumic acid in different pH with initial ozone concentration of 2.0 mg L <sup>-1</sup> with and without scavenger .....	54
5.2 Measurement of the residual aqueous ozone during NA ozonation .....	55
5.3 Samples analysis .....	56
5.4 Estimation of NA removal during ozonation process .....	57
5.5 Identification of possible TPs .....	57
5.5.1 Suspect screening .....	57
5.5.2 Non-target screening .....	59

5.5.3 Interpretation of MS and MS/MS spectra .....	59
5.5.4 Communication of the achieved level of confidence .....	60
5.5.5 Retention time prediction .....	60
5.6 Ozonation of the most abundant TP of NA and investigation of possible second generation TPs.....	60
<b>CHAPTER 6: RESULTS AND DISCUSSION .....</b>	<b>62</b>
6.1 Determination of NA removal during ozonation .....	62
6.1.1 Effect of the initial ozone concentration in NA removal .....	62
6.1.2 Effect of different pH values and presence or absence of scavenger in NA removal .....	64
6.2 Determination of residual ozone .....	66
6.3 Identification of NA transformation products .....	67
6.3.1 Fragmentation pattern of NA .....	67
6.3.2 Identification of TPs found by suspect screening .....	72
6.3.2.1 NA-298.....	72
6.3.2.2 NA-262.....	79
6.3.2.3 NA-161.....	82
6.3.2.4 NA-138.....	83
6.3.3 Identification of TPs found by non-target screening .....	91
6.3.3.1 NA-272.....	91
6.3.3.2 NA-286.....	95
6.3.3.3 NA-242.....	97
6.3.3.4 NA-243.....	101
6.3.3.5 NA-232.....	104
6.3.3.6 NA-228.....	106
6.3.3.7 NA-204.....	108

6.4 Determination of 2-aminopyridine-3-carboxylic acid (NA-138) removal during ozonation .....	115
6.5 Identification of NA second generation-transformation products .....	116
6.5.1 NA <sup>1</sup> -98 .....	116
6.5.2 NA <sup>1</sup> -154 .....	118
6.5.3 NA <sup>1</sup> -88 .....	119
<b>CHAPTER 7: CONCLUSIONS-FUTURE PERSPECTIVES .....</b>	<b>121</b>
<b>ABBREVIATIONS AND ACRONYMS .....</b>	<b>123</b>
<b>REFERENCES.....</b>	<b>125</b>

## INDEX OF FIGURES

<b>Fig.1:</b> Occurrence of ECs and their TPs in WWTPs [7].....	22
<b>Fig.2:</b> Release of pharmaceuticals and their metabolites into the environment [10].....	23
<b>Fig.3:</b> Sewage Treatment Process.....	24
<b>Fig.4:</b> Schematic diagram for reactions of O <sub>3</sub> with substrate (S) and the O <sub>3</sub> -decomposition reactions compete for ozone consumption [27]. ....	26
<b>Fig.5:</b> Advanced oxidation processes [34].....	29
<b>Fig.6:</b> 2-D structure, chemical formula and exact mass of Niflumic acid. ....	31
<b>Fig.7:</b> Distribution of NA species versus pH. ....	31
<b>Fig.8:</b> Flow chart of screening procedures of TPs. ‘Known’ TPs have been confirmed or confidently identified before, other TPs are considered ‘Unknown’ [39].....	33
<b>Fig.9:</b> Proposed identification confidence levels in HR-MS analysis by Schymanski et al. (2014) [53].....	38
<b>Fig.10:</b> 2-D structure, chemical formula and exact mass of Diclofenac.....	42
<b>Fig.11:</b> Proposed transformation pathway of Diclofenac during ozonation and UV/H <sub>2</sub> O <sub>2</sub> oxidation by Vogna et al. (2004) [71].....	44
<b>Fig.12:</b> 2-D structure, chemical formula and exact mass of Ibuprofen .....	44
<b>Fig.13:</b> Proposed transformation pathway of Ibuprofen during photo-Fenton reaction by Mendez-Arriaga et al. (2010) [74].....	46
<b>Fig.14:</b> Setup for production of saturated ozone stock solution.....	51
<b>Fig.15:</b> The UHPLC-QToF-MS system.....	52
<b>Fig.16:</b> Decolorization of indigo reagent in reaction with different ozone concentration. ....	55

<b>Fig.17:</b> NA degradation under various initial ozone concentrations in pH 7.0 in the presence of <i>t</i> -BuOH ( $C_t$ : concentration of treated sample, $C_o$ : 3.0 mg L <sup>-1</sup> ).....	63
<b>Fig.18:</b> % NA mean removal under various initial ozone concentrations in pH7.0 in the presence of scavenger ( $C_{o,NA}$ : 3.0 mg L <sup>-1</sup> ).....	63
<b>Fig.19:</b> NA degradation at different pH values with or without <i>t</i> -BuOH, initial $C_{O_3}$ : 2.0 mg L <sup>-1</sup> ( $C_t$ : concentration of treated sample, $C_o$ : 3.0 mg L <sup>-1</sup> ). .....	65
<b>Fig.20:</b> % NA mean removal at different pH values with or without scavenger, initial $C_{O_3}$ : 2.0 mg L <sup>-1</sup> ( $C_{o,NA}$ : 3.0 mg L <sup>-1</sup> ). .....	65
<b>Fig.21:</b> Standard curve: absorbance of indigo reagent versus ozone concentration.....	66
<b>Fig.22:</b> Analytical data for NA in RP(+); (a) EICs of NA and its adduct at zero-time sample, (b) MS and (c) MS/MS spectrum showing the fragmentation and proposed fragments of NA. ....	68
<b>Fig.23:</b> Analytical data for NA in RP(-); (a) EICs of NA and its in-source fragment at zero-time sample and (b) MS spectrum. ....	69
<b>Fig.24:</b> Analytical data for NA in RP(-); MS/MS spectrum showing the fragmentation and proposed fragments of NA.....	70
<b>Fig.25:</b> Proposed structures for NA-298 isomers.....	72
<b>Fig.26:</b> Analytical data for NA-298 isomers in RP(+); (a) EIC of NA-298 and (b) MS spectra of : (1) NA-298a, (2) NA-298b, (3) NA-298c.....	74
<b>Fig.27:</b> Analytical data for NA-298 isomers in RP(+); MS/MS spectrum showing the fragmentation and proposed fragments of NA-298a. ....	75
<b>Fig.28:</b> Analytical data for NA-298 isomers in RP(+); (a) MS/MS spectrum showing the fragmentation and proposed fragments of NA-298b and (b) bbCID mode MS spectrum showing characteristic proposed fragment of NA-298c..	76
<b>Fig.29:</b> NA-298 isomers production trend in correlation with $O_3$ initial concentration.....	77
<b>Fig.30:</b> Analytical data for NA-298 isomers in RP(-); (a) EIC of NA-298 and their in-source fragments (b) MS spectra. ....	78

<b>Fig.31:</b> <i>Proposed structure for NA-262</i> .....	79
<b>Fig.32:</b> <i>Analytical data for NA-262 in RP(+); (a) EICs of NA-262 and its adduct, (b) MS and (c) MS/MS spectrum showing the fragmentation and proposed fragments of NA-262</i> .....	80
<b>Fig.33:</b> <i>Analytical data for NA-262 in RP(-); (a) EIC of NA-262, (b) MS and (c) MS/MS spectrum</i> .....	81
<b>Fig.34:</b> <i>Proposed structure for NA-161</i> .....	82
<b>Fig.35:</b> <i>Analytical data for NA-161 in RP(-); EIC of NA-161</i> .....	82
<b>Fig.36:</b> <i>Analytical data for NA-161 in RP(-); (a) MS and (b) MS/MS spectrum showing the fragmentation and proposed fragments of NA-161</i> .....	83
<b>Fig.37:</b> <i>Proposed structure for NA-138</i> .....	84
<b>Fig.38:</b> <i>Analytical data for NA-138 in RP(+); EICs of NA-138, its adduct and its in-source fragment</i> .....	84
<b>Fig.39:</b> <i>Analytical data for NA-138 in RP(+); (a) MS spectra of NA-138 and its reference standard, (b) MS/MS spectra showing the fragmentation and proposed fragments of NA-138 and its reference standard</i> .....	85
<b>Fig.40:</b> <i>NA-138 production trend in correlation with O<sub>3</sub> initial concentration</i> ...	86
<b>Fig.41:</b> <i>Analytical data for NA-138 in RP(-); (a) EICs for NA-138 and its in-source fragment, (b) MS spectra of NA-138 and its reference standard</i> .....	87
<b>Fig.42:</b> <i>Proposed structure for NA-272</i> .....	92
<b>Fig.43:</b> <i>Analytical data for NA-272 in RP(+); (a) EICs for NA-272 and its adduct, (b) MS spectrum</i> .....	92
<b>Fig.44:</b> <i>Analytical data for NA-272 in RP(+); MS/MS spectrum showing the fragmentation and proposed fragments of NA-272</i> .....	93
<b>Fig.45:</b> <i>Analytical data for NA-272 in RP(-); (a) EIC of NA-272, (b) MS and (c) MS/MS spectrum showing the fragmentation and proposed fragments of NA-272</i> .....	94
<b>Fig.46:</b> <i>Proposed structure for NA-286</i> .....	95

<b>Fig.47:</b> Analytical data for NA-286 in RP(+); (a) EIC of NA-286, (b) MS and (c) MS/MS spectrum showing the fragmentation and proposed fragments of NA-286 .....	96
<b>Fig.48:</b> Analytical data for NA-286 in RP(-); (a) EIC of NA-286, (b) MS spectrum .....	97
<b>Fig.49:</b> Proposed structures for NA-242 .....	97
<b>Fig.50:</b> Analytical data for NA-242a, b in RP(+); (a) EIC of NA-242, (b) MS spectra of: (1) NA-242a and (2) NA-242b.....	98
<b>Fig.51:</b> Analytical data for NA-242a, b in RP(+); MS/MS spectra showing the fragmentation and proposed fragments of (a) NA-242a and (b) NA-242b.....	99
<b>Fig.52:</b> Analytical data for NA-242 in RP(-); (a) EIC of NA-242, (b) MS spectra and (c) MS/MS spectrum of NA-242 eluted at $t_R$ 6.9 min .....	100
<b>Fig.53:</b> Proposed structures for NA-243a .....	101
<b>Fig.54:</b> Proposed structure for NA-243b .....	101
<b>Fig.55:</b> Analytical data for NA-243a, b in RP(-); (a) EIC of NA-243 and (b) MS spectra of: (1) NA-243a, (2) NA-243b.....	102
<b>Fig.56:</b> Analytical data for NA-243a, b in RP(-); MS/MS spectra showing the fragmentation and proposed fragments of (a) NA-243a and (b) NA-243b.....	103
<b>Fig.57:</b> Proposed structure for NA-232 .....	104
<b>Fig.58:</b> Analytical data for NA-232 in RP(-); (a) EICs of NA-232 and its in-source fragments, (b) MS and (c) MS/MS spectrum showing the fragmentation and proposed fragments of NA-232 .....	105
<b>Fig.59:</b> Proposed structure for NA-228 .....	106
<b>Fig.60:</b> Analytical data for NA-228 in RP(-); (a) EICs of NA-228 and its in-source fragment, (b) MS and (c) MS/MS spectrum showing the fragmentation and proposed fragments of NA-228 .....	107
<b>Fig.61:</b> Proposed structures for NA-204a, NA-204b, NA-204c .....	108
<b>Fig.62:</b> Analytical data for NA-204a, b and c in RP(+); (a) EIC of NA-204, (b) MS spectra of: (1) NA-204a, (2) NA-204b and (3) NA-204c.....	109

<b>Fig.63:</b> Analytical data for NA-204 in RP(+); MS/MS spectra showing the fragmentation and proposed fragments of (a) NA-204a and (b)NA-204c. ....	110
<b>Fig.64:</b> Ozonation transformation products of NA (TP marked with dashed frame is available as commercial standard, the other TPs reach the 2b level of identification) .....	114
<b>Fig.65:</b> % NA-138 mean removal under various initial ozone concentrations in pH7.0 with scavenger .....	115
<b>Fig.66:</b> Proposed structure for NA'-98.....	116
<b>Fig.67:</b> Analytical data for NA'-98 in RP(+); (a) EICs of NA'-98 and its adduct, (b) MS and (c) MS/MS spectrum showing the fragmentation and proposed fragments of NA'-98.....	117
<b>Fig.68:</b> Analytical data for NA'-154 in RP(+); (a) EIC and (b) MS spectrum..	118
<b>Fig.69:</b> Analytical data for NA'-88 in RP(+); (a) EIC and (b) MS spectrum ...	119

## INDEX OF TABLES

<b>Table 1:</b> The most frequently identified molecules in WWTPs.....	30
<b>Table 2:</b> Range of concentrations of the most popular NSAIDs in WWTPs influents and effluents in different countries. ....	39
<b>Table 3:</b> Range of concentrations of the most popular NSAIDs in Greek WWTPs and their removal efficiencies.....	41
<b>Table 4:</b> Occurrence of the most popular NSAIDs in surface water in Greece (sampling site: Aisonas River).....	41
<b>Table 5:</b> Identified TPs of Diclofenac. ....	43
<b>Table 6:</b> Identified TPs of Ibuprofen.....	45
<b>Table 7:</b> NA removal under various initial ozone concentrations in pH 7.0 in the presence of t-BuOH 50mM.....	62
<b>Table 8:</b> NA removal at different pH in absence or presence of scavenger ( $C_{0,NA} = 3.0 \text{ mg L}^{-1}$ , $C_{0,O_3} = 2.0 \text{ mg L}^{-1}$ ) .....	64
<b>Table 9:</b> Absorption measurements in 600 nm for Indigo method std curve ...	66
<b>Table 10:</b> Elemental composition of NA, its adduct and fragment ions along with the measured m/z, the theoretical m/z and the mass error in ppm in RP(+). ....	71
<b>Table 11:</b> Elemental composition of NA, its in-source fragment and fragment ions along with the measured m/z, the theoretical m/z and the mass error in ppm in RP(-). ....	71
<b>Table 12:</b> Predicted and experimental retention time of three isomers NA-298 in RP(+). ....	73
<b>Table 13:</b> Elemental composition of TPs, their adduct and/or in-source fragments and fragment ions along with the measured m/z, the theoretical m/z and the mass error in ppm in RP(+), detected with suspect screening. ....	88

<b>Table 14:</b> Elemental composition of TPs, their in-source fragments and fragment ions along with the measured m/z, the theoretical m/z and the mass error in ppm in RP(-),detected with suspect screening..	90
<b>Table 15:</b> Elemental composition of TPs, their adducts and fragment ions along with the measured m/z, the theoretical m/z and the mass error in ppm in RP(+),detected with non-target screening.	111
<b>Table 16:</b> Elemental composition of TPs, their in-source fragments and fragment ions along with the measured m/z, the theoretical m/z and the mass error in ppm in RP(-),detected with non-target screening.	113
<b>Table 17:</b> NA-138 removal under various initial ozone concentrations in pH 7.0 in the presence of t-BuOH 50mM.	115
<b>Table 18:</b> Elemental composition of second generation TPs of NA, their adducts and fragment ions along with the measured m/z, the theoretical m/z and the mass error in ppm in RP(+),detected with suspect screening.	120
<b>Table 19:</b> Abbreviations and acronyms	122

## PREFACE

This master thesis was conceived and performed at the Laboratory of Analytical Chemistry (Department of Chemistry, University of Athens, Greece) under the supervision of the Associate Professor, Nikolaos Thomaidis.

First of all, I would like to thank my supervisor, Dr. Nikolaos Thomaidis, for giving me the opportunity to become a member of his research group as well as for the cooperation regarding this master thesis.

A special thanks to all of my colleagues and friends in the Laboratory of Analytical Chemistry, for providing a great work environment and an enjoyable atmosphere in the lab and, in particular to Maristina Nika, Katerina Psoma, Dimitris Damalas, Anna Bletsou, and Anthi Panara, for their constant guidance, assistance and cooperation.

Last but not least, I would like to express my appreciation to my beloved sister, my parents and my friends for their enormous support of my decision to continue my studies for a master's degree and their encouragement throughout these two years and my life in general.

# CHAPTER 1

## PHARMACEUTICALS IN THE ENVIRONMENT

### 1.1. Emerging Contaminants (ECs)

Hazardous compounds such as metals and persistent organic pollutants (POPs) have been of great interest of researchers since 1990 and are until now part of intensive monitoring programs due to their impact on the environment. Today, the existence of these compounds has been dramatically eliminated as appropriate measures and laws have been applied to our society.

Presently, the focus of environmental analysis has shifted from the classic contaminants to the emerging pollutants (EPs). This category, is also called trace organic compounds (TrOCs), and encompasses a wide range of compounds including pharmaceuticals, personal care products (PPCPs), pesticides, hormones, musk fragrances and disinfectants which are chemical compounds widely used by humans the last decades [1]. These compounds are a source of concern because they are used and released in large quantities and their physical and chemical properties contribute to their widespread distribution into the environment [2].

The molecular structure of PPCPs and pharmaceuticals are typically large and complex containing functional groups such as hydroxyl, carboxyl, amine and ketone. Simultaneously, it would be counter-productive not to emphasize the fact that the classification of pharmaceuticals by their active substances does not imply that they can be treated as groups with similar chemical behavior. That is to say, small changes in the chemical structures can provoke significant effects on the properties like solubility and polarity of these compounds which in turn affects their environmental distribution in air, water, soil and animals [3].

The analysis and risk assessment of the EPs, especially drugs and their metabolites are of major concern nowadays since they are detected in secondary effluents of wastewater treatment plants (WWTPs) and surface water worldwide [4, 5]. However, there are no existing water-quality regulations

in order to define guidelines for EPs and their transformation products (TPs) concentrations in WWTPs, drinking water or the environmental samples. Thus, they are considered to be potential threats to human's health and safety and as well as to the environmental ecosystem in conjunction with having been connected with chronic toxicity, endocrine disruption and the development of pathogen resistance [2, 6].



**Fig.1:** Occurrence of ECs and their TPs in WWTPs [7].

## 1.2. Occurrence, fate and transformation of pharmaceuticals in the environment

Pharmaceuticals due to their widespread consumption and after having an internal curing effect in human body, are released from hospitals and private households to sewer system. Afterwards, they enter the WWTPs through urine and feces as a mixture of metabolites, conjugates or unchanged substances, depending on the pharmacology of each medical substance [8]. Moreover, pharmaceuticals end up to the sewage through pharmaceutical industries and wasted expired drugs. Three are the possible routes concerning the fate of ECs, during the processes that take place in the WWTPs:

- i) be completely mineralized to carbon dioxide and water, e.g. aspirin
- ii) undergo some form of metabolism or rather partial degradation ,e.g. penicillin
- iii) stay persistent, e.g. clofibrate.

Hence, the effluents of WWTPs contain preserved and partially degraded pharmaceutical chemicals, which in turn end up in the receiving surface waters and may therefore affect the aquatic organisms [9].

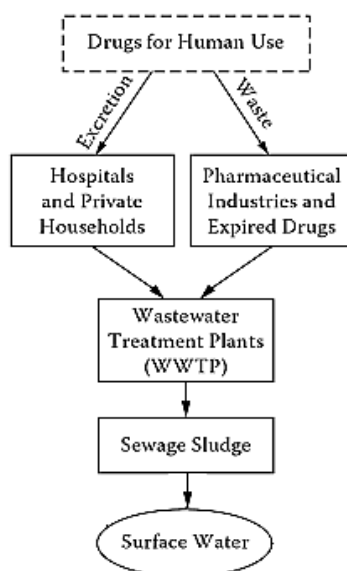


**Fig.2:** Release of pharmaceuticals and their metabolites into the environment [10].

Veterinary drugs which can be divided into substances used as growth promoters, therapeutics in livestock production or for treatment of livestock on fields (e.g. antiparacetic agents) and feed additives in fish farms, ensue similar pathways and are presented in the aquatic environment.

### 1.3. Conventional wastewater treatment

WWTPs are designed to remove oxygen demand, suspended solids and pathogens coupled with eliminating carbon and nitrogen loads in sewage water [11, 12]. However, several types of micropollutants have been detected in secondary effluents of WWTPs which cannot be fully degraded by current treatment systems and they are discharged to receiving waters [13]. This is the reason why the treatment processes of WWTPs are extensively studied and especially the process of disinfection.

### 1.3.1. Primary and Secondary treatment

Primary treatment decreases the organic loading on downstream of sewage by removing a large amount of settleable matter and suspended solids through sedimentation. A sufficient operated primary treatment system typically removes up to 90% of the settleable solids, 40% to 60% of the suspended solids and 20% to 40% of incoming biochemical oxygen demand (BOD). Primary settling tanks blast away the floating scum, called skimmings, with a surface collector. In addition, they remove and collect the settled sludge in order to transfer it to disposal or for further treatment [14].

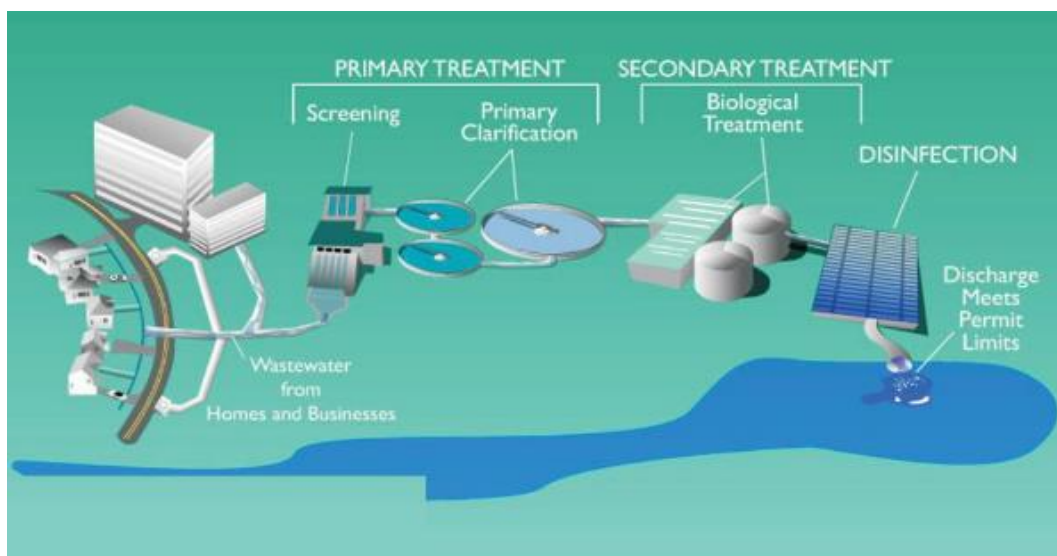


**Fig.3:** Sewage Treatment Process.

The main target of secondary treatment, referred as biological treatment, is to achieve a higher percentage of removal of BOD than the one accomplished in the primary treatment. There are three commonly used approaches: the trickling filter or its variations, the rotating biological contractor (RBC) and the activated sludge process. All of the aforementioned processes use the ability of microorganisms to convert dissolved, colloidal and suspended organic wastes to more stable, low-energy compounds which can either be removed by settling or discharged to the environment without being harmful. As defined by the Clean Water Act (CWA), secondary treatment produces an effluent with no more than 30 mg/L BOD<sub>5</sub> and 30 mg/L total suspended solids [15].

### **1.3.2. Disinfection**

The important treatment process which aims to the destruction or deactivation of pathogenic microorganisms and the total removal of organic matter in WWTPs is called disinfection [16]. It includes the use of chemical agents such as compounds of chlorine, and/or nonchemical agents such as ultraviolet (UV) light. In order to choose the most suitable disinfectant process, the desired effectiveness to destroy microorganisms and the absence or minimal level of its attendant by-products which are often toxic, mutagenic and carcinogenic, should be taken into account [17].

#### **1.3.2.1 Chlorination**

Chlorination is the most common disinfection method used in WWTPs [18]. Chlorine is delivered into the treatment system in liquid or gaseous form and the applied technology is targeted toward efficiency and effectiveness of the disinfectant, taking into consideration its distribution in it. Chlorine dose usually varies from 5 to 20 mg L<sup>-1</sup> depending on chlorine demand, wastewater characteristics and discharge requirement of a particular WWTP [19]. Although, the main purpose of chlorination is to eliminate pathogens, investigations have shown that chlorine reacts with micropollutants and natural organic matter in water and forms halogenated by-products which are toxic and can cause long-term health effects [18, 20].

It is recommended that the process of chlorination must be followed by dechlorination in order to remove the free and combined chlorine residuals. Thus, it is crucial to decrease the toxicity of effluents before they end up in receiving waters [20].

#### **1.3.2.2. UV Disinfection**

UV light is a growing technology for wastewater treatment disinfection. UV disinfection generally involves the use of electromagnetic energy generated from low pressure or medium pressure high intensity mercury arc lamps to inactivate efficiently several pathogens such as bacteria and viruses. The effectiveness of this method is determined by the quality of wastewater, the intensity of UV irradiation and the exposure time of microorganisms [17]. The required dose of UV irradiation which is used for disinfection purposes is 400

$\text{J/m}^2$  [21]. In addition, it has been noticed that the above mentioned dose of UV light may be sufficient to cause an important transformation of organic chemical components in water, both natural organic matter (NOM) and micropollutants [22]. Disinfection of wastewater by UV irradiation is incubated as a promising alternative to chemical disinfection due to the absence of undesirable transformation products after treatment [23, 24].

### 1.3.2.3. Ozonation

Ozone is a very strong oxidant and virucide. It is produced when oxygen molecules are separated by an energy source into oxygen atoms and instantly collide with an oxygen molecule to form an unstable gas. Due to its instability, ozone is decomposed to elemental oxygen within very short time and thus it is generated at the point of application [25]. In WWTPs, ozonation can be suitable as a disinfection method after the secondary treatment, in order to remove the resistant substances remaining in the effluents [26]. Furthermore, it is considered as a more effective disinfectant than chlorine or UV.

Ozonation is a technique of chemical oxidation which leads to complete or partial degradation of organic pollutants. Ozone is a very powerful oxidizing agent that can react with most species containing multiple bonds, such as  $\text{C}=\text{C}$ ,  $\text{C}=\text{N}$ ,  $\text{N}=\text{N}$  [27], but not with species containing single bonds like  $\text{C}-\text{C}$ ,  $\text{C}-\text{O}$ ,  $\text{O}-\text{H}$ , at high rates. This fact occurs because there is no easy chemical pathway for the oxidation to take place.

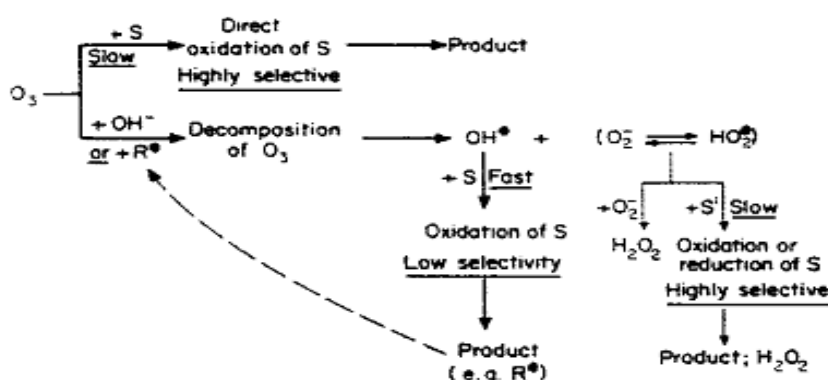


**Fig.4:** Schematic diagram for reactions of  $\text{O}_3$  with substrate (S) and the  $\text{O}_3$ -decomposition reactions compete for ozone consumption [27].

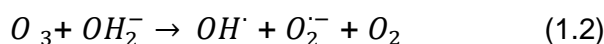
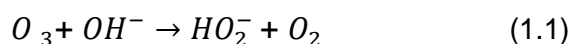
Moreover, ozone reacts with simple oxidizable ions such as  $S^{-2}$ . It is important to mention that the action of ozone usually depends on how it reacts with the pollutants. This means that the kinetic factors are determinant to know if ozone will oxidize a pollutant in a favorable time frame [28].

It has to be mentioned that, according to the literature, some operational parameters concerning the ozonation process can be optimized in order to achieve the maximum extend of pollutants' degradation in an energy efficient way [28]. Some of these important parameters are:

- *pH of the reaction solution*
- *Ozone partial pressure*
- *Contact time with the pollutant and interfacial area*
- *Presence of radical scavengers*
- *Operating temperature*
- *Combination with other oxidation processes (ex.  $O_3/UV$  ,  $O_3/US$  (Ultrasonic irradiation))*

In addition, the reactions of ozone are characterized by high selectivity. However, ozone can be decomposed before the reactions with the pollutants-substrates take place. Beyond a critical parameter, the pH-value, decomposition products of ozone, usually the hydroxyl radicals ( $OH^\bullet$ ), become the main oxidants. These reactions are unselective [29].

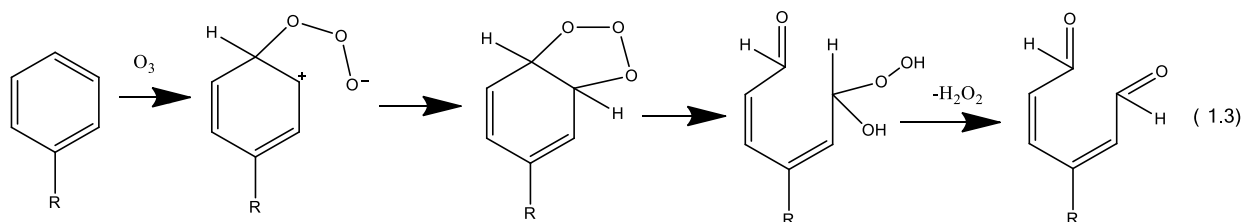
The reaction of ozone in aquatic solutions can be described with the following decomposition reactions:



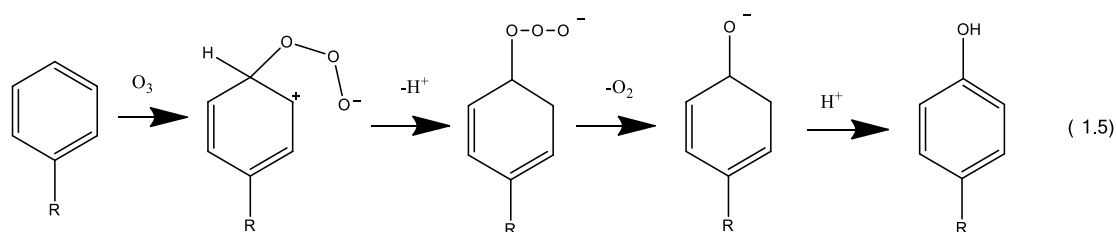
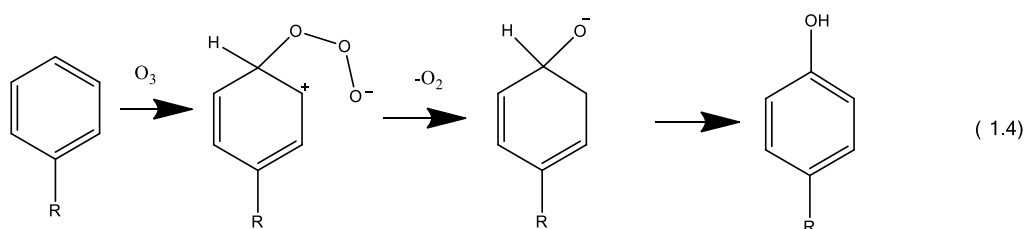
In order to control exclusively the process of oxidation with ozone, it is necessary to use scavengers. Scavengers are usually carbonate ions and less bicarbonate. They offer a protective effect due to electron transfer from  $CO_3^{-2}$  to  $OH^-$  and they act as inhibitors for the  $OH^\bullet$ -radical reactions with the substrate. Other substances, such as tertiary butanol (t-BuOH) and acetate, are used as  $OH^\bullet$  scavengers and prolong the lifetime of ozone [30].

Some common reactions of ozone with aromatic compounds are presented below. First of all, the most predominant reaction between  $O_3$  and aromatic

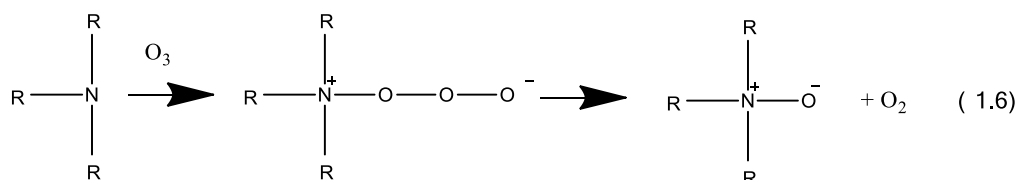
compounds is the formation of an ozonide, its breakdown and the formation of aldehyde groups:



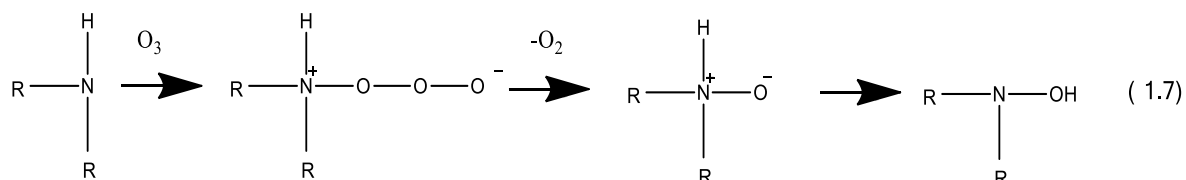
Another process that usually takes place is the hydroxylation of the starting material by two different pathways:



Furthermore, ozone reacts with tertiary amines in the following way, leading to the formation of N-oxides:



For secondary amines, the corresponding N-oxide is only a short-lived intermediate which rearranges into isomeric hydroxylamine:



Despite the effectiveness of ozone, issues like the formation of carcinogenic products, bromate an N-nitrosodimethylamine (NMDA) must be taken into consideration [31, 32]. Furthermore, this application of ozonation is under question because of the undetermined toxicity of the mostly unknown

transformation products [7, 33]. Nowadays, the researchers make an effort to identify these oxidation TPs and specify if they are non-toxic or at least less toxic than the parent compound [12].

#### 1.3.2.4. Advanced oxidation processes

Advanced oxidation processes (AOPs) gain popularity as disinfection methods in WWTPs. Despite the fact that they all use different reacting systems, they are having a common chemical feature which is the production of OH radicals. Some of the AOPs systems are presented in Fig.5 below.

- $\text{H}_2\text{O}_2 / \text{Fe}^{2+}$  (Fenton)
- $\text{H}_2\text{O}_2 / \text{Fe}^{3+}$  (Fenton - like)
- $\text{H}_2\text{O}_2 / \text{Fe}^{2+} (\text{Fe}^{3+}) / \text{UV}$  (Photo assisted Fenton)
- $\text{H}_2\text{O}_2 / \text{Fe}^{3+}$  - Oxalate
- $\text{Mn}^{2+}$ /Oxalic acid/Ozone
- $\text{TiO}_2 / \text{h}\nu / \text{O}_2$  (Photocatalysis)
- $\text{O}_3 / \text{H}_2\text{O}_2$
- $\text{O}_3 / \text{UV}$
- $\text{H}_2\text{O}_2 / \text{UV}$

**Fig.5:** Advanced oxidation processes [34].

OH radicals are chemical species which react with organic compounds with a range of constant rates from  $10^{-6}$  to  $10^{-9} \text{ M}^{-1}\text{s}^{-1}$  [35]. As it was mentioned before in subsection 1.3.2.3, OH radicals are characterized by low selectivity of attack which enables them to be strong oxidants in order to solve pollution problems in WWTPs. Moreover, the adaptability of AOPs in WWTPs is enhanced by offering various possible ways for OH radicals production, thus allowing a better compliance with the specific treatment requirements [34].

#### 1.4. Nonsteroidal Anti- inflammatory drugs as ECs

Nonsteroidal anti-inflammatory drugs (NSAIDs), including compounds used as analgesics, are the most important groups of pharmaceuticals worldwide due to their wide use [33]. They include a wide variety of individual compounds within the general groups of carboxylic acids (salicylic, propionic, pyranocarboxylic, acetic and fenamic acids) and enolic acids (benzotriazines, oxicams and pyrazolones). These are weak organic acids which have high affinity for lipids in acidic media and plasma proteins, sharing therapeutic actions for controlling a varying degree of pain (analgesic), inflammation (anti-inflammatory) and fever (antipyretics). Their annual production is estimated to be in the range of several kilotons and one of them which called ibuprofen, is the third most popular drug in the world [36]. NSAIDs are enlisted in the most investigated molecules in WWTPs (Table 1) [1].

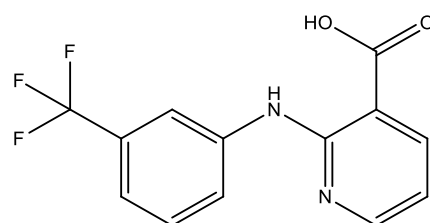
**Table 1:** The most frequently identified molecules in WWTPs [1].

ECs class	Frequency (%) *
Hormones	30
Analgesic, Anti-inflammatory drugs	20
Antibiotics	8.7
Lipid regulators	4.4
Anti-epileptics	4.0
Metabolites	3.9
Betablockers	2.8
Personal care products	2.7
Contrast products	1.1
Disinfectants	0.8
Vasodilators	0.7
Antidepressants	0.6
<b>TOTAL</b>	<b>80</b>

\* Frequency of citation in one database (117 papers, 6641 data, 148 molecules)

### 1.4.1. Niflumic Acid (NA)

Niflumic acid (2-[3-(trifluoromethyl)phenyl]aminopyridine-3-carboxylic acid) is an analgesic and anti-inflammatory drug used in the treatment of rheumatoid arthritis, osteoarthritis and spondylosis. It is also categorized as an inhibitor of cyclooxygenase. Some of its brand names in different countries are: Niflamol (Greece), Niflactol (Spain), Niflugel (Belgium), Donalgin (Hungary) etc. This drug has low solubility in water, 19 mg/L at 25°C. The recommended dosage of niflumic acid is 250 mg per time, 3-4 times daily by mouth. Two well-known metabolites of niflumic acid are 4'-hydroxynilumic acid and 5-hydroxyniflumic acid [37]. The structure of NA is presented in Fig.6, while different ionic species of NA are shown in Fig.7. It is important to be mentioned that the various forms of ionic species of the drug have different reactivity with ozone.



Chemical Formula:  $C_{13}H_9F_3N_2O_2$   
Exact Mass: 282.0616

**Fig.6:** 2-D structure, chemical formula and exact mass of niflumic acid.

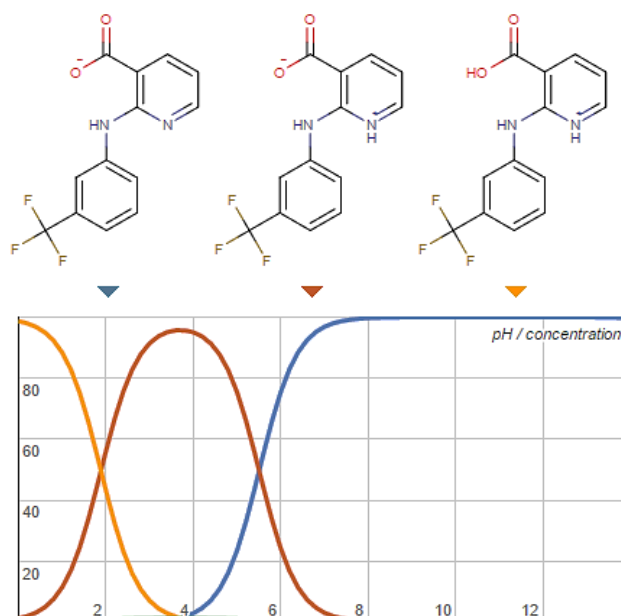


**Fig 7:** Distribution of NA species versus pH.

## CHAPTER 2

# APPROACHES FOR TPs IDENTIFICATION- LITERATURE REVIEW FOR OCCURRENCE AND TRANSFORMATION OF NONSTEROIDAL ANTIFLAMMATORY DRUGS

### 2.1. Introduction

The rapid development of very sensitive analytical methods allowed researchers to reach parts per-quadrillion (sub-ng/L) detection limits for TrOCs and their TPs [38]. Especially, Liquid Chromatography coupled to tandem Mass Spectrometry (LC-MS/MS) permits great performance in terms of sensitivity and selectivity. LC is an ideal technique for molar and thermolabile molecules and their TPs which are usually more polar than their parent compounds [39]. LC-MS using atmospheric pressure ionization (API), atmospheric pressure chemical ionization (APCI) and electrospray ionization (ESI) has dramatically changed the analytical methods used to determine polar compounds in aqueous environmental samples. ESI has become the most dominant ionization technique in MS coupling with LC for the identification of low molecular mass and polar compounds [40, 41]. High resolution analytical instruments, like quadrupole time-of-flight (Q-ToF) mass spectrometry, are extensively used for real time detection and identification of oxidation by-products [42], due to their high confirmatory capabilities, derived from the high resolving power and the mass accuracy in MS and MS/MS modes, along with the developed sophisticated software. These two facts have contributed to the increase of the number and interest of scientific investigations into the occurrence and transport of TrOCs and their TPs in natural and engineered systems and finally the effort of their removal. Furthermore, identification of TPs is a challenging task because of the unknown nature of these molecules and usually the absence of analytical standards to confirm their identity. Moreover, it must be emphasized that difficulties in analysis are presented by their complexity, their different physicochemical properties, the formation of isomer compounds which are difficult to differentiate and the co-elution of compounds with similar structures.

## 2.2. Identification of TPs- Analytical approaches

As it was already mentioned above, LC coupled to MS is the most appropriate and promising analytical technique in TPs investigation. The development of high- resolution mass spectrometric systems (HR-MS) which includes mass analyzers such as time-of-flight (TOF), Fourier transform-ion cyclotron resonance (FT-ICR), Orbitrap or new hybrid approaches (e.g. quadrupole time-of-flight (Q-ToF), is a driving force in development of TPs identification methodologies because of their sensitivity and high mass accuracy [39]. Three different analytical approaches for this procedure were presented by Krauss et al. (2010):

- Target analysis, a quantitative analytical approach using reference standards
- Suspect screening, a qualitative approach for candidate TPs without using reference standards
- Non-target screening, a qualitative approach for unknown TPs [43].

These workflows are depicted step by step in Fig.8 and analysed in subchapters below.

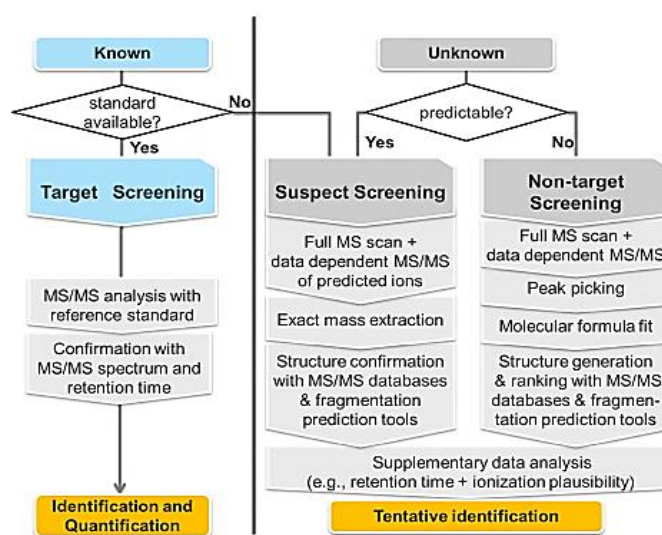


**Fig.8:** Flow chart of screening procedures of TPs. 'Known' TPs have been confirmed or confidently identified before, other TPs are considered 'Unknown' [39].

### **2.2.1. Target analysis**

In target analysis, as shown in Fig.8, TPs are already known and their reference standards are available in order to confirm their structure. As a result, they can be included within a defined MS method and be monitored in routine analysis. LC in combination with triple-quadrupole mass spectrometric detection (LC-QqQ MS/MS) dominates in target analysis. The QqQ analyzer permits application of MS/MS modes [e.g., production scan, precursor-ion scan, neutral-loss scan and selected reaction monitoring (SRM), which is the most predominant]. The SRM mode provides several advantages and interesting characteristics for target analysis, such as increased selectivity, reduced interferences and high sensitivity, which allows robust quantification [39]. However, it focuses on a predefined list of compounds to be tested for, because the transitions must be preselected.

The SRM limitations can be handled by HR-MS target analysis. Practically, all compounds present in a sample can be detected simultaneously with HR-MS instrument operating in full scan mode, making it unnecessary to pre-select compounds and associated SRM transitions [43]. Target compounds included in an accurate-mass database are screened in the sample based on retention time ( $t_R$ ), theoretical mass, isotopic pattern and MS/MS fragments [44, 45]. Additionally, hybrid instruments have the option of data-dependent MS/MS acquisition, where MS/MS analysis is triggered if a compound from a target-ion list is detected in the full scan [46]. Due to their high mass resolving power, these instruments improve the identification of isobaric compounds and thus permit more reliable identification process of target analytes [47].

### **2.2.2 Suspect screening**

Contrary to target analysis, suspect screening approach does not depend on reference standards for confirmation. Despite the fact that a large number of possible ECs and their candidate TPs have not currently reference standards available, compound-specific information for suspected molecules, such as molecular formula and structure can be used for the identification and confirmation process. The molecular formula allows the calculation of the exact  $m/z$  of the expected ion which is in turn extracted from the high resolution full-

scan chromatogram [43]. In case of positive findings, several confirmatory steps must be followed in order to reach structure-derived information [48].

A critical step in suspect screening is the prediction of potential TPs. Several commercially available or freely accessible programs are currently applied to predict microbial transformation pathways of xenobiotics and the structures of likely TPs. These tools include programs such as:

- META
- CATABOL
- the University of Minnesota Pathway Prediction System (UM-PPS, now exclusively provided from EAWAG as EAWAG-Biocatalysis/Biodegradation Database Pathway Prediction System, EAWAG-BBD PPS, <http://eawag-bbd.ethz.ch/predict/> (last visited: September 2016))

EAWAG-BBD PPS contains sets of transformation rules that predict likely microbial transformations based on compound substructure recognition. As this tool is freely accessible and all rules applied are clearly assigned, it is the most common prediction tool in suspect screening. Due to the fact that EAWAG-BBD PPS has accumulated data generated from microbial metabolic reactions, the predicted pathways may not be completely appropriate for environmental systems [49]. In addition, this program does not contain reactions of hydroxylation which are the most common reactions in oxidation processes. Other *in silico* prediction tools used for the prediction step in environmental analysis such as Meteor and PathPred, are available.

Prediction of TPs is followed by the HR-MS analysis; the exact mass for each of the predicted TPs is extracted from the chromatogram and checked by comparing it with control samples. An intensity-threshold value is applied to cut off unclear spectra. The plausibility of the chromatographic  $t_R$ , isotopic pattern, and ionization efficiency are used as further filters to narrow down the number of candidate peaks. Furthermore, using MS/MS or MS<sup>n</sup>, structures of suspected TPs are suggested based on the observed fragmentation pattern and diagnostic fragment ions. Depending on the above criteria, there are different confidence levels of identification in HR-MS analysis of TPs.

### 2.2.3 Non-target screening

Non-target screening is the analytical approach for investigation of TPs which can be detected in the samples but no previous information is available. It is usually performed after target analysis and suspect screening. Full identification of the non-target extracted  $m/z$  is a difficult task and for this reason HR-MS instrumentation is necessary in order to obtain high resolution data from full scan and MS/MS mode and elucidate reliably the detected mass [39, 50].

The assessment of massive quantities of data which offer HR instruments and finally the export of results require post-acquisition data-processing programs which offer rapid, accurate and efficient data mining. Thus a lot of open-source and commercial software exist, some of which are indicatively presented below:

- MZmine
- XCMS
- enviMass
- Bruker Metabolite Tools and Profile Analysis
- Waters MassLynx and MetaboLynx
- Thermo Scientific MetWorks.

The first and most critical step in non-target screening is peak peaking. This step gives the opportunity to exclude irrelevant peaks by the comparison of the sample with control or blank samples. Afterwards, the removal of noise peaks, mass recalibration, componentization of isotopes and adducts follow.

Exploration of online databases such as ChemSpider and PubChem or structure generation may lead to possible structures of TPs. Also, information like molecular formula and substructures of the parent compound could be helpful for the purpose of the search restriction.

Even after filtering, strict criteria and thresholds, the number of peaks which correspond to non-target compounds is enormous and their interpretation would demand a great amount of effort and time. Therefore, the most intense peaks are chosen in order to be interpreted [51].

#### 2.2.4 Structure elucidation and identification confidence levels in HR-MS

High mass accuracy coupled with high isotopic abundance accuracy is fundamental to elicit a reliable molecular formula generated by the software incorporated in the HR-MS instruments. The acceptable deviation of the experimental  $m/z$  from its corresponding theoretical of parent ions is usually defined at 5 ppm. This limit guarantees the correct prediction of their molecular formula. Higher errors, generally below 10 ppm, are acceptable in the workflow regarding their characteristic fragment ions. In spite of the fact that the accurate extrapolation of the elemental composition of a TP is essential, it is not sufficient to lead in a correct structure proposal.

A process which is very helpful in structure investigation is the observation of the presence or absence of similar characteristic ions in the fragmentation pattern between the parent compounds and its TPs. In addition, information from experimental MS/MS spectra can be compared with *in silico* mass spectral fragmentation tools (e.g. MetFrag, MetFusion, Mass Frontier, MOLGEN-MS and ACD/MS Fragmenter) or with mass spectra in libraries (e.g. MassBank and MetLin) [39]. On the other hand, the use of mass spectral libraries is restricted for LC/MS-MS data because they do not have a great amount of available data and mass spectra of different instruments are not so comparable [52].

Consequently, the HR-MS based identifications of TPs differ among studies and compounds because it is not always possible to synthesize each compound and confirm it. In order to make easier the communication of identification confidence of TPs, Schymanski et al. (2014) proposed a level system which is described below (Fig. 9) [53].

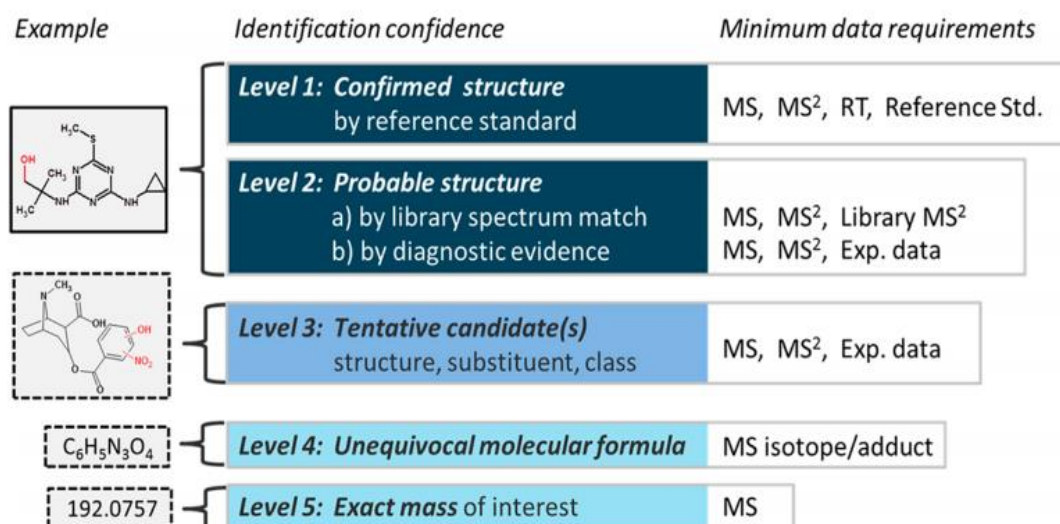


**Fig.9:** Proposed identification confidence levels in HR-MS analysis by Schymanski et al. (2014) [53]

- **Level 1: Confirmed structure** is the perfect situation where the candidate structure is confirmed by the measurement of a reference standard with MS, MS/MS and retention time matching.
- **Level 2: Probable structure** refers to a proposal for an exact structure based on different evidence.
- **Level 2a: Library** which includes indisputable matching between literature or library spectrum data and experimental.
  - **Level 2b: Diagnostic** which refers in the case of no other structure fits in experimental data, but no standard or literature information is available.
- **Level 3: Tentative candidate(s)** is the situation where there is evidence for possible structure(s) but the experimental information is insufficient to the exact proposal.
- **Level 4: Unequivocal molecular formula** describes the case of an unambiguous formula which is assigned by the spectral information but there is no sufficient evidence to propose possible structures.
- **Level 5: Exact mass (m/z)** is detected in the sample but no experimental information exists in order to propose even a formula.

## 2.3 Occurrence of NSAIDs in WWTPs worldwide

Occurrence data from the most popular NSAIDs in WWTPs influent and effluent are presented in the Table 2. The referred concentrations of NSAIDs show significant spatial and temporal variations due to a number of factors such as the rate of production, specific sales, humans metabolism, water consumption each person per day, the size of WWTPs and finally effectiveness of wastewater treatment processes [54]. Some pharmaceutical compounds from NSAIDs category like ibuprofen and naproxen present high occurrence concentrations. To be more precise, ibuprofen was the most abundant compound detected in the effluent of four WWTPs in Spain with concentration levels varying from 3.73 to 603  $\mu\text{g L}^{-1}$  [55]. The detected high levels could be justified by the high consumption rate and easy accessibility of this compound as it is considered to be the third most consumed drug in the world.

**Table 2:** Range of concentrations of the most popular NSAIDs in WWTPs influents and effluents in different countries.

Compound	Sampling sites	Concentration in influent samples ( $\mu\text{g L}^{-1}$ )	Concentration in effluent samples ( $\mu\text{g L}^{-1}$ )	References
<b>Diclofenac</b>	EU-wide, Greece, Korea, Sweden, UK, WB*	<0.001-94.2	<0.001-0.69	[56], [57], [58], [59], [60], [61]
<b>Ibuprofen</b>	EU-wide, Greece, Spain, Korea, Sweden, UK, WB*, USA	<0.004-603	ND** -55	[56], [57], [55], [62], [58], [59], [60], [61], [63]
<b>Ketoprofen</b>	EU-wide, Greece, Spain, Korea, UK, WB*	<0.004-8.56	<0.003-3.92	[56], [64], [55], [62], [58], [60], [61]

Compound	Sampling sites	Concentration in influent samples ( $\mu\text{g L}^{-1}$ )	Concentration in effluent samples ( $\mu\text{g L}^{-1}$ )	References
<b>Naproxen</b>	Greece, Spain, Korea, Sweden, UK, WB*	<0.002-52.9	<0.002-5.09	[57], [55], [62], [58], [59], [60], [61]

\*WB: Western Balkan Region (including Bosnia and Herzegovina, Croatia and Serbia)

\*\*ND: not detected

The compound of concern in this study, Niflumic acid, has not been researched extensively. It is enlisted in substances of possible concern in Oslo and Paris Commission for the protection of the Marine Environment of the North East Atlantic (OSPAR) website (<http://www.ospar.org/work-areas/hasec/chemicals/possible-concern/list>, last visited: August 2016). In addition, a recent investigation has shown that the concentration of NA in samples of surface water and effluents of WWTPs in UK is approximately  $5 \text{ ng L}^{-1}$  [65].

#### **2.4 Occurrence of NSAIDs in WWTPs and surface water in Greece**

Subsequently, Table 3 and 4 present the occurrence data of the most popular NSAIDs in two WWTPs, that serves cities of Athens (WWTPa) and Mytilene (WWTPb), and in surface water, respectively. The presence of the compounds in the environmental samples shows the necessity of further investigation of the efficiency of wastewater treatment processes and of their fate in Greek aquatic environment.

**Table 3:** Range of concentrations of the most popular NSAIDs in Greek WWTPs and their removal efficiencies [64].

Compound	WWTPa			WWTPb		
	Concentration in influent samples ( $\mu\text{g L}^{-1}$ )	Concentration in effluent samples ( $\mu\text{g L}^{-1}$ )	Removal (%)	Concentration in influent samples ( $\mu\text{g L}^{-1}$ )	Concentration in effluent samples ( $\mu\text{g L}^{-1}$ )	Removal (%)
Diclofenac	1.04-2.17	0.18-0.88	75	0.86-1.86	0.15-1.07	39
Ibuprofen	0.30-1.44	<0.30	100	0.49-1.23	<0.30	100
Ketoprofen	0.36-3.15	<0.09-0.12	89	<0.09-0.78	<0.09	83
Naproxen	0.60-1.42	0.01-0.09	95	0.28-2.67	0.002-0.11	91

**Table 4:** Occurrence of the most popular NSAIDs in surface water in Greece (sampling site: Aisonas River) [66].

Compound	Concentration ( $\text{ng L}^{-1}$ )
Diclofenac	0.8-1043
Ibuprofen	1-67
Ketoprofen	0.4-395
Naproxen	3-322

#### 2.4.1 Occurrence of Niflumic Acid in WWTPs and surface water in Greece

Niflumic acid was detected in samples obtained from Psyttalia WWTP in Athens in April 2011 in concentration levels ranging from 420 to 675  $\text{ng L}^{-1}$  by Danesaki and Thomaidis (2015) [67]. It was also detected in all twenty four flow proportional samples of secondary wastewater samples collected from the same WWTP in Athens in October 2014 by Ibáñez et al. (2016) [68].

Additionally, Niflumic acid was detected in all treated sewage sludge samples collected from five WWTPs of Santorini in July 2013 in a mean concentration of 40.9 ng g<sup>-1</sup> d.w. by Ferrero et al. (2015) [69].

Last but not least, this pharmaceutical was detected, with occurrence frequency equal or above 50% in samples collected from seawater of Eastern Mediterranean Sea, Saronikos Gulf and Elefsina Bay during December 2013 by Alygizakis et al. (2016) [70].

All previous information indicates the importance of further investigation for Niflumic acid removal in wastewater treatment processes in order to prevent its distribution in the aquatic environment.

## 2.5 Formation of transformation products of diclofenac and ibuprofen through ozonation and advanced oxidation processes

Nowadays, researchers are in concern of the identification of transformation products of NSAIDs originated by several degradation processes. The main target is to investigate their fate in the aquatic environment and determine their toxicity. To our knowledge published studies for NA transformation do not exist yet. Thus, some of the identified TPs of the most studied NSAIDs, diclofenac and ibuprofen, formed during ozonation and advanced oxidation processes will be briefly presented in the tables 5 and 6 respectively. Also, the analytical technique used for each identification process is mentioned. In fig. 11 and 13, tentative transformation pathways of the two pharmaceuticals by oxidation are shown.

- **Diclofenac TPs**

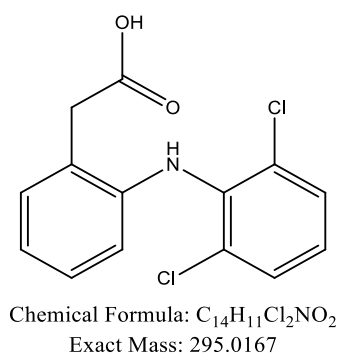


**Fig.10:** 2-D structure, chemical formula and exact mass of Diclofenac.

**Table 5:** Identified TPs of Diclofenac

<b>Molecular formula of TP</b>	<b>Degradation process</b>	<b>Analytical Technique</b>	<b>Reference</b>
C <sub>14</sub> H <sub>11</sub> Cl <sub>2</sub> NO <sub>3</sub>	Ozonation, UV/H <sub>2</sub> O <sub>2</sub>	GC-Ion Trap MS	[71]
	Sonolysis*, Sonophotocatalysis**	UPLC-QToF-MS	[72]
C <sub>14</sub> H <sub>11</sub> Cl <sub>2</sub> NO <sub>4</sub>	Sonolysis*, Sonophotocatalysis**	UPLC-QToF-MS	[72]
C <sub>14</sub> H <sub>12</sub> ClNO <sub>3</sub>	Ozonation, UV/H <sub>2</sub> O <sub>2</sub>	GC-Ion Trap MS	[71]
C <sub>13</sub> H <sub>9</sub> Cl <sub>2</sub> NO	Sonolysis*, Sonophotocatalysis**	UPLC-QToF-MS	[72]
C <sub>8</sub> H <sub>8</sub> O <sub>4</sub>	Ozonation, UV/H <sub>2</sub> O <sub>2</sub>	GC-Ion Trap MS	[71]
C <sub>8</sub> H <sub>8</sub> O <sub>3</sub>	Ozonation, UV/H <sub>2</sub> O <sub>2</sub>	GC-Ion Trap MS	[71]
C <sub>8</sub> H <sub>9</sub> NO <sub>2</sub>	Ozonation, UV/H <sub>2</sub> O <sub>2</sub>	GC-Ion Trap MS	[71]
C <sub>6</sub> H <sub>5</sub> Cl <sub>2</sub> N	Ozonation, UV/H <sub>2</sub> O <sub>2</sub>	GC-Ion Trap MS	[71]
C <sub>6</sub> H <sub>5</sub> Cl <sub>2</sub> NO	Sonolysis*, Sonophotocatalysis**	UPLC-QToF-MS	[72]
C <sub>6</sub> H <sub>4</sub> Cl <sub>2</sub> O <sub>2</sub>	Ozonation, UV/H <sub>2</sub> O <sub>2</sub>	GC-Ion Trap MS	[71]

\*Sonolysis: TiO<sub>2</sub> photocatalysis driven by UV-A or simulated solar irradiation.

\*\*Sonophotocatalysis: UV-A photocatalysis integrated with ultrasound irradiation.

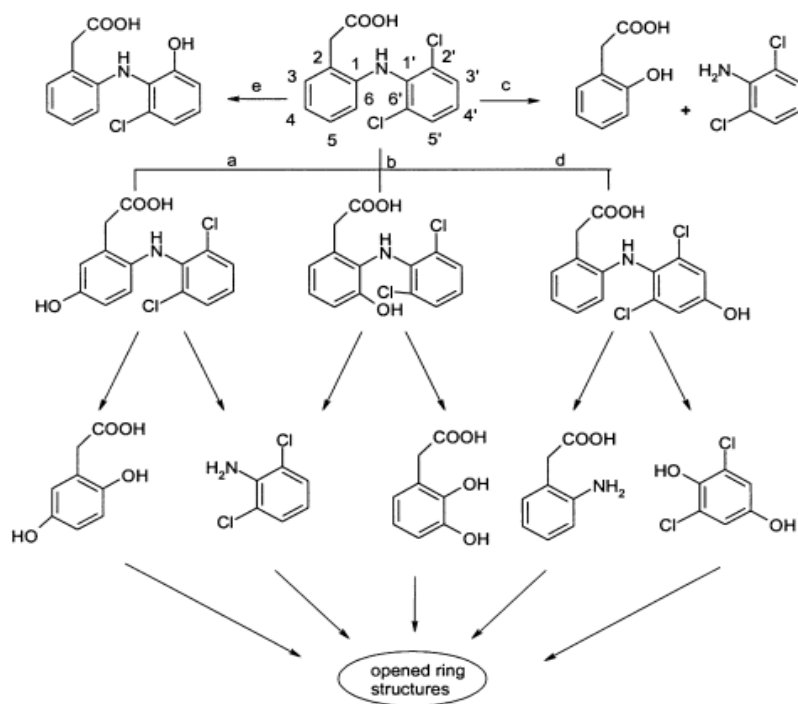
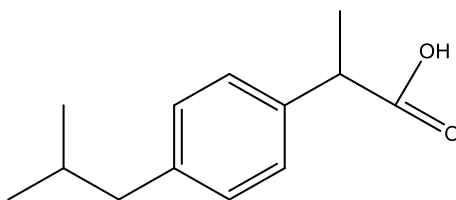


**Fig.11:** Proposed transformation pathway of Diclofenac during ozonation and UV/  $H_2O_2$  oxidation by Vogna et al. (2004) [71].

- **Ibuprofen TPs**



Chemical Formula:  $C_{13}H_{18}O_2$   
 Exact Mass: 206.1307

**Fig.12:** 2-D structure, chemical formula and exact mass of Ibuprofen.

**Table 6:** Identified TPs of Ibuprofen

<b>Molecular formula of TP</b>	<b>Degradation process</b>	<b>Analytical Technique</b>	<b>Reference</b>
C <sub>13</sub> H <sub>18</sub> O <sub>3</sub>	Ozonation	UPLC-QToF-MS	[73]
	photo-Fenton	LC-ToF-MS	[74]
	Sonolysis, Photocatalysis, sonophotocatalysis	HPLC-MS, UPLC-QToF-MS	[75], [72]
C <sub>13</sub> H <sub>18</sub> O <sub>4</sub>	photo-Fenton	LC-ToF-MS	[74]
	Sonolysis, Photocatalysis, sonophotocatalysis	HPLC-MS	[75]
C <sub>12</sub> H <sub>16</sub> O	Ozonation	UPLC-QToF-MS	[73]
	photo-Fenton	LC-ToF-MS	[74]
	Sonolysis, Photocatalysis, sonophotocatalysis	HPLC-MS, UPLC-QToF-MS	[75], [72]
C <sub>12</sub> H <sub>16</sub> O <sub>2</sub>	photo-Fenton	LC-ToF-MS	[74]
	Sonolysis, sonophotocatalysis	UPLC-QToF-MS	[72]
C <sub>12</sub> H <sub>16</sub> O <sub>5</sub>	Ozonation	UPLC-QToF-MS	[73]
C <sub>12</sub> H <sub>18</sub> O	Ozonation	UPLC-QToF-MS	[73]
	photo-Fenton	LC-ToF-MS	[74]
	Sonolysis, sonophotocatalysis	UPLC-QToF-MS	[72]
C <sub>10</sub> H <sub>12</sub> O <sub>2</sub>	photo-Fenton	LC-ToF-MS	[74]

Molecular formula of TP	Degradation process	Analytical Technique	Reference
C <sub>9</sub> H <sub>10</sub> O	Ozonation	UPLC-QToF-MS	[73]
	Sonolysis, sonophotocatalysis	UPLC-QToF-MS	[72]

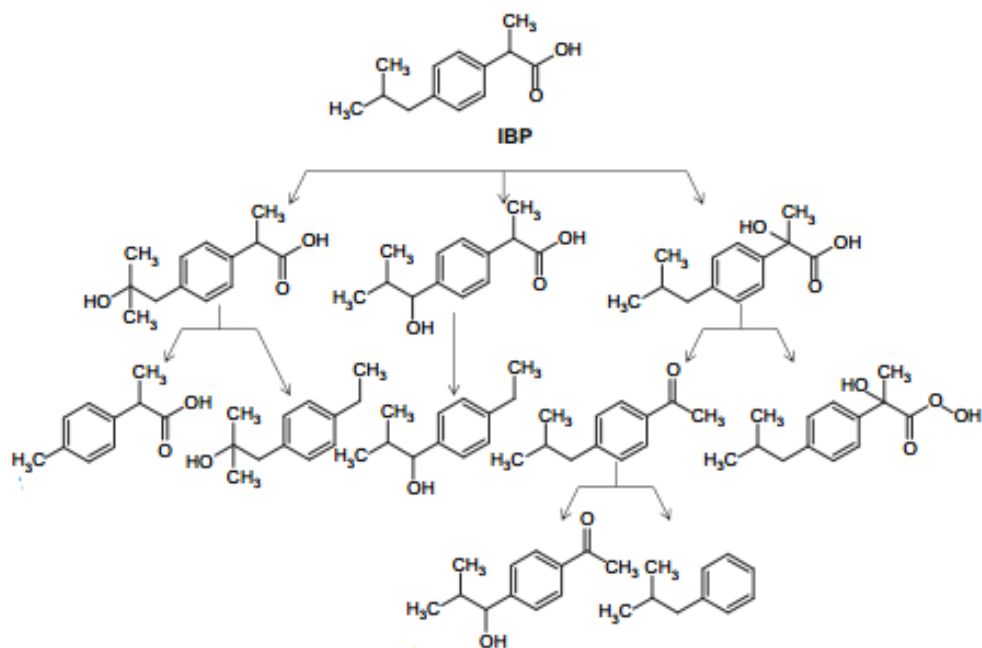


**Fig.13:** Proposed transformation pathway of Ibuprofen during photo-Fenton reaction by Mendez-Arriaga et al. (2010) [74].

## CHAPTER 3

### SCOPE AND OBJECTIVES

Recent studies have demonstrated that an exaggerate number of pharmaceutical compounds reach the environment mainly through anthropogenic sources of pollution. After the insufficient removal in wastewater treatment, these substances are discharged in receiving surface waters and are detected in various concentrations, from ng to  $\mu\text{g}$  per litter, depending on their physicochemical properties and biodegradability.

Various oxidation processes have been proposed in order to be applied as tertiary treatment in wastewater treatment plants in order to enhance the degradation of these micropollutants. Ozonation is a promising process which has been proven to be an effective oxidation technique and has gained popularity the recent years. Therefore, the complete mineralization of the contaminants is not achieved and consequently ozone-oxidation products with unknown toxicity may be produced. Thus the investigation of the precursors' degradation, the identification of probable produced TPs, their origin and their fate in aquatic environment are fields of great concern.

Among pharmaceuticals, NSAIDs and particularly the selected compound, niflumic acid (NA), has demonstrated incomplete removal by the conventional processes applied in WWTPs and is thus detected in surface water samples. The removal of NA in ultrapure water and wastewater samples, as well as the probable formation of its TPs through the application of degradation processes and especially oxidation processes have not been studied so far.

So, the aim of this master thesis is to assign knowledge on the removal and transformation of NA during ozonation. Particularly, the objectives of this study are:

- the systematic investigation of NA removal in ultra-pure water matrix, using a lab-scale ozonation system and the influence of two operational parameters (pH value, initial concentration of oxidant) were studied
- the detection, identification and structural elucidation of the main TPs after LC-QToF-MS analysis, through the application of suspect and non-

target screening techniques. Both positive and negative electrospray ionization modes were applied during the MS analysis

- the investigation of the fate of the most abundant TP of NA during ozonation and the study of second generation TPs.

Concluding, in the end of the present master thesis, future perspectives and work to be done are discussed.

## CHAPTER 4

### MATERIALS AND INSTRUMENTATION

#### 4.1 Reagents, standards and solvents

For the HPLC-HR/MS-MS system:

- Methanol (MeOH hypergrade for LC-MS, Sigma-Aldrich)
- Ultrapure water (18.2 MΩ cm<sup>-1</sup>, produced by a Milli-Q water purification system)
- Acetonitrile (ACN LC-MS grade, Merck)
- Formic acid (LC-MS Ultra, Fluka Analytical, Sigma-Aldrich)
- Ammonium formate (Fluka, Sigma-Aldrich)
- Ammonium acetate (Fluka, Sigma-Aldrich).

For the experimental procedure:

- Niflumic acid and 2-aminopyridine-3 carboxylic acid (Sigma-Aldrich, high purity grade) 1000 mg L<sup>-1</sup> standard solutions. Standard solutions of 1000 mg L<sup>-1</sup> were prepared for each analyte. 0.01g was weighed and diluted in MeOH in 10 mL volumetric flask. Then the solutions were stored at -20 °C in amber glass bottles to prevent photodegradation.

Additionally, the bellow mentioned solutions are required:

- CH<sub>3</sub>COONH<sub>4</sub> 0.001 M buffer solutions for pH values 4.0, 7.0 and 9.0. Firstly, solution CH<sub>3</sub>COONH<sub>4</sub> 0.001 mol L<sup>-1</sup> was prepared by weighing 0.0077 g of CH<sub>3</sub>COONH<sub>4</sub> (MW: 77.08 g mol<sup>-1</sup>), dissolving them in ultrapure water and diluting in volumetric flask of 100 mL. Then, the desirable pH value was adjusted by the addition of CH<sub>3</sub>COOH 0.1% (v/v) or NH<sub>3</sub> 0.1% (v/v) solution.
- Na<sub>2</sub>SO<sub>3</sub> 0.238 M stock solution. 0.3000 g of Na<sub>2</sub>SO<sub>3</sub> (Sigma-Aldrich, ≥98%) (MW: 126.04 g mol<sup>-1</sup>) were weighed and dissolved in ultrapure water and diluted in 10 mL volumetric flask.
- Tert-Butanol (t-BuOH) 4 M stock solution. 2.9648 g of t-BuOH (Sigma-Aldrich, 99.5%) (MW: 74.12 g mol<sup>-1</sup>) were weighed and dissolved in ultrapure water and diluted in 10 mL volumetric flask.

For residual ozone measurements:

- Indigo Reagent 0.001 M stock solution. 0.6167 g of potassium indigotrisulfonate (Sigma-Aldrich) (MW: 616.72 g mol<sup>-1</sup>) were weighed and dissolved with 1 mL of H<sub>3</sub>PO<sub>4</sub> (Sigma-Aldrich, 85%) in ultrapure water and diluted in 1 L volumetric flask.
- Phosphate buffer solution (pH 2). 28 g of NaH<sub>2</sub>PO<sub>4</sub>·2·H<sub>2</sub>O (Sigma-Aldrich, ≥99%) were weighed and dissolved with 21 mL of H<sub>3</sub>PO<sub>4</sub> (Sigma-Aldrich, 85%) in ultrapure water and diluted in 1 L volumetric flask.

All the necessary dilutions was performed to standards and stock solutions according to the experimental requirements, in order to prepare solutions of lower concentrations. All working solutions were stored in the refrigerator.

#### **4.2 Experimental setup used for the production of ozone stock solution**

Ozone stock solution was produced from industrial/ biomedical grade oxygen (Revival Bottled Gas, 99.5%) using AZCOZON VMUS-2 ozone generator. The experimental setup is presented in Fig. 14. All tubes and materials used in this configuration, are resistant in corrosion which ozone provokes. The O<sub>2</sub> gas flow is adjusted by an air valve and is kept constant in 40 L h<sup>-1</sup>. O<sub>3</sub> generator converts the O<sub>2</sub> molecules into ozone. Then the produced ozone is transferred by pipeline and through a sintered sparger at the bottom of 1 L glass reactor which contains ultrapure water. The surplus O<sub>3</sub> which is not dissolved in water, is removed by a pipeline which ends up in the waste. The glass reactor is placed in a bucket made by insulation material, filled with ice. The low temperature helps the dissolving process of ozone in the water (ozone solubility strongly depends on temperature, is about twice as high at 0 °C than at room temperature) and simultaneously averts the ozone decay.

Thus, a saturated ozone stock solution was prepared daily. The concentration of dissolved ozone in stock solution was determined by direct absorption determination in a UV-photometer at 260 nm ( $\epsilon = 2900 \text{ cm}^{-1} \text{ mol}^{-1} \text{ L}$ ) [76] and was calculated by Beer-Lambert law:

$$A = \epsilon b C \quad (4.1)$$

where  $\epsilon$ :  $\text{cm}^{-1} \text{mol}^{-1} \text{L}$ ,  $b$ :  $\text{cm}$ ,  $C$ :  $\text{mol L}^{-1}$ .

In order to convert the concentration from  $\text{mol L}^{-1}$  to  $\text{mg L}^{-1}$ , the equation 4.2 was used:

$$C' = C 1000 MW_{O_3} \quad (4.2)$$

where  $MW$  of  $O_3$  is  $48 \text{ g mol}^{-1}$ .

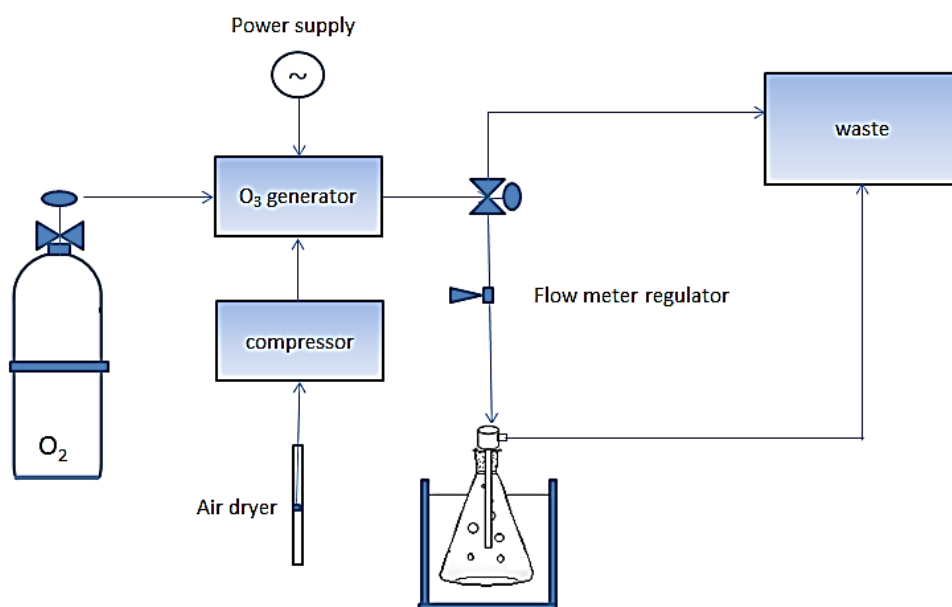


**Fig. 14:** Setup for production of saturated ozone stock solution.

### 4.3 UHPLC-HRMS/MS system and analysis

Ozonation samples analysis was carried out using an UHPLC-QToF-MS system composed of:

- An UHPLC rapid separation pump system, Dionex UltiMate 3000 (Thermo Fisher Scientific)
- Autosampler
- QToF mass spectrometer, Maxis Impact (Bruker Daltonics)

Mass spectra acquisition and data analysis was processed with DataAnalysis 4.1, TargetAnalysis 1.3 (Bruker Daltonics, Bremen, Germany) and Metabolite Tools 2.0, SR4 Bruker's software (Germany). The QToF-MS system is equipped with an ESI source, operating in positive and negative ionization mode. The chromatographic separation was performed on reversed-phase (RP) chromatographic system.

In RP mode, an Acclaim RSLC C18 column (2.1 × 100 mm, 2.2 μm) from Thermo Fisher Scientific, connected to an ACQUITY UPLC BEH C18 1.7 μm, VanGuard Pre-Column from Waters, and thermostated at 30 °C, was used.



**Fig.15:** *The UHPLC-QToF-MS system*

For positive ionization mode, the aqueous phase consisted of H<sub>2</sub>O:MeOH 90:10 with 5 mM ammonium formate and 0.01% formic acid. The organic phase was MeOH with 5 mM ammonium formate and 0.01% formic acid.

For negative ionization mode, the aqueous phase consisted of H<sub>2</sub>O:MeOH 90:10 with 5 mM ammonium acetate and the organic phase comprised of MeOH with 5 mM ammonium acetate.

The elution gradient program for both ionization modes started with 1% of organic phase (flow rate 0.2 mL min<sup>-1</sup>) for one minute, increasing to 39 % by 3 min (flow rate 0.2 mL min<sup>-1</sup>), and then to 99.9 % (flow rate 0.4 mL min<sup>-1</sup>) in the following 11 min. These almost pure organic conditions were kept constant for 2 min (flow rate 0.48 mL min<sup>-1</sup>) and then initial conditions were restored within 0.1 min, kept for 3 min and then the flow rate decreased to 0.2 mL min<sup>-1</sup> for the last minute. The injection volume was set to 5 μL.

A QToF-MS external calibration was daily performed with a sodium formate solution, and a segment (0.1–0.25 min) in every chromatogram was used for internal calibration, using a calibrant injection at the beginning of each run. The sodium formate calibration mixture consisted of 10 mM sodium formate in a mixture of water/isopropanol (1:1). The theoretical exact masses of calibration ions with formulas  $\text{Na}(\text{NaCOOH})_{1-14}$  in the range of 50–1000 Da were used for calibration. The instrument provided a typical resolving power of 36000–40000 during calibration (39274 at  $m/z$  226.1593, 36923 at  $m/z$  430.9137, and 36274 at  $m/z$  702.8636).

## CHAPTER 5

### STUDY OF REMOVAL AND IDENTIFICATION OF TRANSFORMATION PRODUCTS OF NIFLUMIC ACID DURING OZONATION EXPERIMENTS

#### 5.1 Removal of niflumic acid during ozonation

##### 5.1.1 Removal of niflumic acid in pH 7.0 ± 0.2 with different initial ozone concentrations and scavenger

A saturated stock solution of O<sub>3</sub> was prepared and its concentration was determined, with the procedure described in subchapter 4.2. At the same time, in a 25 mL volumetric flask, aqueous buffer solution (pH 7.0 ± 0.2) of NA of 3.0 mg L<sup>-1</sup>, with scavenger (t-BuOH) of 50 mM were prepared. Then the solutions were transferred into amber glass bottles, where the ozonation reaction would take place. A zero-time sample was withdrawn before the addition of ozone. A desirable amount of Na<sub>2</sub>SO<sub>3</sub> was added in all vials used for the sampling as immediate quencher of the reaction and its final concentration was 300 mg L<sup>-1</sup>. This concentration is high enough to quench the residual ozone, even when 7.0 mg L<sup>-1</sup> were used as initial ozone dose. Aliquots of the saturated stock solution of O<sub>3</sub> were transferred into the sealed bottles in order to achieve initial ozone concentrations of 0.4, 1.0, 2.0, 5.0 mg L<sup>-1</sup> respectively. The reaction started immediately and samples were collected in several time points (0 s, 15 s, 30 s, 1 min, 5 min, 10 min, 20 min, 30 min). A blank sample, comprised of aqueous buffer solution pH 7.0 ± 0.2, ozone, t-BuOH and Na<sub>2</sub>SO<sub>3</sub>, was also prepared as control sample.

##### 5.1.2 Removal of niflumic acid in different pH with initial ozone concentration of 2.0 mg L<sup>-1</sup> with and without scavenger

The same procedure described in paragraph 5.1.1 was followed. For the investigation of pH value influence, the initial solution of NA 3.0 mg L<sup>-1</sup> was prepared in 25 ml volumetric flask containing:

- aqueous buffer solution of pH 4.0 ± 0.2 with t-BuOH 50 mM
- aqueous buffer solution of pH 4.0 ± 0.2
- aqueous buffer solution of pH 7.0 ± 0.2 with t-BuOH 50 mM

- aqueous buffer solution of pH  $7.0 \pm 0.2$
- aqueous buffer solution of pH  $9.0 \pm 0.2$  with t-BuOH 50 mM
- aqueous buffer solution of pH  $9.0 \pm 0.2$ .

Then the solutions were transferred in amber glass bottles and  $O_3$  was added. After the beginning of the reaction, samples in the same time points were withdrawn. Likewise the corresponding blank samples were prepared.

## 5.2 Measurement of the residual aqueous ozone during NA ozonation.

The determination of the residual aqueous ozone during the experiments was carried out using the indigo method [77, 78]. Aqueous solutions of indigo trisulfonate absorb light at 600 nm ( $\epsilon = 23800 \text{ cm}^{-1} \text{ mol}^{-1} \text{ L}$ ). The indigo molecule contains only one C=C double bond which can signify that reacts in a very high rate with ozone. Parallel, at pH below 4, the amino groups are protonated and therefore become unreactive. Ozonolysis of the reactive C=C double bond produces sulfonate isatin and similar products and as a result has the elimination of its absorbance at 600nm. This decrease in absorbance of indigo reagent is linear with ozone residual.

A standard curve of indigo absorbance in 600 nm versus ozone concentration was made with solutions containing from  $0.01 \text{ mg L}^{-1}$  to  $0.10 \text{ mg L}^{-1}$   $O_3$  in order to cover this range of residual concentrations. Some of these solutions are depicted in Fig.16. The solutions except from the required quantity of ozone, contained 10 mL phosphate buffer for pH 2.0 and 250  $\mu\text{L}$  of Indigo reagent 1 mM diluted in ultrapure water in volumetric flasks of 100 mL.

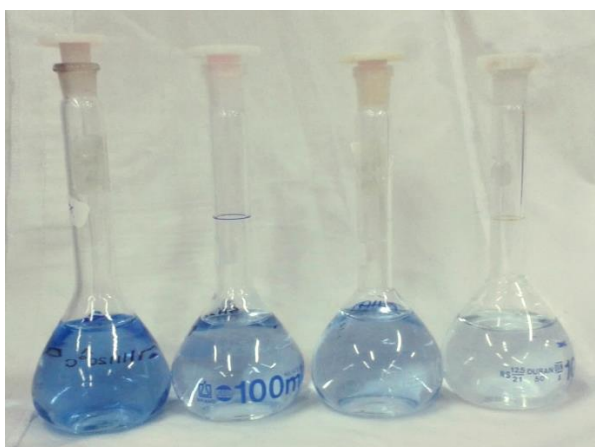


**Fig.16:** Decolorization of indigo reagent in reaction with different ozone concentration.

Then, 20 mL of an experimental solution of ozonation process at time point of 30 s which had initial concentrations of NA  $3.0 \text{ mg L}^{-1}$  and  $\text{O}_3$   $2.0 \text{ mg L}^{-1}$  was added with 10 mL phosphate buffer for pH 2.0 and 250  $\mu\text{L}$  of Indigo reagent 1mM in ultrapure water in volumetric flask of 100 mL. The absorbance of this sample was measured in 600 nm and compared with the standard curve and thus the residual concentration of ozone was calculated. This procedure was followed in order to examine the time-point where the ozone was totally depleted in every experiment.

### 5.3 Samples analysis

Ozonation samples were analyzed by the UHPLC-QToF-MS system described in paragraph 4.3. The selected chromatographic system was RP and the ESI which operated in positive and negative ionization (PI and NI) mode had the following operational parameters:

- end plate offset: 500 V
- capillary voltage: 2500 V for PI, 3500 for NI
- nebulizer gas pressure ( $\text{N}_2$ ): 2 bar
- drying gas ( $\text{N}_2$ ):  $8 \text{ L min}^{-1}$
- drying temperature:  $200 \text{ }^\circ\text{C}$

For each sample, in both ionization modes, full scan mass spectra were recorded over a range of 50-1000 m/z. The Bruker bbCID (broadband collision-induced dissociation) mode provides MS and MS/MS spectra at the same time working at two different collision energies; at low collision energy (4 eV), MS spectra is acquired, where all of the ions from the preselected mass range are heading towards the flight tube without isolation at the quadrupole and there is no collision-induced dissociation at the collision cell. At high collision energy (25 eV), no isolation is taking place at the quadrupole, and the ions from the preselected mass range are fragmented at the collision cell. This mode provides high MS sensitivity but the acquired MS/MS spectra are noisy and not compound-specific. For this reason, when the first screening was completed and the m/z of possible TPs were known, a second analysis with data dependent acquisition mode (autoMS) was performed. Data dependent acquisition can be performed either by fragmenting the five most abundant m/z per scan or by fragmenting predefined m/z which are included in a list. The

applied collision energy was set to predefined values, according to the mass and the charge state of every ion. If needed, more than one collision energies were tested in order to reveal more characteristic fragments.

Some samples were pre-concentrated and reanalyzed with the above mentioned acquisition modes as to obtain clearer MS and MS/MS spectra of the investigated m/z.

#### **5.4 Estimation of NA removal during ozonation process**

Samples analysis was followed by the estimation of NA removal during ozonation towards different experimental conditions. The experimental data were processed and NAs extracted ion chromatogram peaks were integrated manually in order to obtain specific peak areas. As the peak area has direct correlation with the analyte's concentration, it was normalized in order to estimate the compound removal in each experiment.

Peak area of NA in zero-time sample of each experiment was normalized as 100. Peak areas of NA in treated samples of the same experiment were normalized and presented as percentage of the zero-time sample's peak area. Thus the percentage of removal was calculated as:

$$\% \text{ NA Removal} = \frac{\text{Normalized Area}_{\text{zero-time sample}} - \text{Normalized area}_{\text{treated sample}}}{\text{Normalized Area}_{\text{zero-time sample}}} \times 100 \quad (5.1)$$

#### **5.5 Identification of possible TPs**

##### **5.5.1 Suspect screening**

A suspect list of candidate TPs was created accumulating several information including NA impurity products, expected TPs derived from the oxidation of the parent compound or through the breakdown of the parent compound's structure and proposed TPs by *in silico* prediction tools. Two different prediction tools were applied in this study. Firstly, the EAWAG-BBD PPS, an artificial intelligence system, was used which predicts microbial metabolic reactions, without the "relative reasoning mode", based on biotransformation rules set in the EAWAG-BBD and scientific literature. Consequently, Metabolite Predict software (Metabolite Tools 2.0, Bruker Daltonics) was utilized. This program proposes products based on rules according to mammals' metabolism reactions (Phase I, II and Cytochrome P450 reactions).

All the suggested TPs were assimilated in the suspect list including the molecular formula, exact mass and structures.

After compiling the list, all samples were scanned for the detection of these plausible TPs. The suspect peak list was acquired by using an automatic database search function Find Compounds-Chromatogram in Target Analysis (Bruker Daltonics) which created the base peak chromatograms for the masses of the list that attained the preselected threshold of intensity, excluding the isotopic peaks.

Some important criteria were applied in order to start the tentative identification procedure:

- absence of compounds in blank or zero-time samples
- mass accuracy threshold of 2 mDa and 5 ppm on the monoisotopic peaks
- maximum of 100 mSigma for the isotopic pattern fit, where mSigma-value represents the goodness of fit between the measured and the theoretical isotopic pattern (mass and ions ratios). However, mSigma was augmented in low intensity peaks.
- intensity threshold of 400 counts.

It is important to mention that the selected thresholds for fragments identification were more lenient due to their lower intensity:

- mass accuracy threshold of 10 ppm
- mSigma value the smaller the better (sometimes could not be calculated by the program due to low intensity of the isotopic ions)

Identification of the compounds was enhanced by the presence of characteristic adducts and in-source fragments:

- $[M+H]^+$ ,  $[M+Na]^+$ ,  $[M+K]^+$  and  $[M+NH_4]^+$  in positive ionization mode
- $[M-H]^-$ ,  $[M-CO-H]^-$ ,  $[M-CO_2-H]^-$  and  $[M+Cl]^-$  in negative ionization mode.

In case of the tentative identified compounds were commercially available, the related standard was purchased to confirm their identity.

### 5.5.2 Non-target screening

The non-target screening was performed using Metabolite Detect software (Metabolite Tools 2.0, Bruker Daltonics). The first step of this procedure was the background subtraction which typically signified that the full scan MS chromatogram of the zero-time sample was subtracted by the full scan MS chromatogram of each treated sample. As a result a new chromatogram was created in which only the more intense peaks in the treated samples than in reference sample were included in the base peak chromatogram. The parameters used to calculate the difference between the two samples were: eXpose mode algorithm, delta time  $\pm 0.1$  min, delta mass  $\pm 0.05$  m/z while a ratio 2 and 3 were tested, so as a mass peak compared to a peak detected in the reference to be accepted as a different peak. The peaks of the new chromatogram that were not presented in the blank samples or in the current suspect database were selected to be treated as suspect peaks of possible TPs. Therefore, the above mentioned criteria were applied in order to start the tentative identification process.

### 5.5.3 Interpretation of MS and MS/MS spectra

The detected TPs were identified using the mass accuracy and isotopic pattern of the precursor ion, the fragmentation pattern and the retention time of the extracted ion chromatographic (EIC) peak. The possible ion formulas of the precursor ion and its fragment ions were evaluated by SmartFormula Manually function, a DataAnalysis built-in tool, based on the accurate mass and isotopic pattern. In addition to C, H, O, and N, the element F had also been taken into account while proposing the possible TPs formulas since the parent compound's structure included three F atoms. The nitrogen rule, ring structures, double bonds and the number of carbon atoms were automatically checked by the program. The maximum mass deviation was set at  $\pm 10$  ppm.

Then possible structures of TPs were proposed according to the characteristic fragmentation (fragmentation pattern) occurred in TPs during MS/MS fragmentation events. It is crucial to be noticed that many TPs have a similar structure to the parent compound and as a consequence have common

fragments. The interpretation of the mass spectral data in order to propose a structure for the TPs is supported by literature [79].

#### **5.5.4 Communication of the achieved level of confidence**

The system presented by Schymanski et al. (2014) (Fig.9) to communicate the level of confidence achieved in the identification of the detected compounds was used. Level 1 corresponds to confirmed structures where a reference standard is available, level 2 to probable structures, level 3 to tentative candidate(s), level 4 to unequivocal molecular formulas and level 5 to exact mass(es) of interest. The detected compounds are characterized by this classification.

#### **5.5.5 Retention time prediction**

Retention time ( $t_R$ ) prediction is used as a complementary tool for the identification of TPs as reference standard solutions are not commercially available for the most of identified compounds. The in-house quantitative structure-retention relationships (QSRR) prediction model [80] (based on an extensive dataset of over 1800 compounds in RP) was employed for this purpose. The prediction is carried out using advanced chemometric tools where the proposed structure, its physicochemical properties and the chromatographic system (analytical column, gradient elution program and pump) used for the analysis are taken into consideration. The predicted  $t_R$  is considered to befit if it is within  $\pm 3\delta$  (standardized residuals) of the measured value as this covers 99.7% of normally distributed data and usually corresponds to  $\pm 2$  min.

#### **5.6 Ozonation of the most abundant TP of NA and investigation of possible second generation TPs**

In almost all experimental conditions tested, 2-aminopyridine-3 carboxylic acid (NA-138) was the most abundant TP. This TP, is commercially available, so it was purchased in order to confirm its structure. Moreover, its fate during ozonation was investigated in order to clarify if it is a recalcitrant TP or not and for the detection and identification of second generation TPs. The experiments of 2-aminopyridine-3 carboxylic acid (NA-138) were performed in similar conditions to NA. The initial concentration of the analyte was  $3.0 \text{ mgL}^{-1}$  in 25

mL aqueous buffer solution. Four different initial concentrations of O<sub>3</sub> (0.4, 1.0, 2.0 and 5.0 mg L<sup>-1</sup>) in pH 7.0 ± 0.2 with scavenger and three different pH values (pH 4.0, pH 7.0 in the presence of scavenger and pH 9.0 in the presence of scavenger) in the same initial O<sub>3</sub> concentration, 2.0 mg L<sup>-1</sup>, were studied. The samples were obtained in 2 and 10 min from the reaction's beginning and analyzed as described in paragraph 5.3. The removal of the precursor was calculated, and the identification of its TPs with suspect and non-target screening was accomplished as described in paragraph 5.5.

## CHAPTER 6

### RESULTS AND DISCUSSION

#### 6.1. Determination of NA removal during ozonation

##### 6.1.1 Effect of the initial ozone concentration in NA removal

Firstly, NA reactivity with aqueous ozone was tested using increasing initial ozone concentrations in the experiments of pH 7.0 in the presence of scavenger. The target was to determine the ozone concentration which was required for the total elimination of NA. The reaction of ozone with NA is extremely fast and is almost completed in most experimental condition within the first minute. As the results show (Table 7), the percentage of NA removal during ozonation is approximately constant in every time point. This fact implies that the reaction is extremely fast and a plateau is formed after the applied ozone dose is depleted. Thus, competitive kinetics should be applied in order to estimate direct constants.

**Table 7:** NA removal under various initial ozone concentrations in pH 7.0 in the presence of t-BuOH 50mM.

Time points (min)	% Removal under different initial O <sub>3</sub> concentrations			
	0.4 mg L <sup>-1</sup> O <sub>3</sub>	1.0 mg L <sup>-1</sup> O <sub>3</sub>	2.0 mg L <sup>-1</sup> O <sub>3</sub>	5.0 mg L <sup>-1</sup> O <sub>3</sub>
0.25	7.9	35.5	69.1	99.8
0.5	24.8	35.4	71.0	99.9
1	33.2	39.8	69.2	99.9
5	24.9	44.5	70.0	99.9
10	24.5	40.1	70.8	99.9
20	22.0	42.1	69.0	99.9
30	33.2	39.4	70.9	99.9

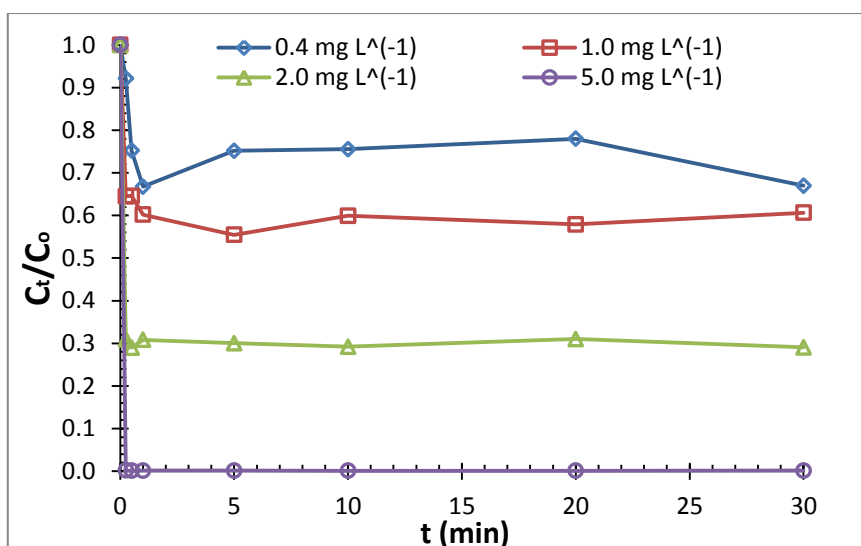


**Fig.17:** NA degradation under various initial ozone concentrations in pH 7.0 in the presence of *t*-BuOH ( $C_t$ : concentration of treated sample,  $C_o$ :  $3.0 \text{ mg L}^{-1}$ ).

NA removal is importantly influenced by the initial ozone concentration, as it is presented in Figure 16. As the initial ozone concentration increases, augmentation is observed in NA removal. An initial concentration of  $2.0 \text{ mg L}^{-1} \text{ O}_3$  is capable of removing 70% NA in the aqueous solution in less than 30 s, while the application of  $5.0 \text{ mg L}^{-1} \text{ O}_3$  leads efficiently in the total elimination of NA (99.9% removal) in almost the first 15 s of the reaction. It is important to highlight the fact that the amount of ozone is instantly consumed by the compound. For this reason, a bar chart (Fig.18), presenting the mean removal of NA in the different  $\text{O}_3$  initial concentrations, provides all the information.

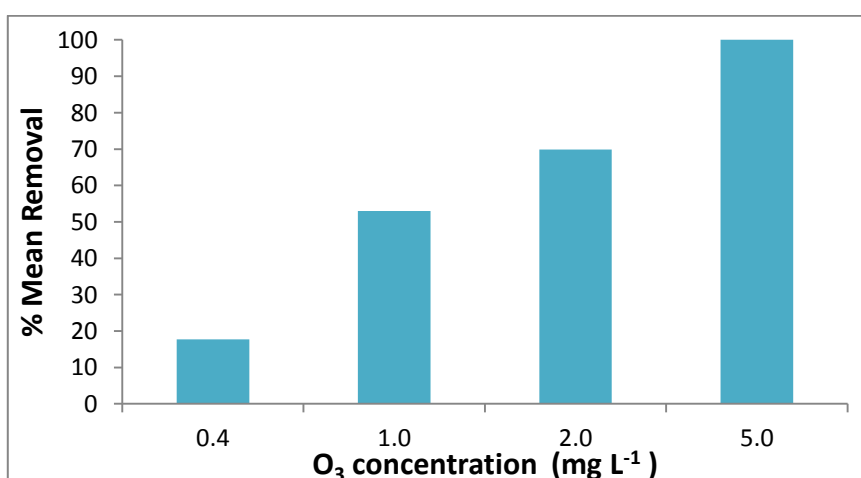


**Fig.18:** % NA mean removal under various initial ozone concentrations in pH 7.0 in the presence of scavenger ( $C_{o,NA}$ :  $3.0 \text{ mg L}^{-1}$ ).

### 6.1.2 Effect of different pH values and influence of the presence of scavenger in NA removal

Ozone aqueous solution is more stable at the acidic conditions, while in pH values >8, ozone decay is fast due to formation of hydroxyl radicals. The scavenger, t-BuOH, acts as inhibitor for the OH-radical reactions with NA and thus it is important in order to be determined if NA degradation occurs by the direct reaction of ozone with the compound.

**Table 8:** NA removal at different pH in absence or presence of scavenger

( $C_{0,NA} = 3.0 \text{ mg L}^{-1}$ ,  $C_{0,O_3} = 2.0 \text{ mg L}^{-1}$ )

Time points (min)	% Removal in different experimental conditions					
	pH 9.0	pH 9.0 (t-BuOH=50mM)	pH 7.0	pH 7.0 (t-BuOH=50mM)	pH 4.0	pH 4.0 (t-BuOH=50mM)
0.25	9.3	44.1	22.9	69.1	47.8	66.9
0.5	13.9	57.9	37.6	71.0	45.5	69.8
2	20.6	47.7	38.2	69.2	46.1	70.7
10	18.9	48.9	40.9	70.8	45.0	68.1
20	20.3	49.4	42.8	69.0	45.7	69.8
30	20.6	52.2	47.1	70.9	45.0	68.0

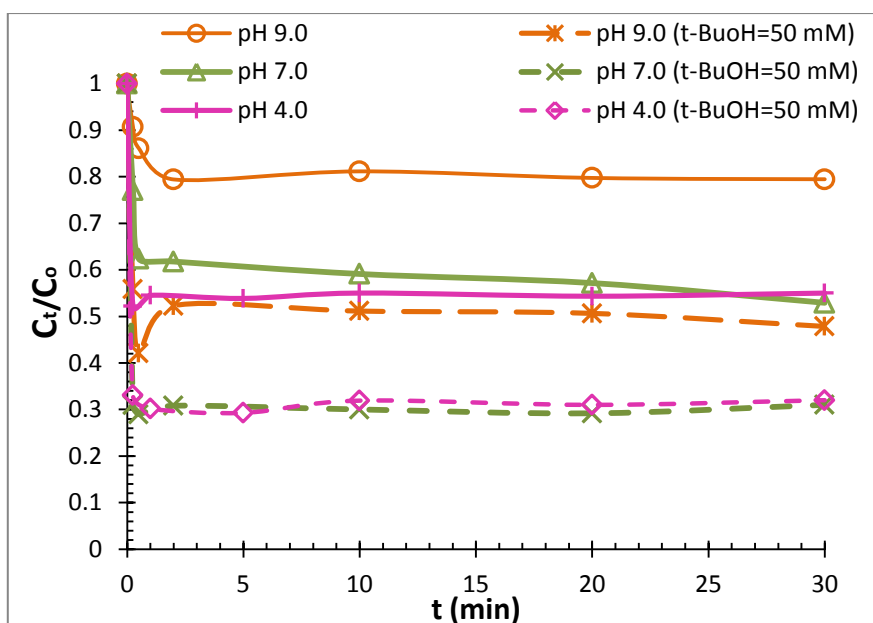


**Fig.19:** NA degradation at different pH values with or without *t*-BuOH, initial  $C_{O_3} : 2.0 \text{ mg L}^{-1}$  ( $C_t$ : concentration of treated sample,  $C_o : 3.0 \text{ mg L}^{-1}$ ).

NA overall removal in all experiments in the presence of scavenger is significantly higher than in related experiments without scavenger. This statement figures out that NA reacts directly with ozone fast and with high selectivity. The same conclusion is derived from the experiment in pH 9.0 (where OH radicals is the most abundant oxidation species) where almost a removal of 20% is achieved, while in pH 4.0 (where  $O_3$  is the most abundant oxidation species) the higher percentage of 45% is observed.

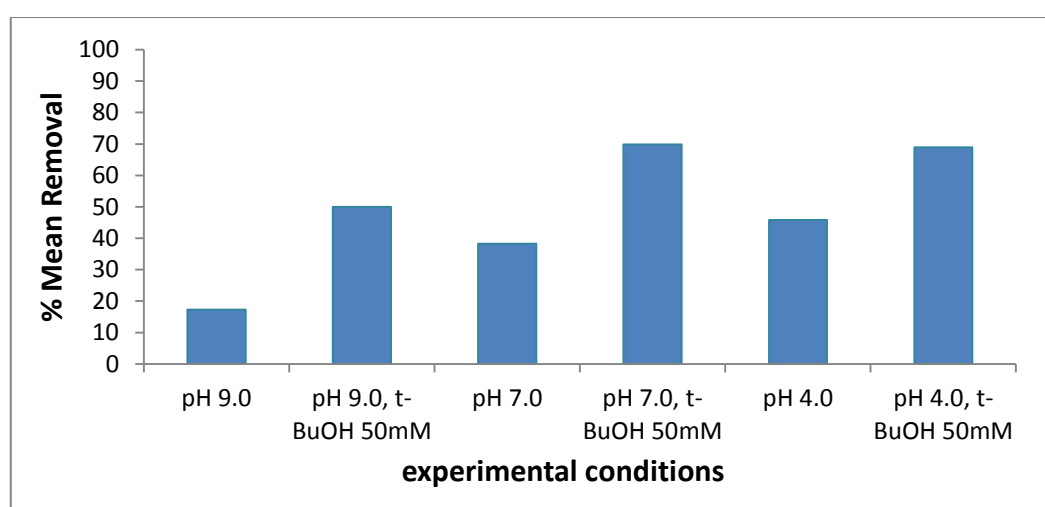


**Fig.20:** % NA mean removal at different pH values with or without scavenger, initial  $C_{O_3} : 2.0 \text{ mg L}^{-1}$  ( $C_{o,NA} : 3.0 \text{ mg L}^{-1}$ ).

## 6.2 Determination of residual ozone

The described Indigo method was used in order to confirm the immediate ozone consumption from NA during the first minute of ozonation process. A standard curve was made for a range of ozone concentrations from 0.01 mg L<sup>-1</sup> to 0.10 mg L<sup>-1</sup>.

**Table 9:** Absorption measurements in 600 nm for Indigo method std curve

O <sub>3</sub> Concentration (mg L <sup>-1</sup> )	Abs (600 nm)
0	0.085
0.01	0.083
0.02	0.079
0.03	0.075
0.05	0.069
0.06	0.062
0.08	0.054
0.10	0.044

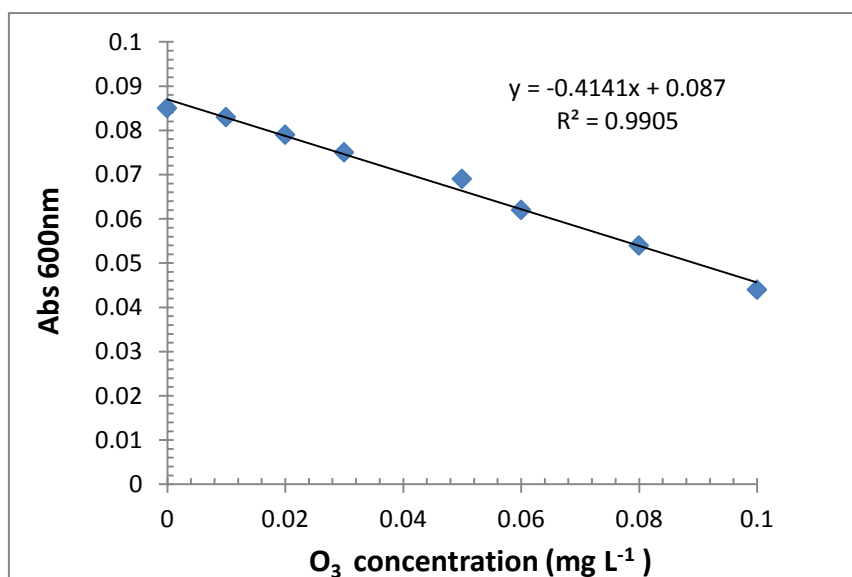


**Fig.21:** Standard curve: absorbance of indigo reagent versus ozone concentration.

Subsequently, the relevant absorption of the experimental sample (20 mL) added in indigo reagent from the first 30 s of ozonation process with initial concentrations  $2.0 \text{ mg L}^{-1} \text{ O}_3$  and  $3.0 \text{ mg L}^{-1} \text{ NA}$  in pH 7.0, was 0.084. The equation extracted from standard curve was used to determine the accurate residual ozone concentration:

- $C_{r,\text{O}_3} / 100 \text{ mL (indigo reagent)} = 0.007 \text{ mg L}^{-1}$ .

Hence the residual ozone concentration in the experimental sample was  $0.035 \text{ mg L}^{-1}$  which implied that approximately 98.3 % of ozone initial concentration had been consumed from NA in the first 30 s of the reaction.

### 6.3 Identification of NA transformation products

In total, seventeen candidate TPs of NA were detected and structurally elucidated using suspect and non-target screening techniques. The produced TPs were formed in the first 15 s as the reaction of NA with ozone has been instantaneously occurred. Analytical data for each TP, like RP Extracted Ion Chromatograms in PI and NI mode, MS and MS/MS spectra are presented below, including information for retention time, elemental formula, proposed structure and mass error (ppm) for the precursor and fragment ions.

#### 6.3.1 Fragmentation pattern of NA

Firstly, the fragmentation pattern of the parent compound in zero-time sample was studied. Taking into account that the TPs are parent compound-structure-like, they may probably generate common fragments, thus making the interpretation of TPs MS/MS spectra easier. NA elutes at  $t_R = 9.6 \text{ min}$  in RP(+) and at  $8.0 \text{ min}$  in RP(-) and its molecular formula is  $\text{C}_{13}\text{H}_9\text{F}_3\text{N}_2\text{O}_2$ .

In RP(+) (Fig. 22b), the MS spectrum shows the molecular ion of  $[\text{M}+\text{H}]^+$ ,  $\text{C}_{13}\text{H}_{10}\text{F}_3\text{N}_2\text{O}_2^+$ , at  $m/z$  283.0695 (1.2 mSigma) and its adduct ion of  $[\text{M}+\text{Na}]^+$ ,  $\text{C}_{13}\text{H}_9\text{F}_3\text{N}_2\text{NaO}_2^+$ , at  $m/z$  305.0519 (12.5 mSigma). The MS/MS spectrum (Fig. 22c) shows the major fragment ion at  $m/z$  265.0589 ( $\text{C}_{13}\text{H}_8\text{F}_3\text{N}_2\text{O}^+$ ) formed by cleaving off a  $\text{H}_2\text{O}$  molecule. Further on,  $m/z$  265 is subjected to the losses of HF molecule, CO group and  $\text{CF}_3$  group which conform to fragment ions at  $m/z$  245.0524 ( $\text{C}_{13}\text{H}_7\text{F}_2\text{N}_2\text{O}^+$ ), 237.0633 ( $\text{C}_{12}\text{H}_8\text{F}_3\text{N}_2^+$ ) and to the charged radical at 196.0628 ( $\text{C}_{12}\text{H}_8\text{N}_2\text{O}^+$ ), respectively. Moreover, a fragment with  $m/z$  217.0575

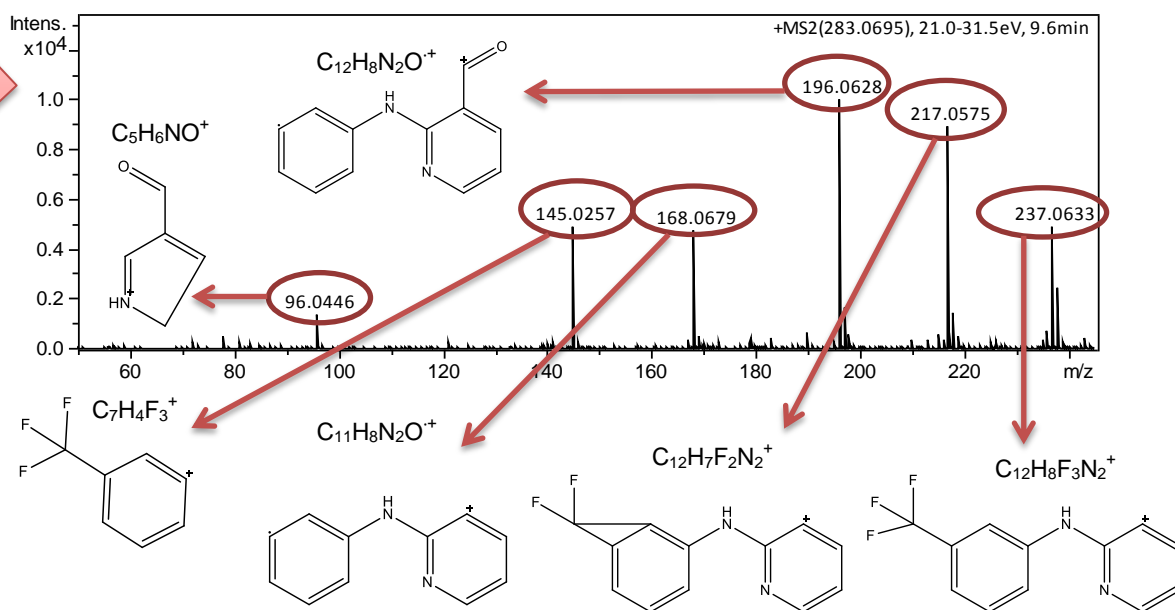
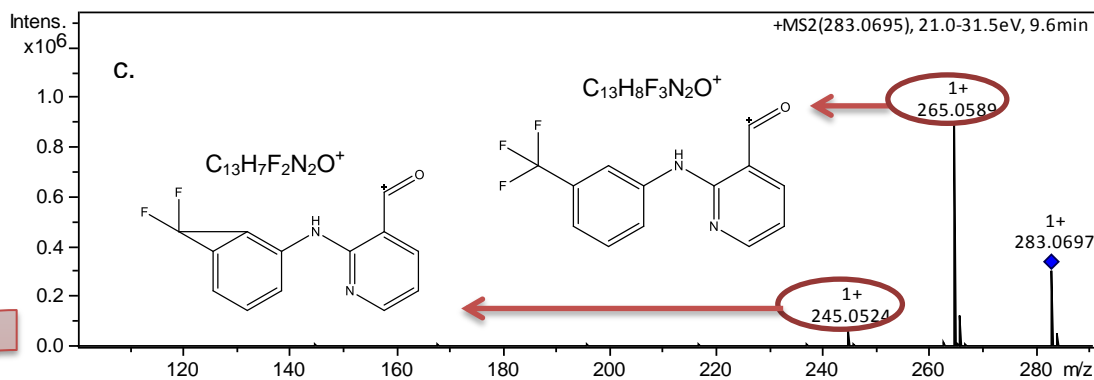
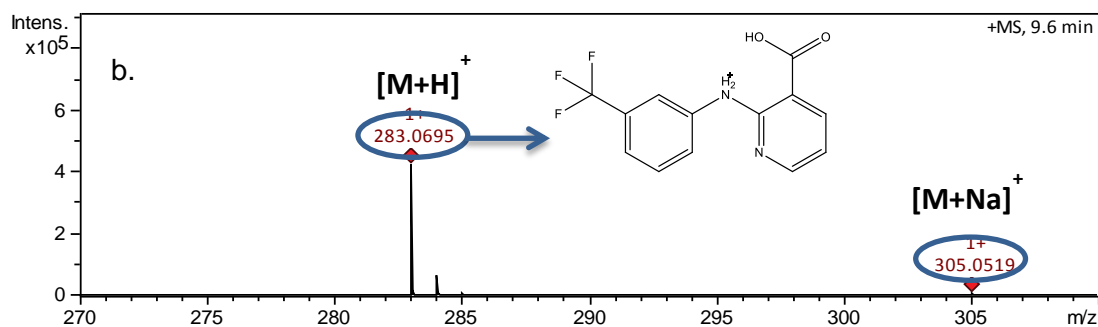
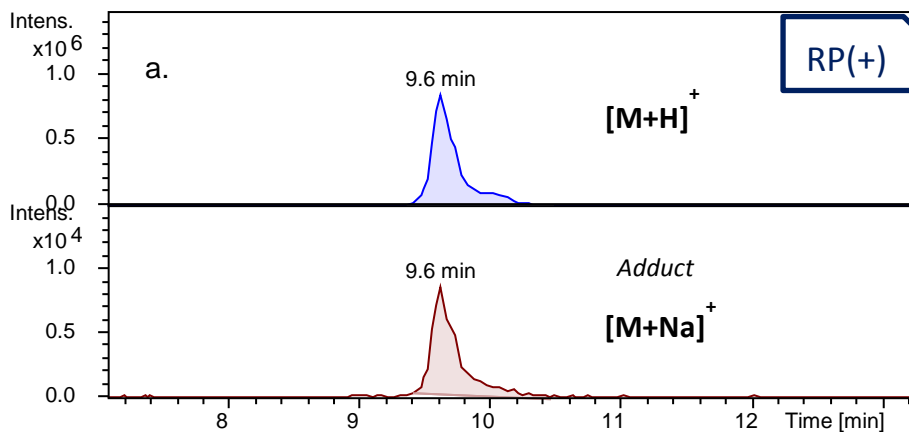


**Fig.22:** Analytical data for NA in RP(+); (a) EICs of NA and its adduct at zero-time sample, (b) MS and (c) MS/MS spectrum showing the fragmentation and proposed fragments of NA.

( $C_{12}H_7F_2N_2^+$ ) is formed by a loss of HF molecule from 237 and the charged radical at  $m/z$  168.0679 ( $C_{11}H_8N_2O^+$ ) arises from the loss of CO group from 196. Additional characteristic fragment ions appear at  $m/z$  145.0257 ( $C_7H_4F_3^+$ ) and 96.0446 ( $C_5H_6NO^+$ ).

In RP (-) (Fig. 23b), the MS spectrum shows the pseudo-molecular ion of  $[M-H]^-$ ,  $C_{13}H_8F_3N_2O_2^-$ , at  $m/z$  281.0549 (21 mSigma) and the loss of  $CO_2$  in the ionization source at  $m/z$  237.0645,  $C_{12}H_8F_3N_2^-$ , with good isotopic fitting (mSigma 17). MS/MS spectrum (Fig. 24) includes the fragment ions at  $m/z$  237.0646 ( $C_{12}H_8F_3N_2^-$ ) and 210.0531 ( $C_{11}H_7F_3N^-$ ) which are formed by the split of  $CO_2$  group and  $(CO_2)CNH$  unit, respectively. A further loss of HF molecule from 237 creates the ion at  $m/z$  217.0575 ( $C_{12}H_7F_2N_2^-$ ). A supplementary fragment ion appears at  $m/z$  160.0381 ( $C_7H_5F_3N^-$ ) which is formed by the cleavage of the  $C_6H_4NO_2$  part of the molecule. Two more characteristic fragments appear at  $m/z$  93.0458 ( $C_5H_5N_2^-$ ) and 68.9955 ( $CF_3^-$ ).

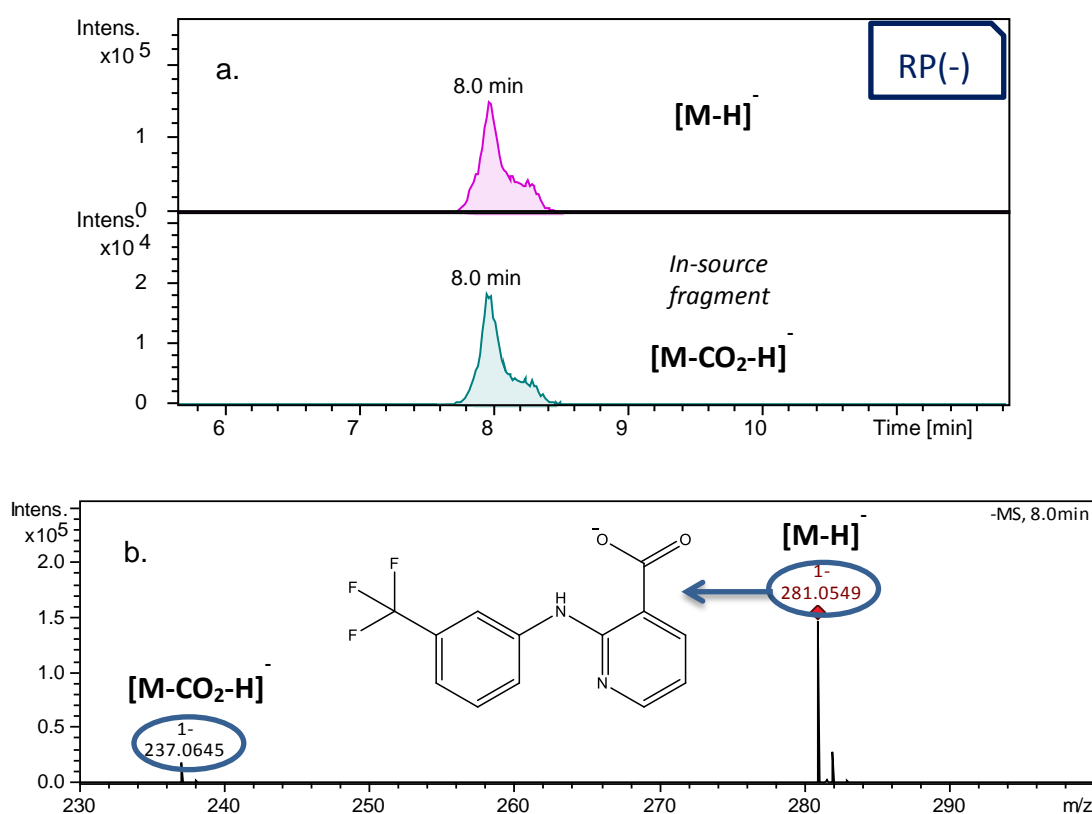


**Fig.23:** Analytical data for NA in RP(-); (a) EICs of NA and its in-source fragment at zero-time sample and (b) MS spectrum

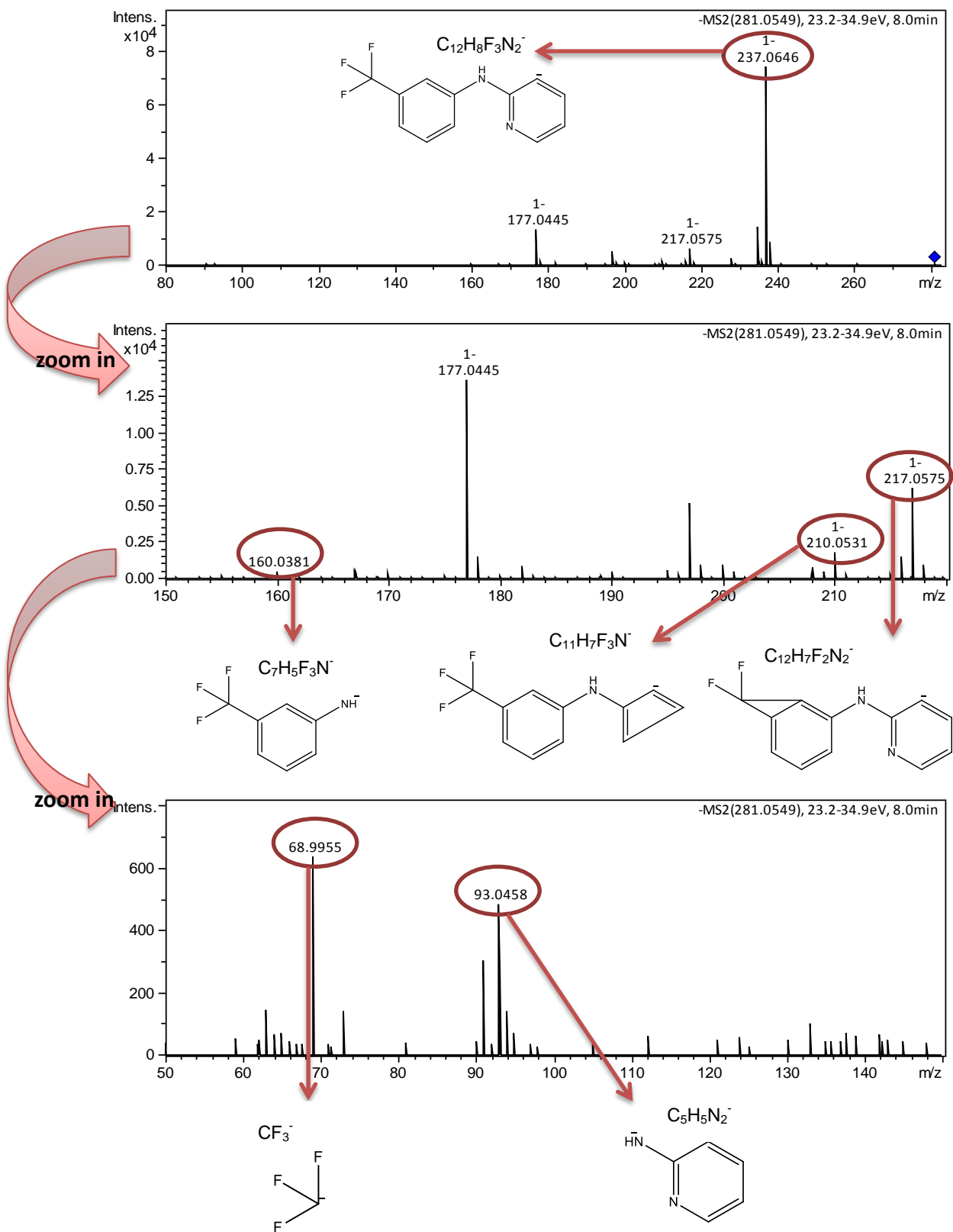


**Fig.24:** Analytical data for NA in RP(-); MS/MS spectrum showing the fragmentation and proposed fragments of NA.

**Table 10:** Elemental composition of NA, its adduct and fragment ions along with the measured m/z, the theoretical m/z and the mass error in ppm in RP(+).

	Ion formula	Theoretical m/z	Measured m/z	Mass error (ppm)
<b>NA</b>	$C_{13}H_{10}F_3N_2O_2^+$	283.0689	283.0695	-2.2
Adduct	$C_{13}H_9F_3N_2NaO_2^+$	305.0508	305.0519	-3.9
Fragments	$C_{13}H_8F_3N_2O^+$	265.0583	265.0589	-2.1
	$C_{13}H_7F_2N_2O^+$	245.0521	245.0524	1.1
	$C_{12}H_8F_3N_2^+$	237.0634	237.0633	-0.3
	$C_{12}H_8N_2O^+$	217.0572	217.0575	-1.3
	$C_{12}H_7F_2N_2^+$	196.0631	196.0628	1.5
	$C_{11}H_8N_2O^+$	168.0682	168.0679	1.8
	$C_7H_4F_3^+$	145.0260	145.0257	1.8
	$C_5H_6NO^+$	96.0444	96.0446	-2.4

**Table 11:** Elemental composition of NA, its in-source fragment and fragment ions along with the measured m/z, the theoretical m/z and the mass error in ppm in RP(-).

	Ion formula	Theoretical m/z	Measured m/z	Mass error (ppm)
<b>NA</b>	$C_{13}H_8F_3N_2O_2^-$	281.0543	281.0549	2.0
In-source fragment	$C_{12}H_8F_3N_2^-$	237.0645	237.0645	0.2
Fragments	$C_{12}H_8F_3N_2^-$	237.0645	237.0646	-0.3
	$C_{12}H_7F_2N_2^-$	217.0583	217.0575	-3.5
	$C_{11}H_7F_3N^-$	210.0536	210.0531	2.3
	$C_7H_5F_3N^-$	160.0380	160.0381	-1.0
	$C_5H_5N_2^-$	93.0458	93.0458	0.3
	$CF_3^-$	68.9955	68.9958	4.1

### 6.3.2 Identification of TPs found by suspect screening

Six TPs of NA were detected by suspect screening, five of which were ionized in both PI and NI mode.

#### 6.3.2.1 NA-298

NA-298a, b and c correspond to three isomers (shown in Fig. 25) with the elemental formula  $C_{13}H_9F_3N_2O_3$ , having one additional oxygen atom in comparison to NA, which were detected at  $t_R= 6.4, 8.1$  and  $9.0$  min in PR(+) and  $5.2, 5.7$  and  $7.3$  min in RP(-). The proposed structures are equivalent to the addition of a hydroxyl group in NA molecule. Hydroxyniflumic acids have been detected also as human metabolites [37].

In RP(+), MS spectra (Fig. 26) show the ions of NA-298a, b and c at  $m/z$  299.0645 (24.8 mSigma), 299.0648 and 299.0650 ( $C_{13}H_{10}F_3N_2O_3^+$ ), respectively. As the intensity of the first eluted isomer (shown in Fig. 26a), NA-298a, is higher than the other two, its fragmentation is extended and permits the structure elucidation of many fragments. The other isomers have lower intensity and as a result their MS/MS spectra provide fewer fragments. As it can be seen from their MS/MS spectra (Fig.27 & 28), there are common fragments verifying their similar structure.

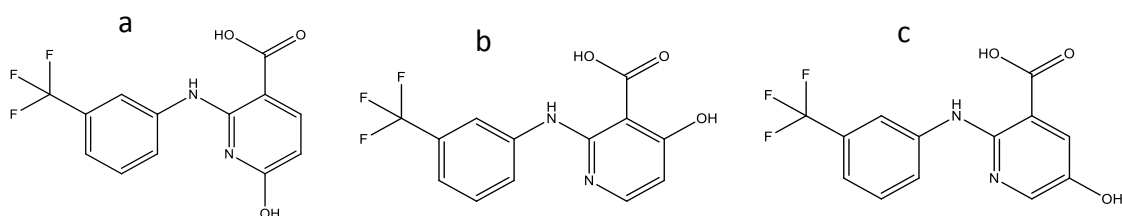


**Fig.25:** Proposed structures for NA-298 isomers.

MS/MS spectrum for NA-298a ( $t_R= 6.4$  min) (Fig. 27) depicts a typical neutral loss of a  $H_2O$  molecule producing the fragment at  $m/z$  281.0541 ( $C_{13}H_8F_3N_2O_2^+$ ) which further loses a HF molecule attributed to the ion at  $m/z$  261.0474 ( $C_{13}H_7F_2N_2O_2^+$ ). The formation of the ion at  $m/z$  233.0528 ( $C_{12}H_7F_2N_2O^+$ ) can be explained by the simultaneous cleavage of a  $CO_2$  group, a HF molecule and two hydrogen atoms from 299. Other fragment ions detected, are  $m/z$  208.0361 ( $C_{11}H_5F_3N^+$ ) and 89.0627 ( $C_4H_8FN^+$ ). More fragments are acquired by increasing the collision energy (to 50 eV) as  $m/z$

205.0578 ( $C_{11}H_7F_2N_2^+$ ) which can be justified by the loss of a CO group from 233. In addition, a charged radical appears at m/z 185.0471 ( $C_{11}H_7NO_2^+$ ) and an ion is exhibited at m/z 158.0384 ( $C_{10}H_5FN^+$ ).

MS/MS spectrum for NA-298b ( $t_R = 8.1$  min) (Fig. 28a) depicts initial fragmentation with the neutral loss of a HF molecule at m/z 279.0564 ( $C_{13}H_9F_2N_2O_3^+$ ). The subsequent loss of a  $H_2O$  molecule leads to the formation of a fragment at m/z 261.0468 ( $C_{13}H_7F_2N_2O_2^+$ ) and the loss of a  $CO_2$  group and two hydrogen atoms can be attributed to m/z 233.0529 ( $C_{12}H_7F_2N_2O^+$ ). By increasing the collision energy to 50 eV two more fragments are generated. The first fragment at m/z 205.0558 ( $C_{11}H_7F_2N_2^+$ ) which is produced in similar way as the described fragmentation pattern of NA-298 a, and an ion is presented at m/z 186.0552 ( $C_{11}H_8NO_2^+$ ).

AutoMS spectrum for NA-298c ( $t_R = 9.0$  min) (Fig. 28b) could not be acquired due to low intensity so the bbCID MS spectra in a range of 8.7 to 9.1 min was studied in order to investigate possible fragments. A characteristic ion at m/z 261.0471 ( $C_{13}H_7F_2N_2O_2^+$ ) with excellent mass accuracy (0.3 ppm) has been detected.

As the fragmentation pattern of the three isomers cannot depict the exact position where the hydroxylation took place, the in-house QSRR prediction model was used to support the proposed structures. As the results show in Table 12, the predicted  $t_R$  of the isomers are clearly separated, indicating which peak can be attributed to each isomeric structure. The theoretical  $t_R$  show a really good fitting with the experimental ones.

Thus, NA-298a, b and c are proposed to be hydroxyniflumic acids achieving a confidence level of 2b.

**Table 12:** Predicted and experimental retention time of three isomers NA-298 in RP(+).

Compound	Predicted $t_R$ (min)	Experimental $t_R$ (min)	$\Delta t_R$ (min)
NA-298a	6.2	6.4	-0.2
NA-298b	7.0	8.1	-1.1
NA-298c	8.9	9.0	-0.1

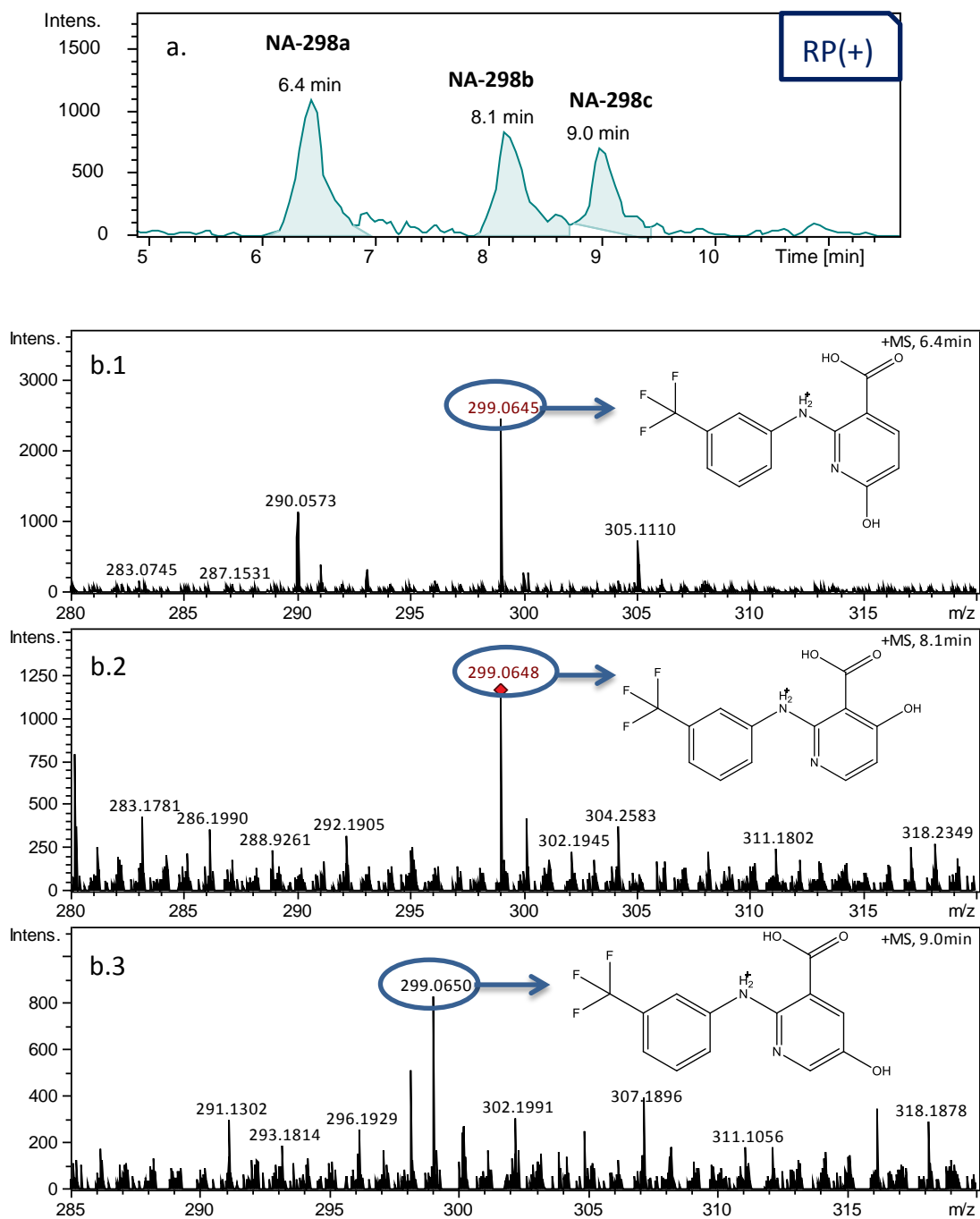


**Fig.26:** Analytical data for NA-298 isomers in RP(+); (a) EIC of NA-298 and (b) MS spectra of: (1) NA-298a, (2) NA-298b, (3) NA-298c

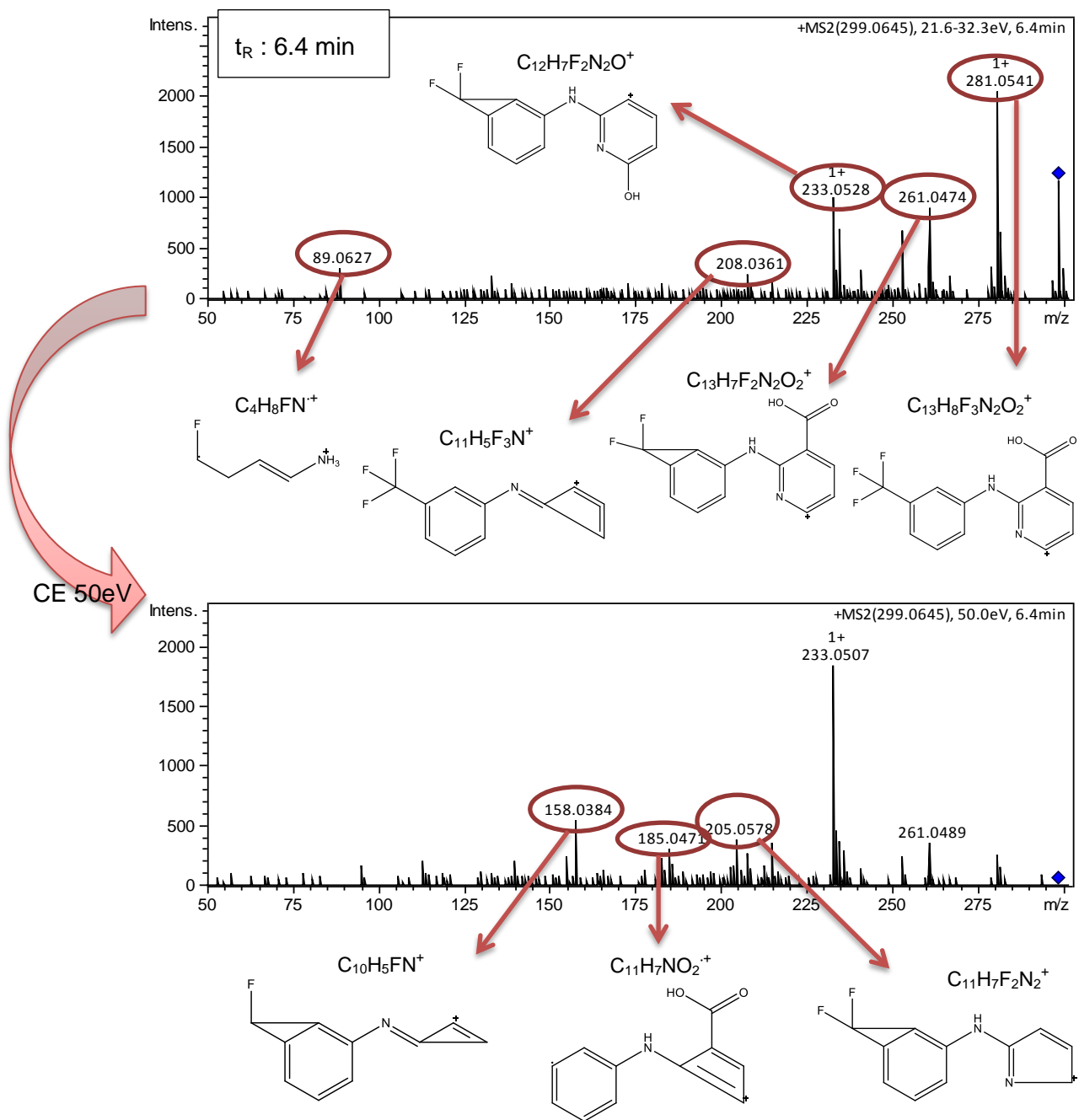


**Fig.27:** Analytical data for NA-298 isomers in RP(+); MS/MS spectrum showing the fragmentation and proposed fragments of NA-298a.

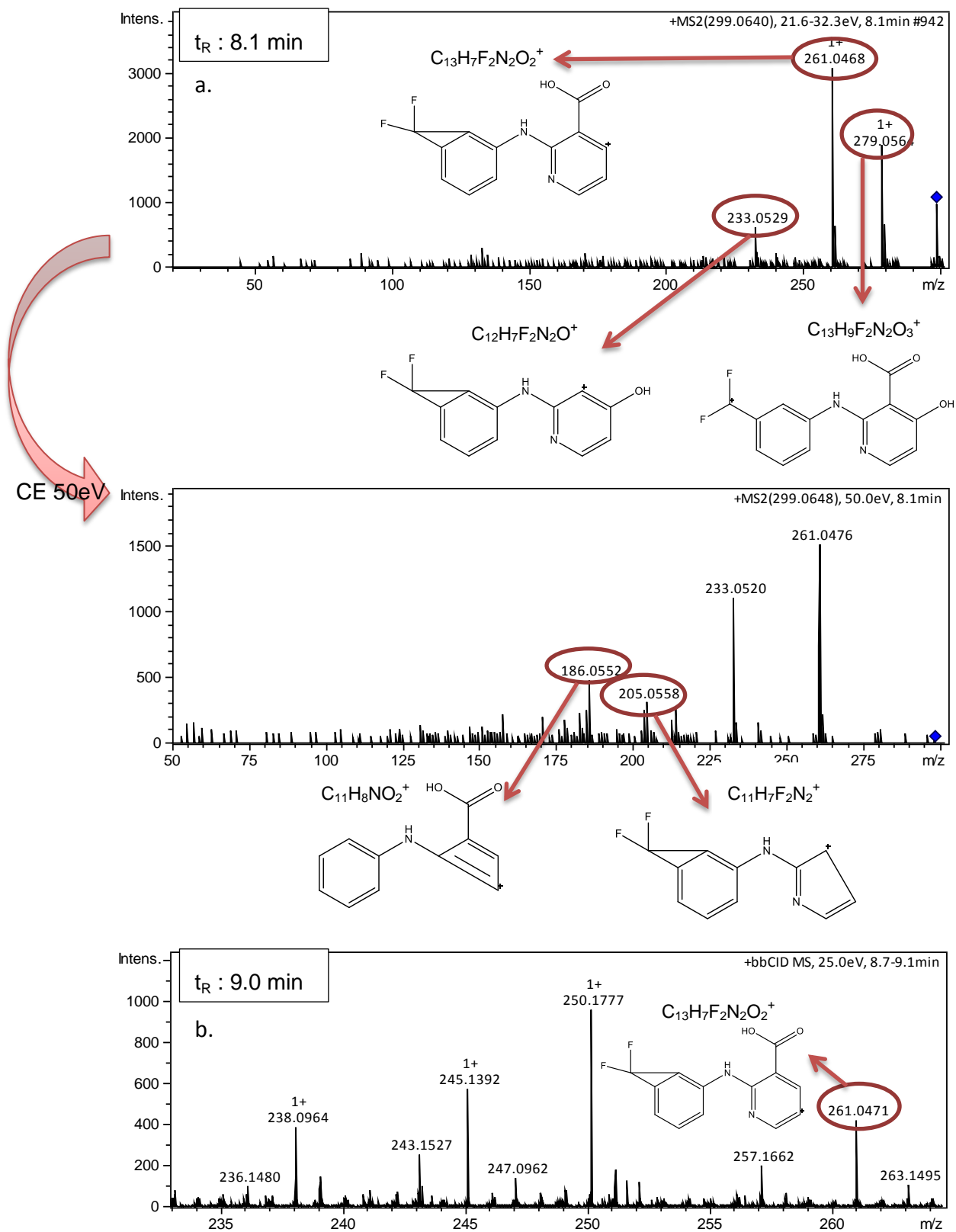


**Fig.28:** Analytical data for NA-298 isomers in RP(+); (a) MS/MS spectrum showing the fragmentation and proposed fragments of NA-298b and (b) bbCID mode MS spectrum showing characteristic proposed fragment of NA-298c.

These TPs are produced by the reaction of NA with O<sub>3</sub>. A hydroxylation of a double bond is the result of the mechanism already been referred in subchapter 1.3.2.3 and it is shown by equations 1.4 and 1.5. This mechanism is highly supported by the fact that the three isomers are produced even in the presence of t-BuOH, where OH radicals are scavenged, so O<sub>3</sub> is the main oxidant. The formation profile of the three isomers is depicted in Fig. 29. Although the removal of NA increases as the O<sub>3</sub> initial concentration increases, the formation profile of NA-298 does not follow the corresponding pattern. Their formation reaches a maximum when the initial O<sub>3</sub> concentration is 2.0 mg L<sup>-1</sup>, while at 5.0 mg L<sup>-1</sup> of O<sub>3</sub>, the intensity of NA 298 a decreases dramatically and the other two isomers were not detected at all, maybe due to further transformation.

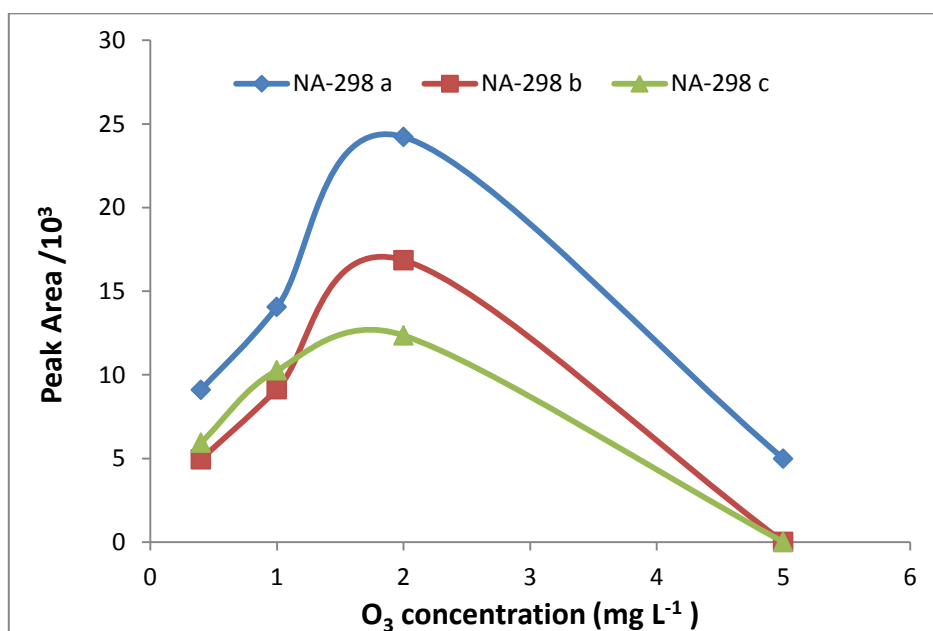


**Fig.29:** NA-298 isomers production trend in correlation with O<sub>3</sub> initial concentration.

In RP(-), the three MS spectra of NA-298 isomers (Fig. 30b) reveal the precursor ions (C<sub>13</sub>H<sub>8</sub>F<sub>3</sub>N<sub>2</sub>O<sub>3</sub><sup>-</sup>) with m/z 297.0482 (34.6 mSigma) , 297.0508 (55.4 mSigma) and 297.0492 (13.9 mSigma). Moreover, the in-source fragments that are also detected, indicate the loss of CO<sub>2</sub> group formatting m/z 253.0581, 253.0589 at t<sub>R</sub> 5.7 and t<sub>R</sub> 7.3 min, respectively.

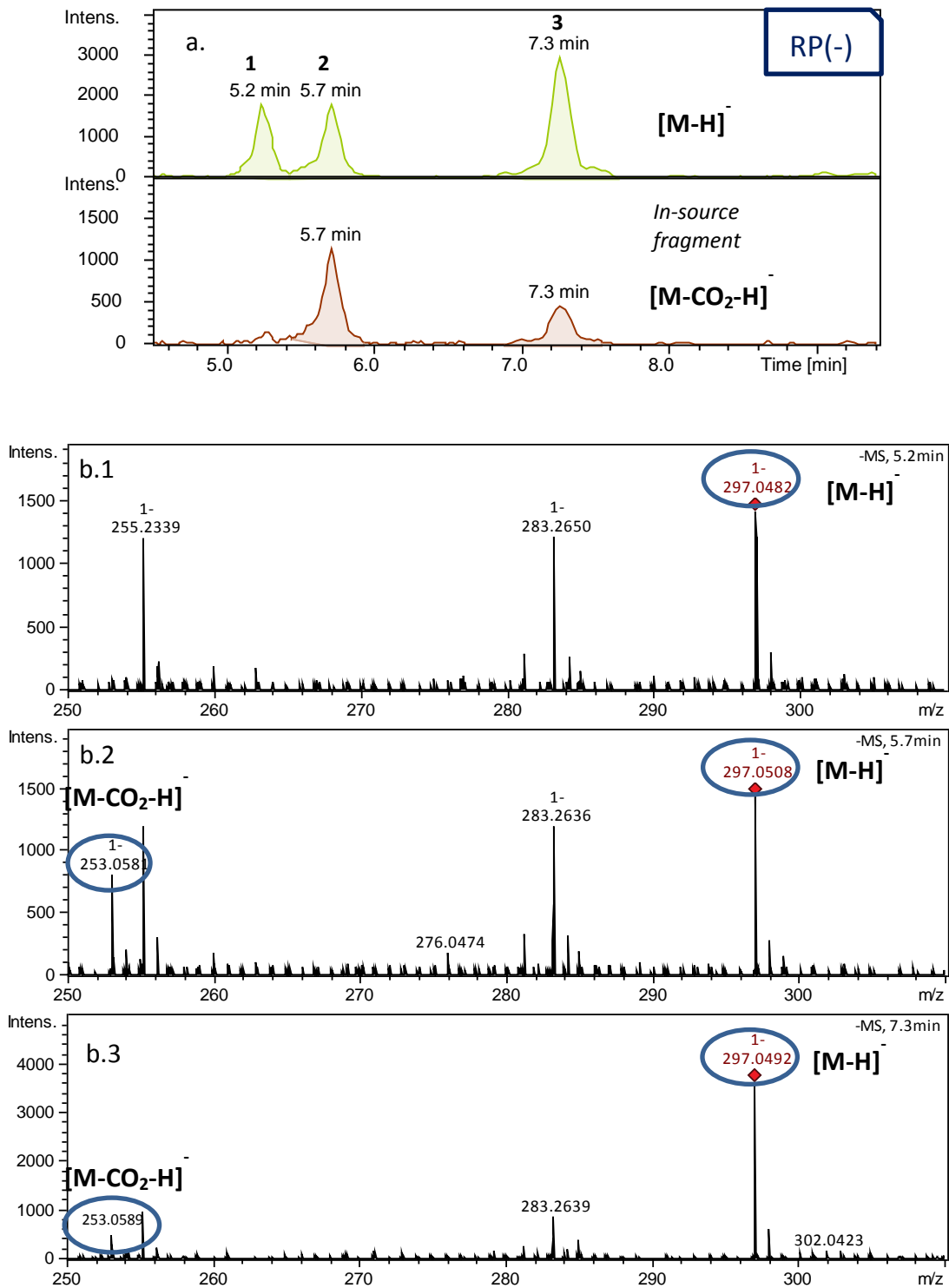


**Fig.30:** Analytical data for NA-298 isomers in RP(-); (a) EIC of NA-298 and their in-source fragments and (b) MS spectra.

### 6.3.2.2 NA-262

The TP NA-262 fits to the elemental formula  $C_{10}H_9F_3N_2O_3$ . This TP has three carbon atoms less and one oxygen atom more than its parent compound. Its structure arises by the breakdown of the heterocyclic ring and the formation of a hydroxylamine. It is eluted at  $t_R$  5.9 min in RP(+) and at 6.1 min in RP(-). In general, ozone does not react with positively charged N atoms. The fact that this compound was not formed in experiments conducted at pH 4.0, where the N atom of the pyridine-like moiety of NA is protonated, indicates that the hydroxylation took place in this nitrogen atom of the heterocyclic ring. The proposed structure of TP NA-262 is presented in Fig. 31.

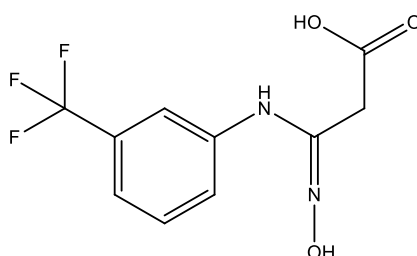


**Fig.31:** Proposed structure for NA-262.

In RP(+), NA-262 ion ( $C_{10}H_{10}F_3N_2O_3^+$ ) is detected at  $m/z$  263.0631 (28.7 mSigma) in the MS spectrum (Fig. 32b) along with its  $[M+K]^+$  adduct ion of ( $C_{10}H_9F_3KN_2O_3^+$ ) at  $m/z$  301.0188. MS/MS spectrum (Fig. 32 c) presents a simultaneous loss of  $CH_2CO_2$  unit and  $NHO$  resulting in the formation of the fragment at  $m/z$  174.0525 ( $C_8H_7F_3N^+$ ) and a following split of  $CH_2NH$  moiety, forming the fragment at  $m/z$  145.0246 ( $C_7H_4F_3^+$ ). Two more ions are depicted at the MS/MS spectra at  $m/z$  127.0342 ( $C_7H_5F_2^+$ ) and a characteristic fragment at  $m/z$  44.0131 ( $CH_2NO^+$ ) which confirms the presence of a hydroxylamine moiety in the structure of the produced TP.

In RP(-), the MS spectrum (Fig. 33b) shows the pseudo-molecular ion of  $[M-H]^-$  at  $m/z$  261.0495 in good fit with the theoretical mass (mass error -1.1 ppm). The intensity of this TP is significantly lower in negative ionization mode and thus the MS/MS spectrum (Fig. 33c) is noisy and the fragments are not clear and abundant. Only one fragment ion at  $m/z$  231.0621 ( $C_9H_9F_2N_2O_3^-$ ) is detected.

Therefore, the identification of this compound is supported clearly by diagnostic evidence reaching the level 2b.

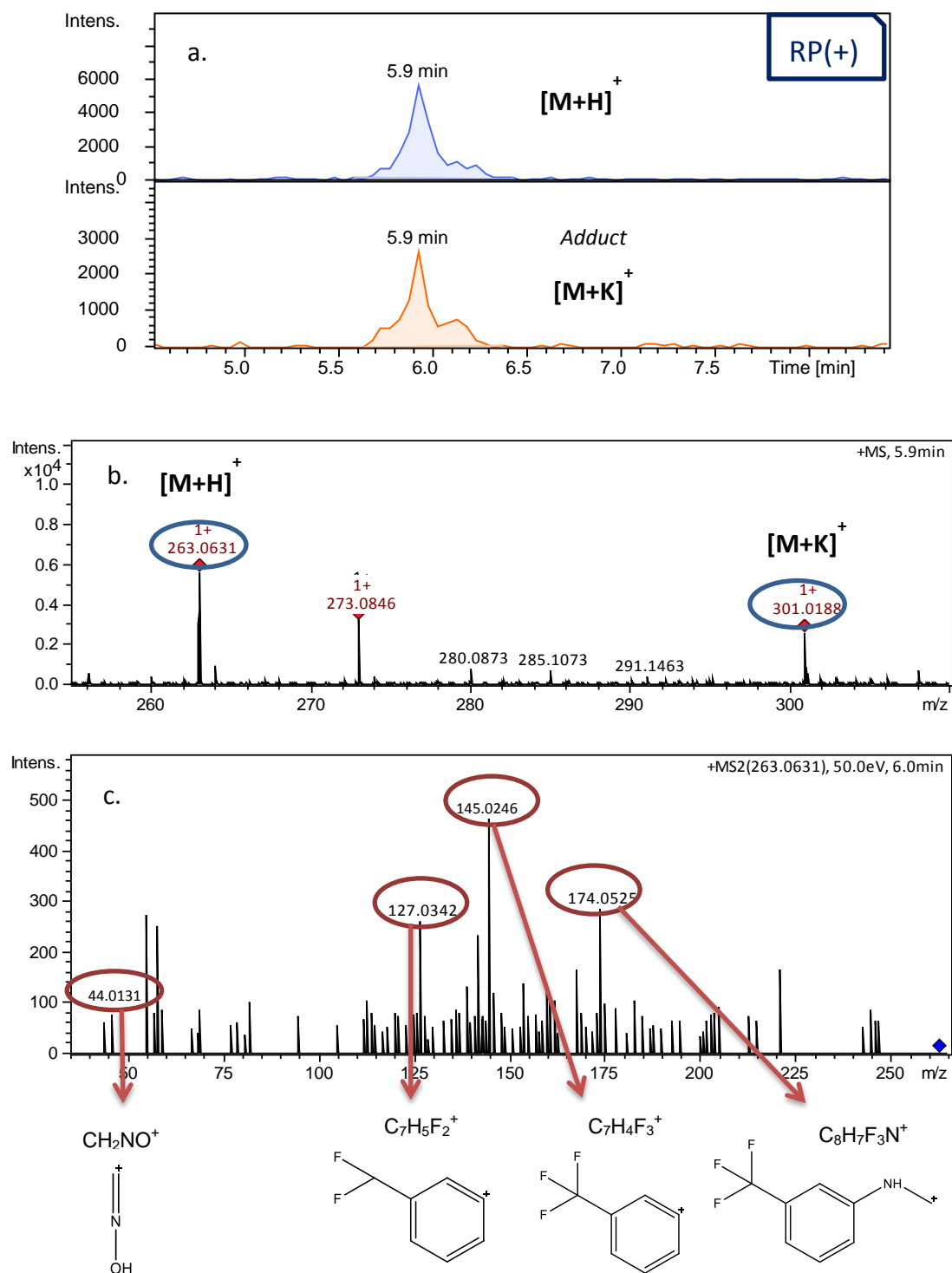


**Fig.32:** Analytical data for NA-262 in RP(+); (a) EICs of NA-262 and its adduct, (b) MS and (c) MS/MS spectrum showing the fragmentation and proposed fragments of NA-262.

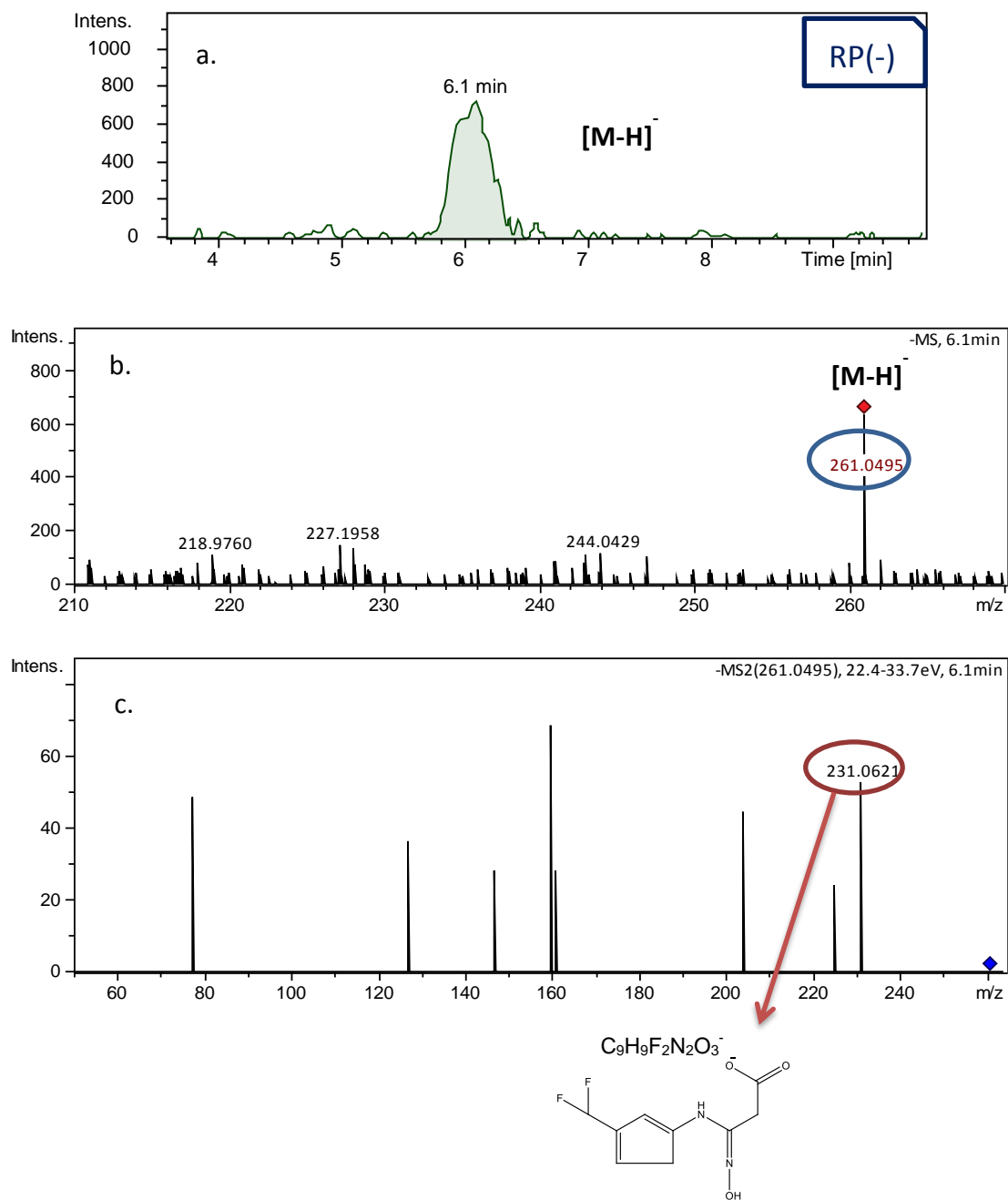


**Fig.33:** Analytical data for NA-262 in RP(-); (a) EIC of NA-262, (b) MS and (c) MS/MS spectrum.

### 6.3.2.3 NA-161

NA-161 is attributed to the elemental formula of  $C_7H_6F_3N$  and is detected only in NI mode at  $t_R$  5.6 min. This TP is formed by the cleavage of the heterocyclic ring part of NA,  $C_6H_4NO_2$ , through the hydroxylation of the N atom, during ozonation. Ozone attack is usually on the benzene ring if it is present in a molecule, however, it is well known that the nature of the substituent on the ring is a strong contributor to the ring's reactivity to ozone. The aromatic ring of this part remains unaffected by ozone attack due to the presence of the three fluoride atoms, which act as electron withdrawing groups.

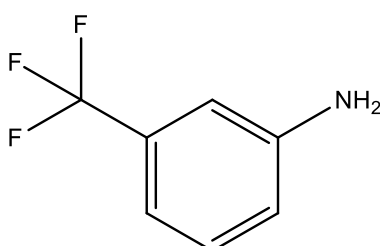


**Fig.34:** Proposed structure for NA-161.

The MS spectrum (Fig. 36a) shows the pseudo-molecular ion of  $[M+H]^+$  at  $m/z$  160.0376 in good matching with the theoretical  $m/z$  (mass error -2.0 ppm). The proposed structure is verified by the formation of two fragments in MS/MS spectrum (Fig. 36b), the  $m/z$  133.0270 ( $C_6H_4F_3^-$ ) produced by the loss of -HCN moiety ( $m/z$  27.0104) and the one at  $m/z$  120.0271 ( $C_7H_3FN^+$ ) caused by the loss of two HF molecules.

Thus, NA-161 is proposed to be 3-(trifluoromethyl)-aniline reaching a confidence level of 2b.

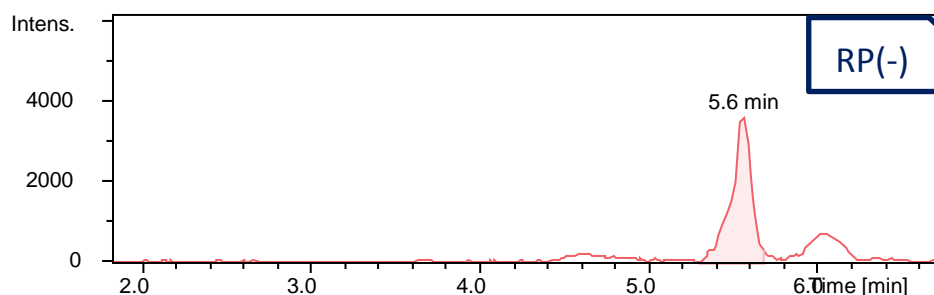


**Fig.35:** Analytical data for NA-161 in RP(-); EIC of NA-161.

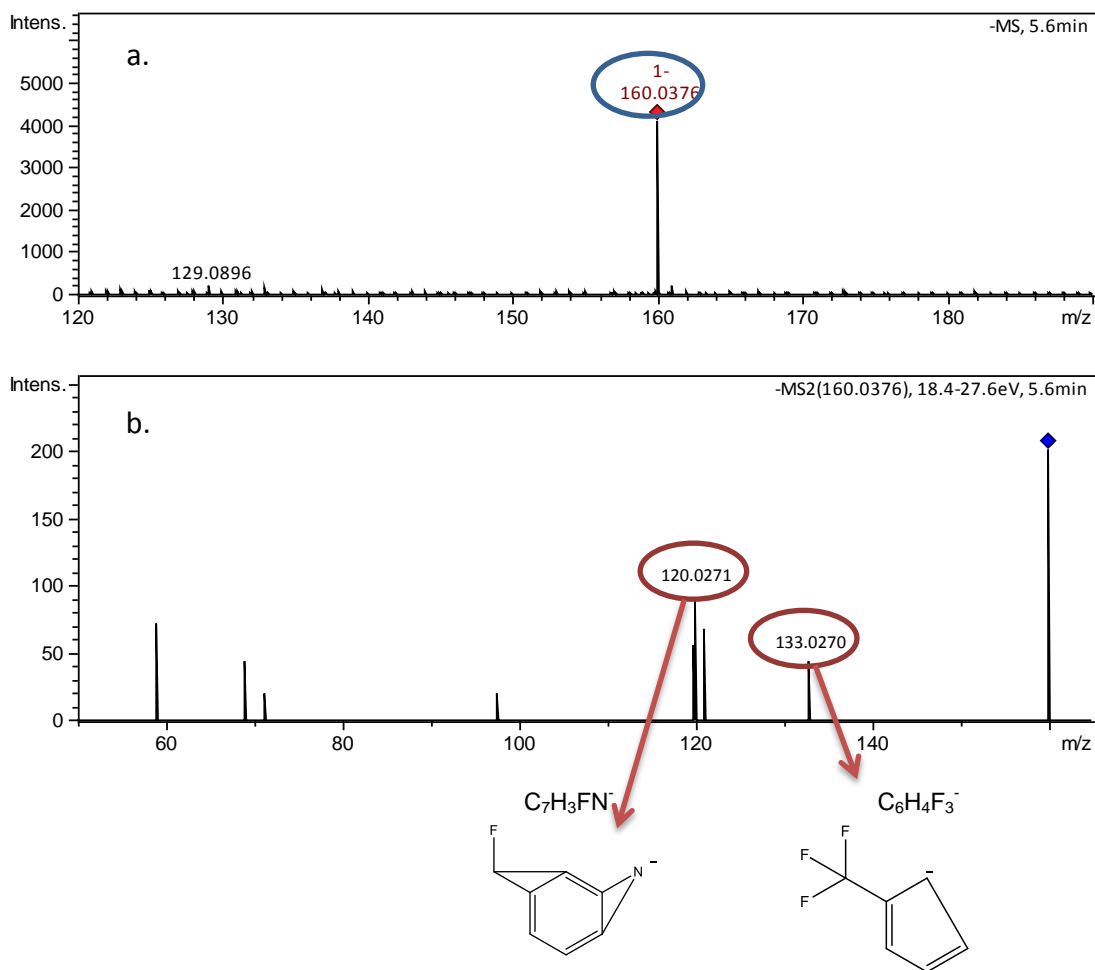


**Fig.36:** Analytical data for NA-161 in RP(-); (a) MS and (b) MS/MS spectrum showing the fragmentation and proposed fragments of NA-161.

#### 6.3.2.4 NA-138

At  $t_R$  1.6 min in RPLC column in both PI and NI mode, NA-138 is detected fitting to the elemental formula  $C_6H_6N_2O_2$ . The left-benzene part is split from NA molecule through amide hydrolysis during ozonation and as a result NA-138 is formed. It is the most abundant TP of NA which appears in all tested experimental conditions, except for the one in pH 9.0 without the addition of scavenger.

In RP(+), the MS spectrum (Fig. 39a) includes the pseudo-molecular ion  $[M+H]^+$  ( $C_6H_7N_2O_2^+$ ) at m/z 139.0499 with excellent isotopic fitting (1 mSigma) and its adduct ion  $[M+Na]^+$  ( $C_6H_6N_2NaO_2^+$ ) at m/z 161.0321. Furthermore, this spectrum indicates a loss of a  $H_2O$  molecule due to the energy applied in the ionization source,  $[M-H_2O+H]^+$  ( $C_6H_5N_2O^+$ ), with m/z 121.0396 in excellent fit

with the theoretical mass (mass error -0.3 ppm). The MS/MS spectrum (fig 39b) presents the direct cleavages of a H<sub>2</sub>O molecule and a CH<sub>2</sub>O<sub>2</sub> moiety (m/z 46.0049) resulting in the formation of the ions m/z 121.0393 (C<sub>6</sub>H<sub>5</sub>N<sub>2</sub>O<sup>+</sup>) and 93.0440 (C<sub>5</sub>H<sub>5</sub>N<sub>2</sub><sup>+</sup>), respectively. The concurrent loss of a CO<sub>2</sub> group and a HCN moiety produces the fragment at m/z 68.0497 (C<sub>4</sub>H<sub>6</sub>N<sup>+</sup>). In addition, a fragment at m/z 111.0552 (C<sub>5</sub>H<sub>7</sub>N<sub>2</sub>O<sup>+</sup>) is observed.

The identity of 2-aminopyridine-3-carboxylic acid, NA-138, is fully confirmed through the purchase and analysis of its reference standard. The retention time, MS and MS/MS spectra of the suspect TP are in accordance with those of the reference standard, thus, the identification confidence reaches the level 1.

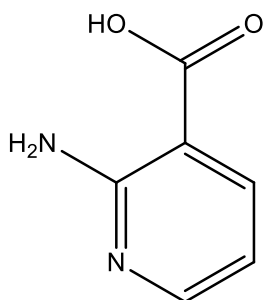


**Fig.37:** Proposed structure for NA-138.

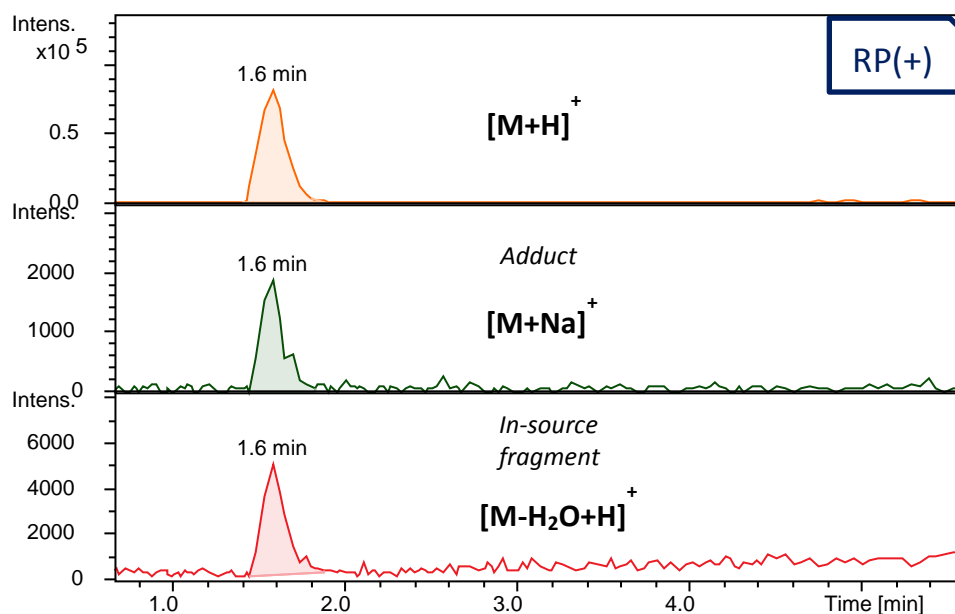


**Fig.38:** Analytical data for NA-138 in RP(+); EICs of NA-138, its adduct and its in-source fragment

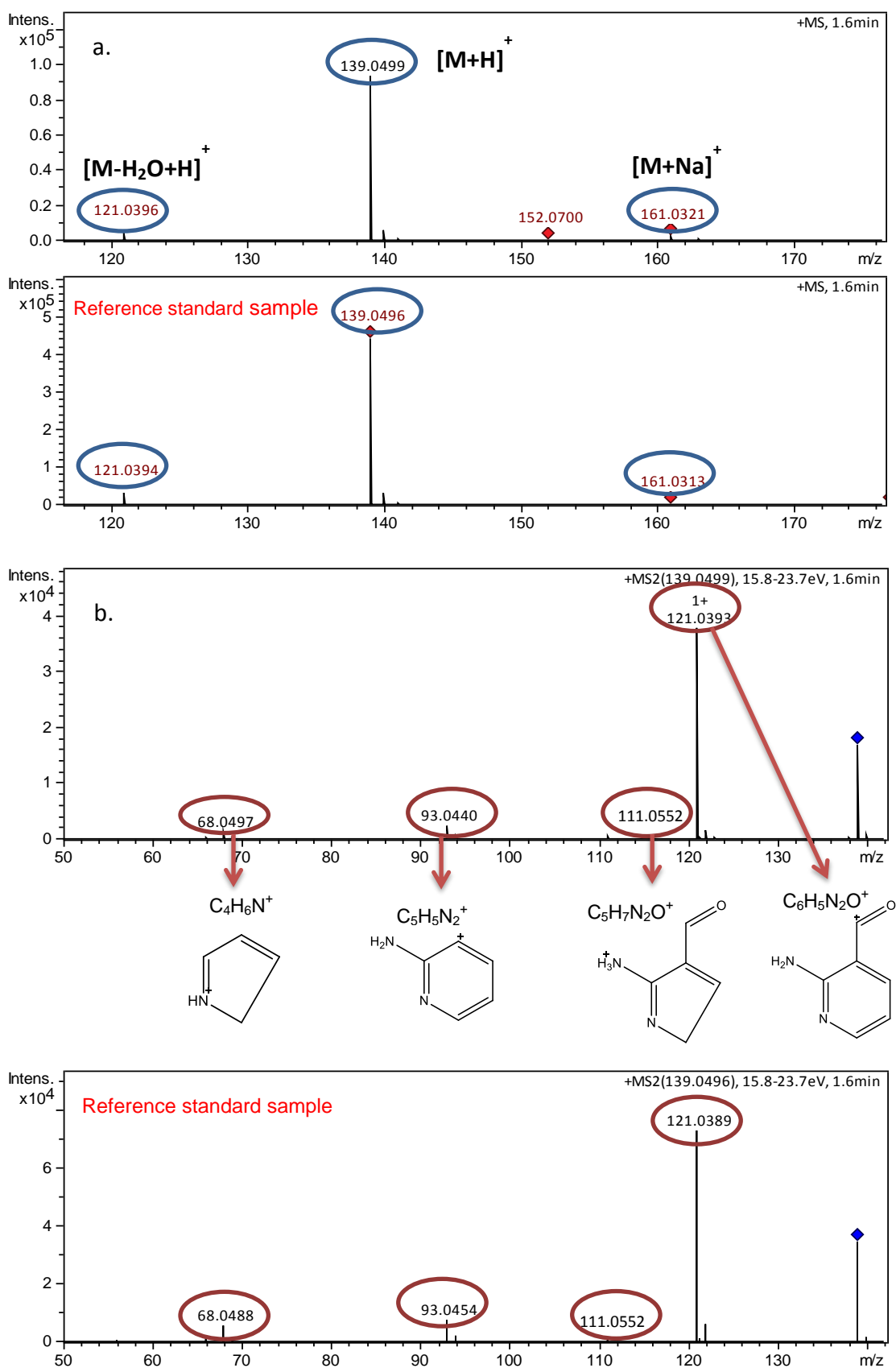


**Fig.39:** Analytical data for NA-138 in RP(+); (a) MS spectra of NA-138 and its reference standard, (b) MS/MS spectra showing the fragmentation and proposed fragments of NA-138 and its reference standard.

This compound is produced by the breakdown of the initial structure of NA during the ozone attack on the amino group as it is proposed from two recent studies [71, 81] and presents an increasing trend of production when the initial ozone concentration increases, as shown in Fig. 40.

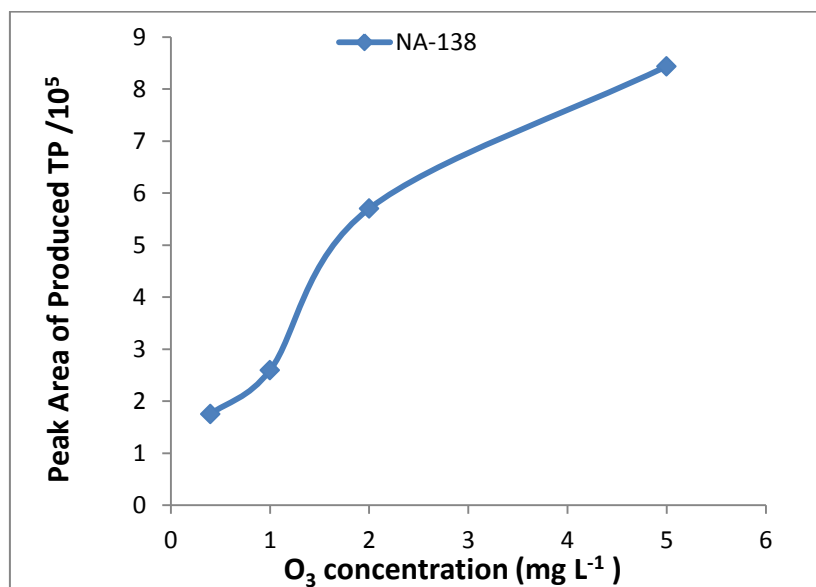


**Fig.40:** NA-138 production trend in correlation with O<sub>3</sub> initial concentration.

In RP(-), the MS spectrum (Fig. 41b) exposes the pseudo-molecular ion [M-H]<sup>-</sup> (C<sub>6</sub>H<sub>5</sub>N<sub>2</sub>O<sub>2</sub><sup>-</sup>) at m/z 137.0355 with excellent mass accuracy and great isotopic fitting (mass error 0.7 ppm and 11.7 mSigma) and its in-source fragment ion produced by the cleavage of CO<sub>2</sub>, [M- CO<sub>2</sub>.H]<sup>-</sup> (C<sub>5</sub>H<sub>5</sub>N<sub>2</sub><sup>-</sup>) at m/z 93.0458.

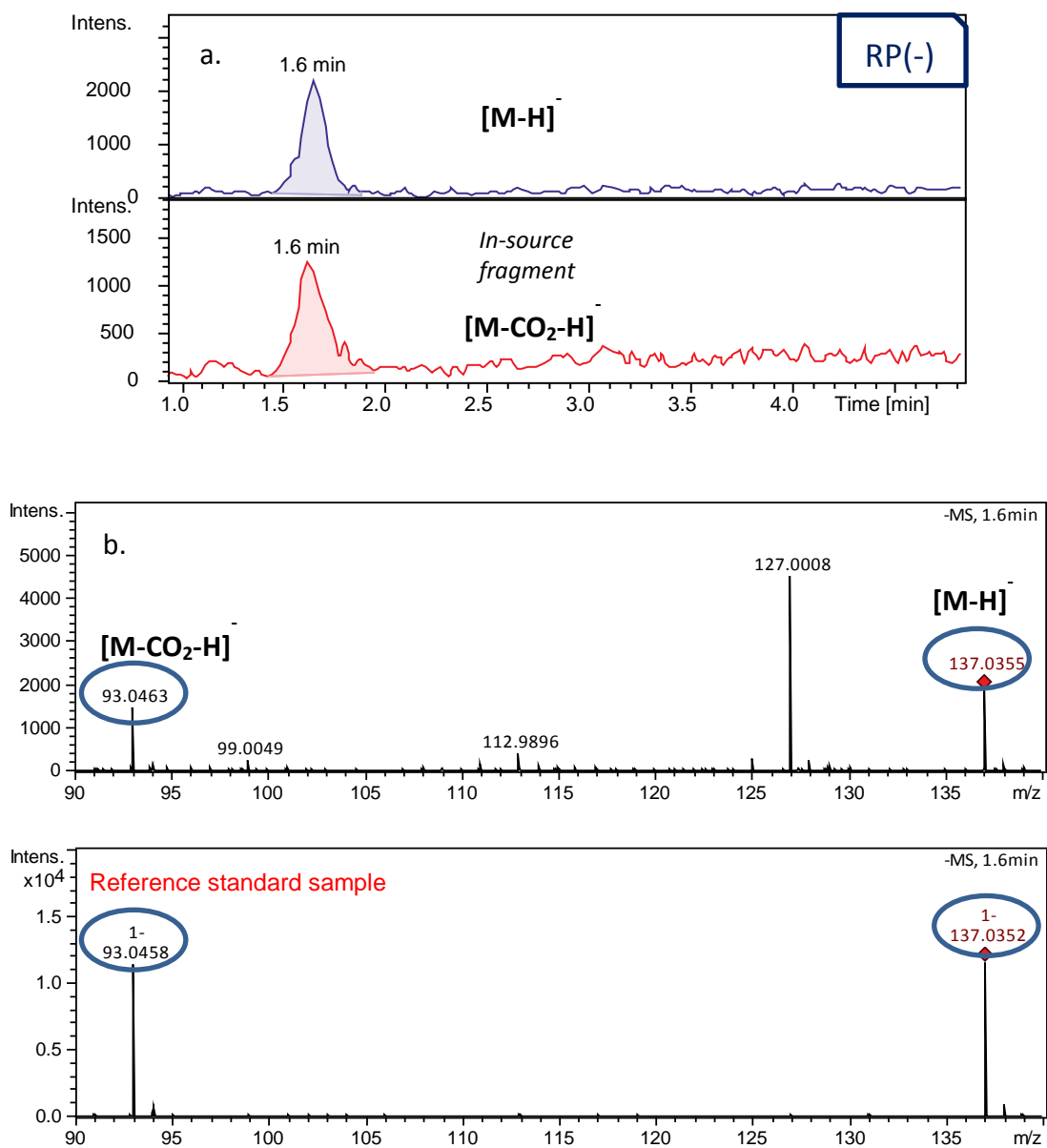


**Fig.41:** Analytical data for NA-138 in RP(-); (a) EICs for NA-138 and its in-source fragment, (b) MS spectra of NA-138 and its reference standard.

**Table 13:** Elemental composition of TPs, their adduct and/or in-source fragments and fragment ions along with the measured m/z, the theoretical m/z and the mass error in ppm in RP(+), detected with suspect screening.

Compound	Ion formula	Theoretical m/z	Measured m/z	Mass error (ppm)
<b>NA-298a</b>	$C_{13}H_{10}F_3N_2O_3^+$	299.0638	299.0645	-2.5
Fragments	$C_{13}H_8F_3N_2O_2^+$	281.0532	281.0541	-3.1
	$C_{13}H_7F_2N_2O_2^+$	261.0470	261.0474	-1.7
	$C_{12}H_7F_2N_2O^+$	233.0521	233.0528	-2.9
	$C_{11}H_5F_3N^+$	208.0369	208.0361	3.8
	$C_{11}H_7F_2N_2^+$	205.0572	205.0578	-2.9
	$C_{11}H_7NO_2^+$	185.0471	185.0471	0.3
	$C_{10}H_5FN^+$	158.0401	158.0384	10.4
	$C_4H_8FN^+$	89.0635	89.0627	9.7
<b>NA-298b</b>	$C_{13}H_{10}F_3N_2O_3^+$	299.0638	299.0648	-3.5
Fragments	$C_{13}H_9F_2N_2O_3^+$	279.0576	279.0564	4.4
	$C_{13}H_7F_2N_2O_2^+$	261.0470	261.0468	1
	$C_{12}H_7F_2N_2O^+$	233.0521	233.0529	3.5
	$C_{11}H_7F_2N_2^+$	205.0572	205.0558	6.7
	$C_{11}H_8NO_2^+$	186.0550	186.0552	-1.4
<b>NA-298c</b>	$C_{13}H_{10}F_3N_2O_3^+$	299.0638	299.0650	-3.9
Fragments	$C_{13}H_7F_2N_2O_2^+$	261.0470	261.0471	-0.3

Compound	Ion formula	Theoretical m/z	Measured m/z	Mass error (ppm)
<b>NA-262</b>	$C_{10}H_{10}F_3N_2O_3^+$	263.0638	263.0631	-2.6
Adduct	$C_{10}H_9F_3KN_2O_3^+$	301.0197	301.0188	3.1
<b>Fragments</b>	$C_8H_7F_3N^+$	174.0525	174.0525	0.3
	$C_7H_4F_3^+$	145.0260	145.0246	9.5
	$C_7H_5F_2^+$	127.0354	127.0342	9.1
	$CH_2NO^+$	44.0131	44.0131	-0.2
<b>NA-138</b>	$C_6H_7N_2O_2^+$	139.0502	139.0499	-2.4
Adduct	$C_6H_6N_2NaO_2^+$	161.0321	161.0321	0.2
In-source fragment	$C_6H_5N_2O^+$	121.0396	121.0396	-0.3
<b>Fragments</b>	$C_6H_5N_2O^+$	121.0396	121.0393	2.8
	$C_5H_7N_2O^+$	111.0552	111.0552	0.4
	$C_5H_5N_2^+$	93.0447	93.0440	8.3
	$C_4H_6N^+$	68.0495	68.0497	-3.4

**Table 14:** Elemental composition of TPs, their in-source fragments and fragment ions along with the measured m/z, the theoretical m/z and the mass error in ppm in RP(-), detected with suspect screening.

Compound	Ion formula	Theoretical m/z	Measured m/z	Mass error (ppm)
<b>NA-298,</b> <b>t<sub>R</sub>=5.2 min</b>	C <sub>13</sub> H <sub>8</sub> F <sub>3</sub> N <sub>2</sub> O <sub>3</sub> <sup>-</sup>	297.0493	297.0482	3.6
<b>NA-298,</b> <b>t<sub>R</sub>=5.7 min</b>	C <sub>13</sub> H <sub>8</sub> F <sub>3</sub> N <sub>2</sub> O <sub>3</sub> <sup>-</sup>	297.0493	297.0508	-5.1
In-source fragment	C <sub>12</sub> H <sub>8</sub> F <sub>3</sub> N <sub>2</sub> O <sup>-</sup>	253.0594	253.0581	5.1
<b>NA-298,</b> <b>t<sub>R</sub>=7.3 min</b>	C <sub>13</sub> H <sub>8</sub> F <sub>3</sub> N <sub>2</sub> O <sub>3</sub> <sup>-</sup>	297.0493	297.0492	0.2
In-source fragment	C <sub>12</sub> H <sub>8</sub> F <sub>3</sub> N <sub>2</sub> O <sup>-</sup>	253.0594	253.0589	-2.0
<b>NA-262</b>	C <sub>10</sub> H <sub>8</sub> F <sub>3</sub> N <sub>2</sub> O <sub>3</sub> <sup>-</sup>	261.0493	261.0495	-1.1
Fragment	C <sub>9</sub> H <sub>9</sub> F <sub>2</sub> N <sub>2</sub> O <sub>3</sub> <sup>-</sup>	231.0587	231.0621	-14.7
<b>NA-161</b>	C <sub>7</sub> H <sub>5</sub> F <sub>3</sub> N <sup>-</sup>	160.0380	160.0376	-2.0
Fragments	C <sub>6</sub> H <sub>4</sub> F <sub>3</sub> <sup>-</sup>	133.0271	133.0270	0.4
	C <sub>7</sub> H <sub>3</sub> FN <sup>-</sup>	120.0255	120.0271	-13.3
<b>NA-138</b>	C <sub>6</sub> H <sub>5</sub> N <sub>2</sub> O <sub>2</sub> <sup>-</sup>	137.0357	137.0355	0.7
In-source fragment	C <sub>5</sub> H <sub>5</sub> N <sub>2</sub> <sup>-</sup>	93.0458	93.0463	-5.1

### 6.3.3 Identification of TPs found by non-target screening

Eleven TPs of NA were detected through the application of non-target screening, four of which were ionized in both PI and NI mode, while three only in PI and the rest of them only in NI.

#### 6.3.3.1 NA-272

At  $t_R$  3.5 min in RP(+) and at 3.1 min in RP(-), NA-272 is eluted which corresponds to the elemental formula  $C_{13}H_8N_2O_5$ . This compound lacks three fluoride atoms and has three additional oxygen atoms in comparison to NA. As the aromatic ring of the left part of parent compound remains intact during ozonation, two oxygen atoms are supposed to be added in the pyridine-like moiety due to the ozone attack in the double C=C bond and the other one is assumed to replace the fluorides. Furthermore, the ring double bond equivalent (RDBE) of the pseudo-molecular ion of NA-272 ( $m/z$  273.0501), which indicates the degree of unsaturation of a structure, is equal to 11.5, implying the formation of an aldehyde or ketone.

In RP(+), the pseudo-molecular ion  $[M+H]^+$  is detected at  $m/z$  273.0501 ( $C_{13}H_9N_2O_5^+$ ) in the MS spectrum (Fig. 43b) with excellent isotopic fitting (mSigma 1.8), while its adduct ion  $[M+K]^+$  is revealed at  $m/z$  311.0057 ( $C_{13}H_8KN_2O_5^+$ ). Furthermore, the proposed structure, shown in Fig. 42, is supported by the MS/MS spectrum (Fig. 44) which shows characteristic neutral losses of a  $H_2O$  molecule and a CO group which can be attributed to  $m/z$  255.0395 ( $C_{13}H_7N_2O_4^+$ ) and to  $m/z$  245.0557 ( $C_{12}H_9N_2O_4^+$ ), respectively. Fragment ion at  $m/z$  227.0442 ( $C_{12}H_7N_2O_3^+$ ) denotes the simultaneous split of an oxygen atom and a  $CH_2O$  molecule, while the further loss of one oxygen atom produces the fragment ion  $m/z$  211.0504 ( $C_{12}H_7N_2O_2^+$ ). The subsequent cleavage of two  $CH_2O$  molecules from the fragment 245 forms the ion at  $m/z$  185.0327 ( $C_{10}H_5N_2O_2^+$ ). One more fragment is detected at  $m/z$  237.0284 ( $C_{13}H_5N_2O_3^+$ ).

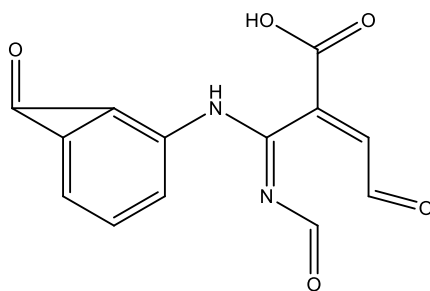


**Fig.42:** Proposed structure for NA-272.

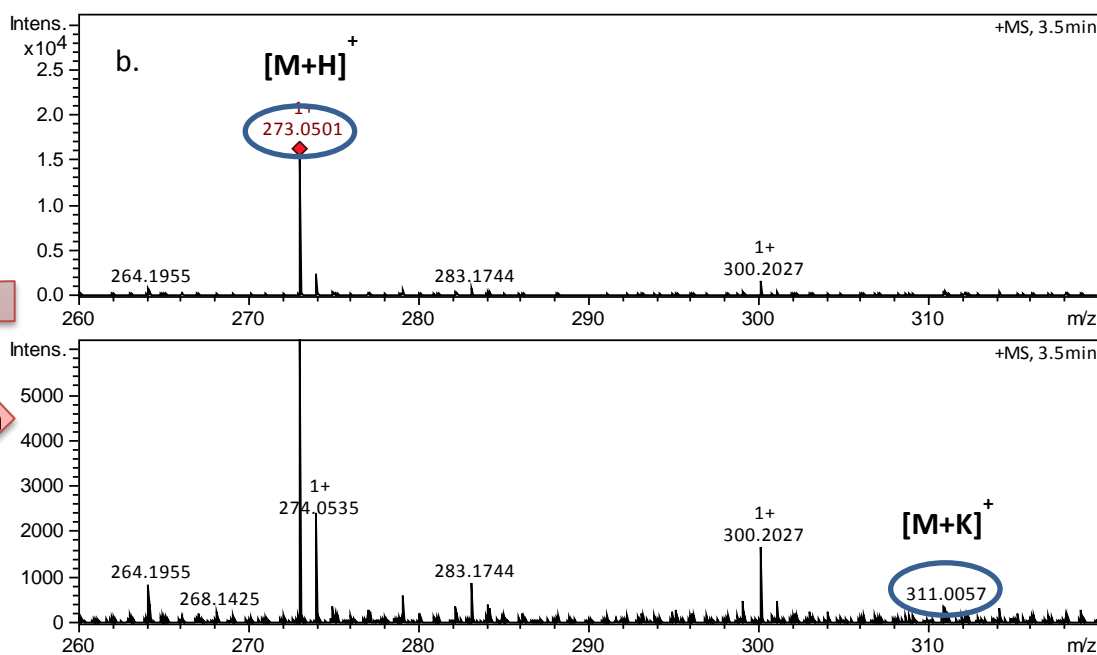
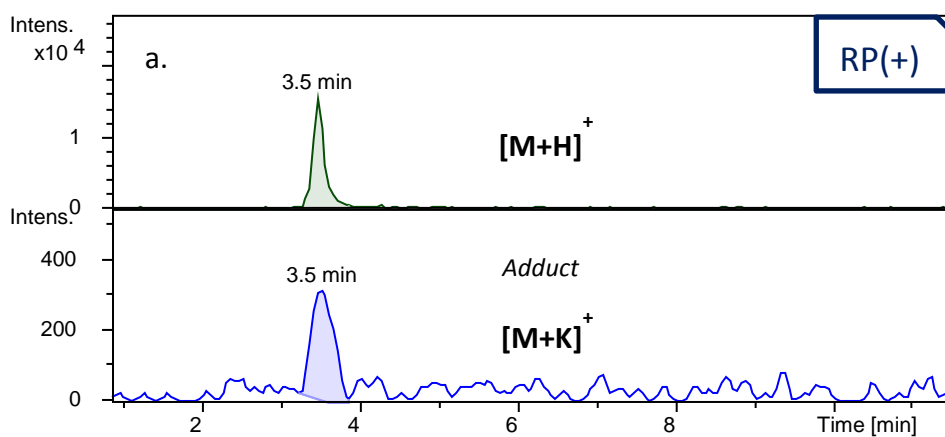


**Fig.43:** Analytical data for NA-272 in RP(+); (a) EICs for NA-272 and its adduct, (b) MS spectrum.

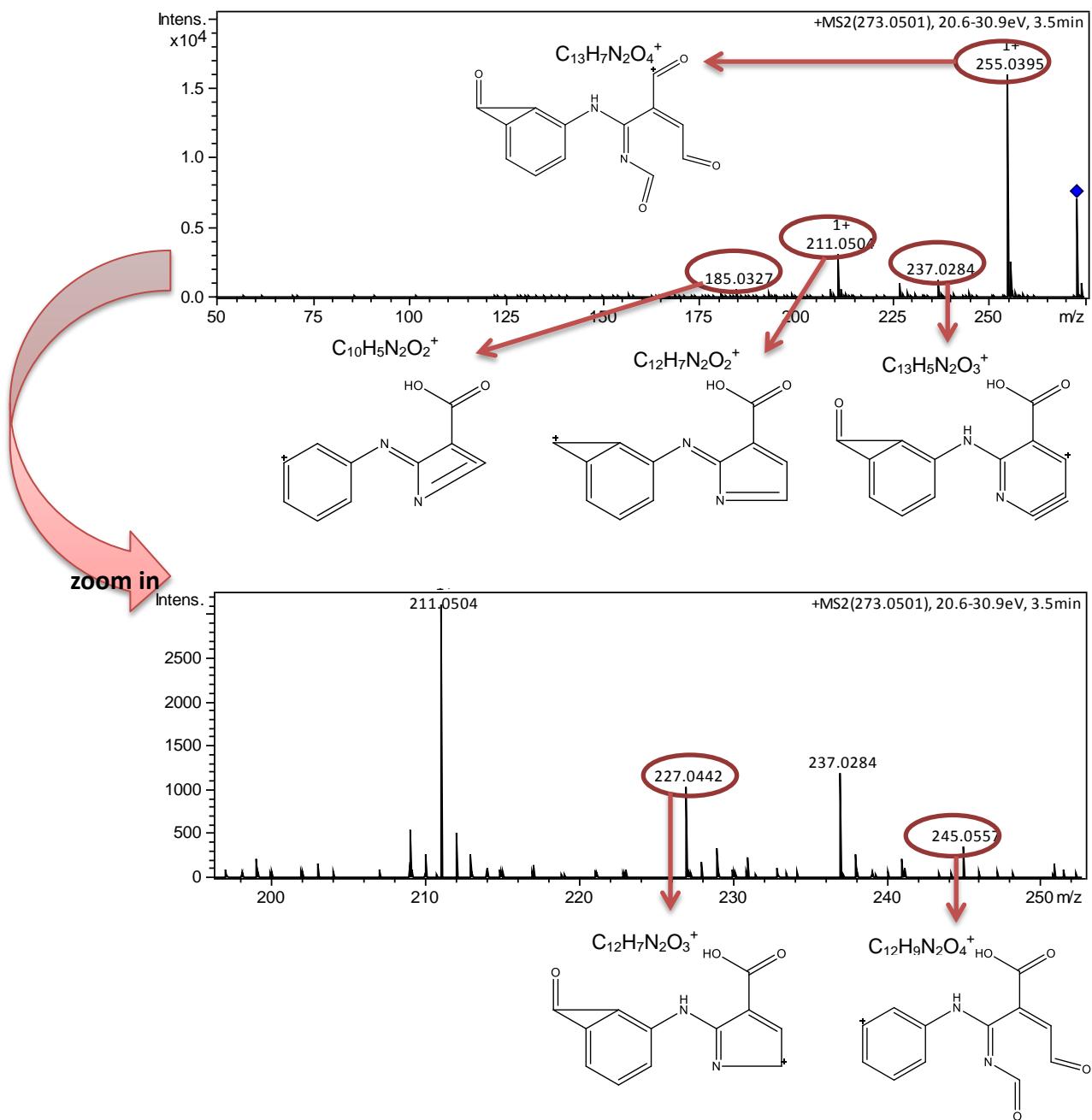


**Fig.44:** Analytical data for NA-272 in RP(+); MS/MS spectrum showing the fragmentation and proposed fragments of NA-272.

In RP(-), the MS spectrum (Fig. 45b) displays the ion  $[M-H]^-$ ,  $C_{13}H_7N_2O_5^-$ , in good fit with theoretical mass (mass error of 1.4 ppm). The fragmentation pattern (Fig 45c) exhibits the concurrent split of a  $CO_2$  group, a CO group and an oxygen atom with the presence of the ion at  $m/z$  183.0553 ( $C_{11}H_7N_2O^-$ ). The subsequent abstraction of a CO group forms the fragment  $m/z$  155.0599 ( $C_{10}H_7N_2^-$ ).

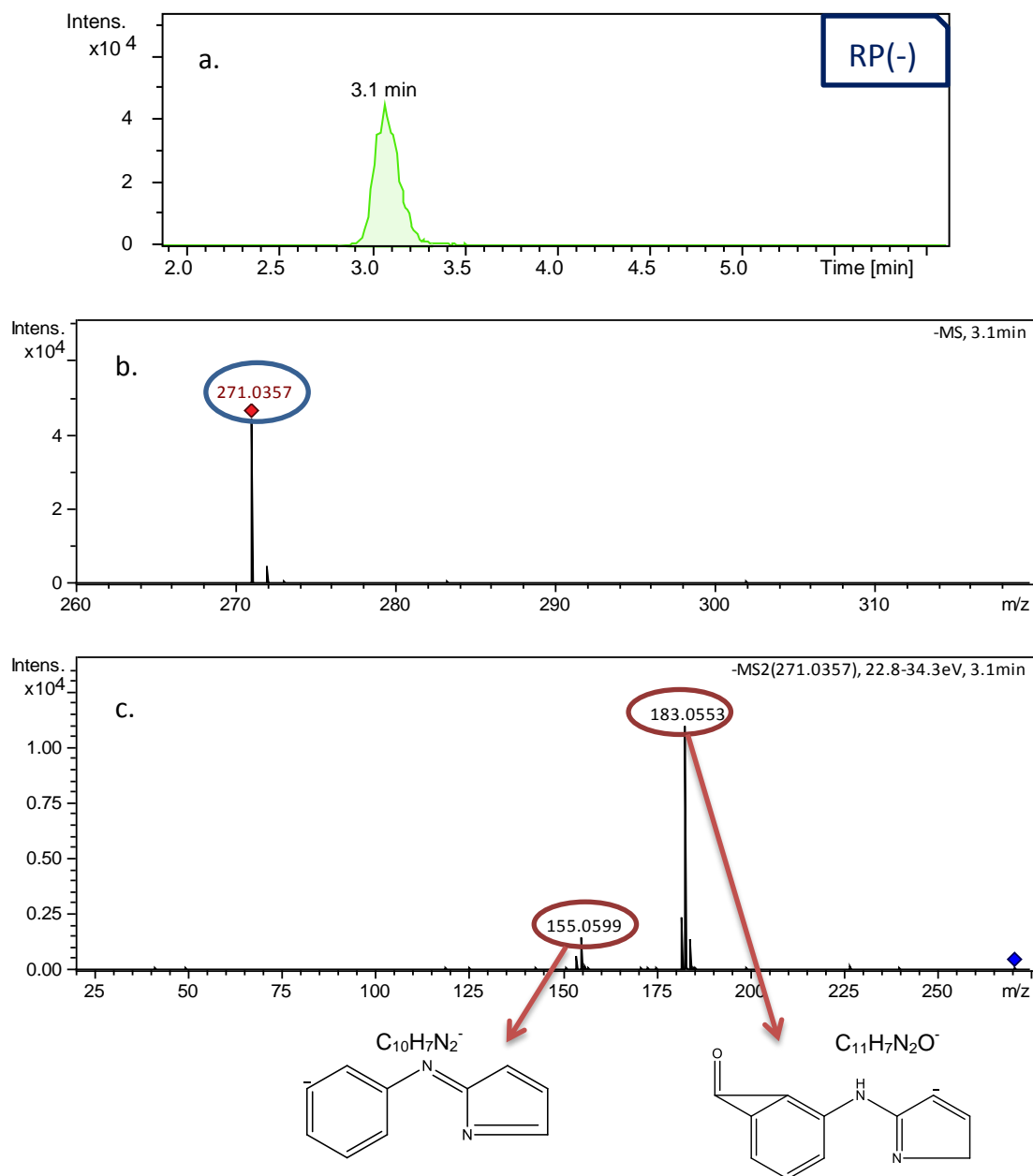


**Fig.45:** Analytical data for NA-272 in RP(-); (a) EIC of NA-272, (b) MS and (c) MS/MS spectrum showing the fragmentation and proposed fragments of NA-272.

### 6.3.3.2 NA-286

NA-286 is detected at  $t_R$  4.3 min in RP(+) and at 6.7 min in RP(-) and matches to the elemental formula  $C_{12}H_9F_3N_2O_3$ . Compared with NA, this TP lacks one carbon atom which is removed during the cleavage of a double bond in the right aromatic ring of the molecule and has one oxygen atom more, which can be attributed to the presence of a hydroxyl group. The proposed structure is presented in Fig.46.

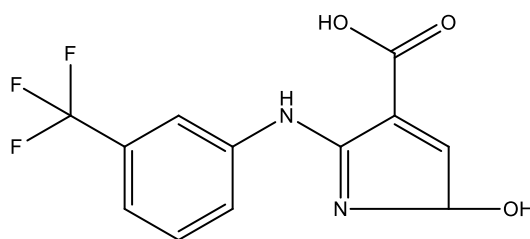


**Fig.46:** Proposed structure for NA-286.

In RP(+), the pseudo-molecular ion of NA-286,  $C_{12}H_{10}F_3N_2O_3^+$  is detected as  $m/z$  287.0638 (mSigma 12). The MS/MS fragmentation spectrum depicts the initial loss of a  $CH_3OH$  group verifying that a hydroxylation took place, resulting in the formation of  $m/z$  255.0385 ( $C_{11}H_6F_3N_2O_2^+$ ) which is the most abundant fragment. In addition, a further split of  $CO_2$  group from 255 corresponds to ion  $m/z$  211.0478 ( $C_{10}H_6F_3N_2^+$ ) and one more fragment appears at  $m/z$  186.0549 ( $C_{11}H_8NO_2^+$ ).

In addition, the in-house QSRR prediction model was used. The predicted  $t_R$  for the hydroxylated structure is 5.4 min ( $\Delta t_R = 1.1$  min) and as a result NA-286 identification confidence reaches level 2b (probable structure).

The MS spectrum in RP(-) demonstrates the molecular ion  $[M-H]^-$  ( $C_{12}H_8F_3N_2O_3^-$ ) at  $m/z$  285.0493 with low mass error (2.4 ppm). MS/MS spectrum has low intensity and as a result does not provide further information for the structure elucidation.

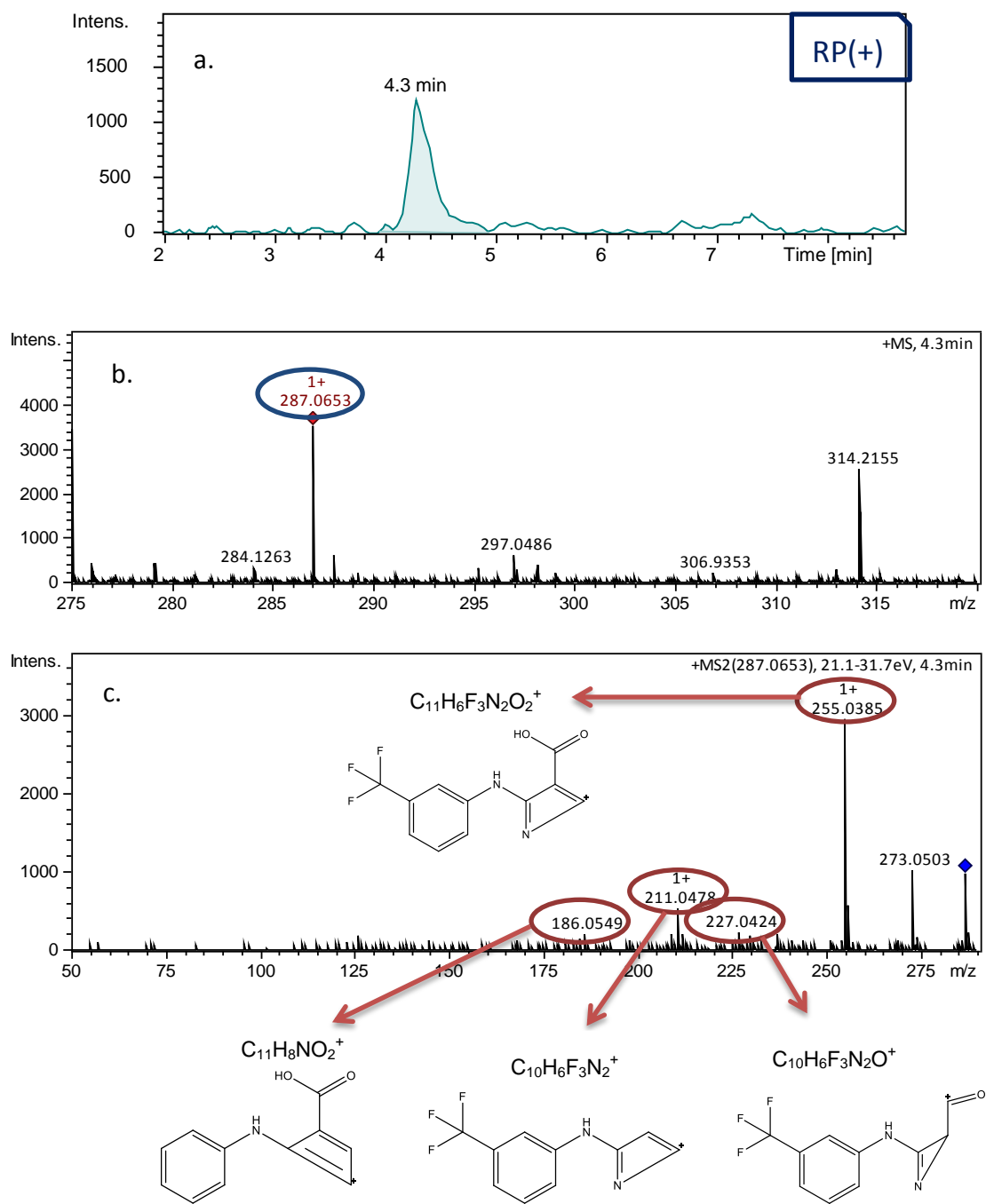


**Fig.47:** Analytical data for NA-286 in RP(+); (a) EIC of NA-286, (b) MS and (c) MS/MS spectrum showing the fragmentation and proposed fragments of NA-286.

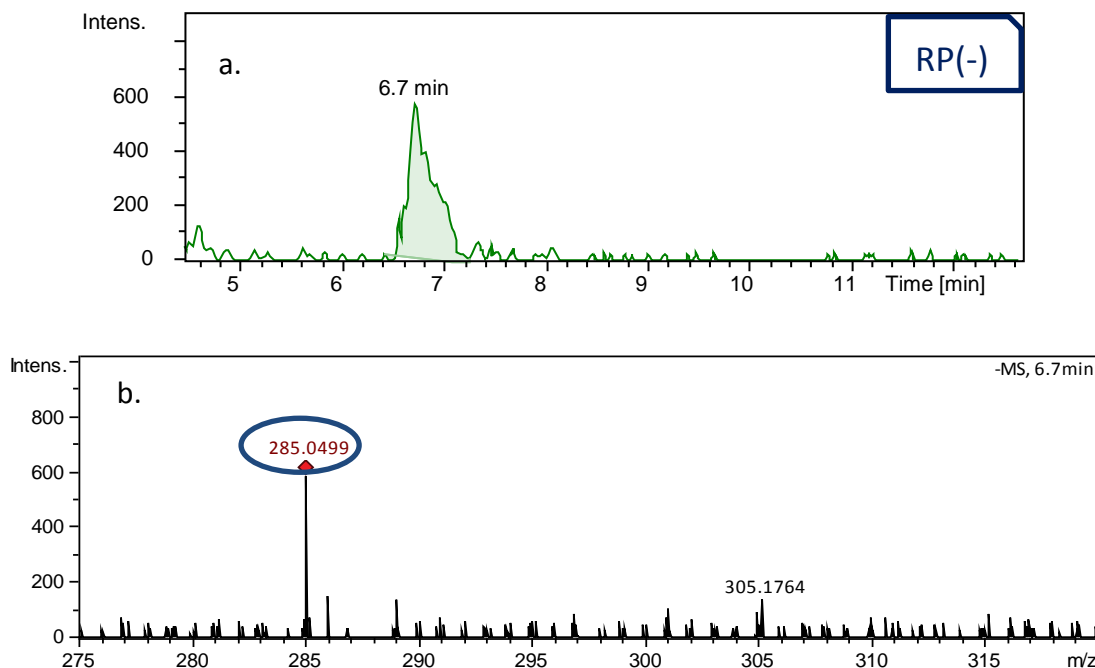


**Fig.48:** Analytical data for NA-286 in RP(-); (a) EIC of NA-286, (b) MS spectrum

### 6.3.3.3 NA-242

NA-242a and NA 242b are detected in the RPLC analysis at  $t_R$  4.4 and 6.8 min in PI mode and at  $t_R$  6.0 and 6.9 min respectively, in NI mode. The elemental formula which fits to both of them is  $C_{11}H_9F_3N_2O$ . The proposed structures relate to the abstraction of the  $CO_2$  group, the loss of a carbon atom and the insertion of an oxygen atom in the heterocyclic ring of NA molecule. The addition of the O atom is supposed to occur after the  $C=C$  bond cleavage of the heterocyclic ring. Based on the experimental data, the oxidation of the first TP can be attributed to the formation of a hydroxyl group and for the second to a N-oxidation of the pyridine-like moiety of NA. Despite the common elemental composition, these isomeric structures provide totally different  $t_R$  and MS/MS spectra.

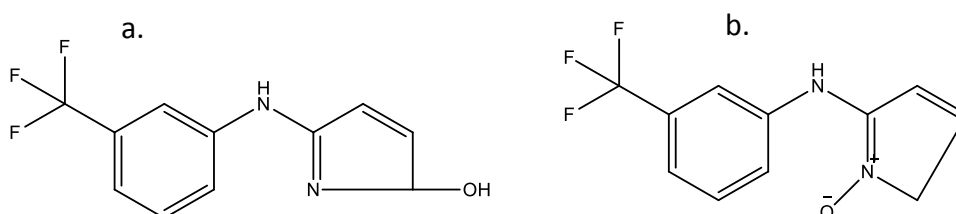


**Fig.49:** Proposed structures for NA-242.

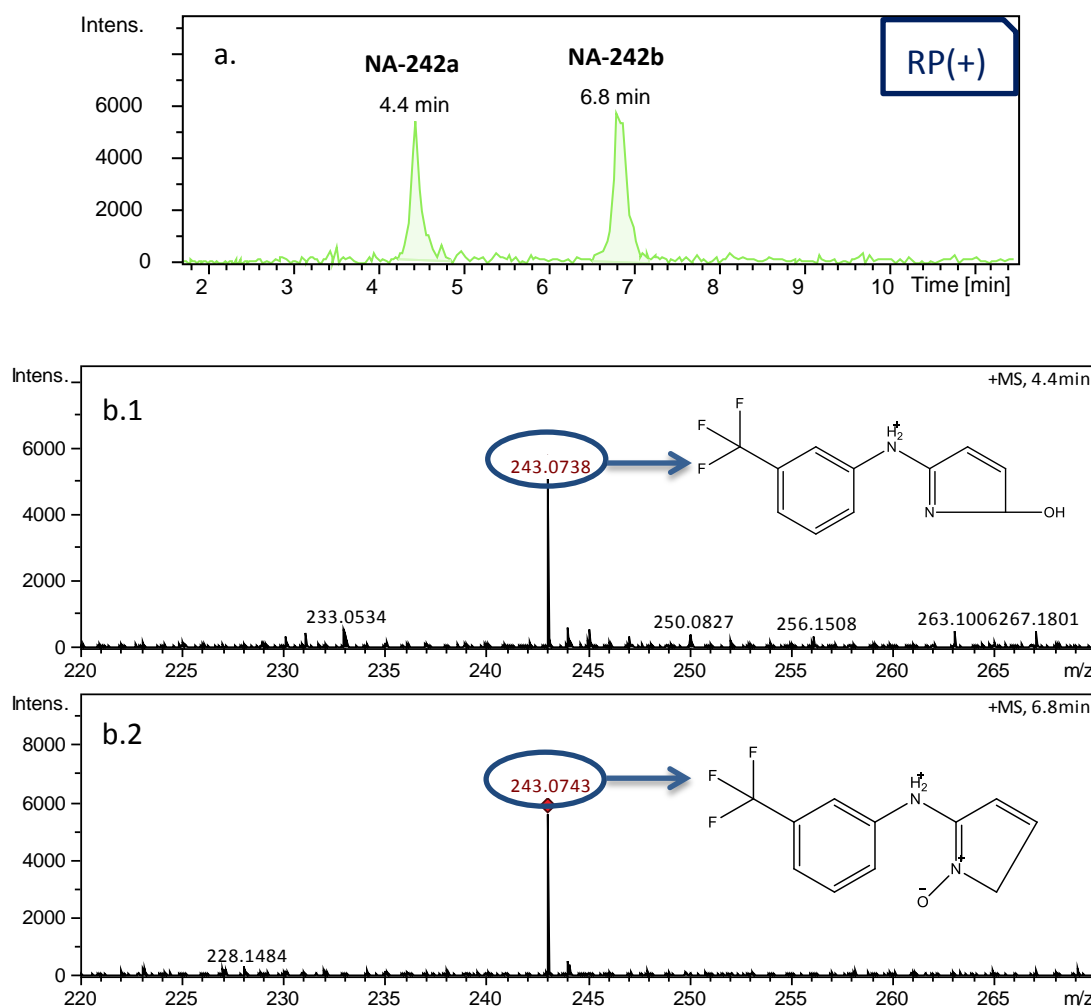


**Fig.50:** Analytical data for NA-242a, b in RP(+); (a) EIC of NA-242a, (b) MS spectra of: (1) NA-242a and (2) NA-242b.

To be more specific, in the case of NA-242a in RP(+), the MS spectrum (Fig. 50b.1) shows the pseudo-molecular ion  $[M+H]^+$  ( $C_{11}H_{10}F_3N_2O^+$ ) at m/z 243.0738 with great mass accuracy and isotopic fitting (mass error of -0.9 ppm, 9.2 mSigma). The MS/MS spectrum presents the initial loss of a HF molecule resulting in the formation of the fragment m/z 223.0674 ( $C_{11}H_9F_2N_2O^+$ ) and the concomitant cleavage of a  $H_2O$  and a  $HCN$  produced the ion at m/z 198.0521 ( $C_{10}H_7F_3N^+$ ). A characteristic fragment appears at m/z 45.0331 ( $C_2H_5O^+$ ) which supports the evidence of hydroxylation in the heterocyclic ring. Two more fragments, m/z 215.0797 ( $C_{10}H_{10}F_3N_2^+$ ) and m/z 173.1093 ( $C_{11}H_{13}N_2^+$ ), are depicted in this spectrum. As a result, a probable structure can be attributed to NA-242a (Fig. 50) and its identification confidence is of the level 2b.

NA-242b pseudo-molecular ion,  $C_{11}H_{10}F_3N_2O^+$ , is figured in the MS spectrum (Fig. 50b.2) of RP(+) at  $m/z$  243.0743 with low mass error and very good isotopic fitting (-1.5 ppm, 17.9 mSigma). The fragmentation pattern demonstrates an initial split of  $CH_3NO$  unit, resulting in the formation of  $m/z$  198.0513 ( $C_{10}H_7F_3N^+$ ) which supports that N-oxidation occurred in the pyridine-like moiety of NA. The fragments with  $m/z$  174.0522 ( $C_8H_7F_3N^+$ ) and  $m/z$  145.0248 ( $C_7H_4F_3^+$ ) verify that the fluoride-containing part of the molecule remained intact during ozonation. The N-oxide characteristic fragment is presented at  $m/z$  44.0129 ( $CH_2NO^+$ ). Therefore, identification confidence of NA-242b reaches the level 2b.

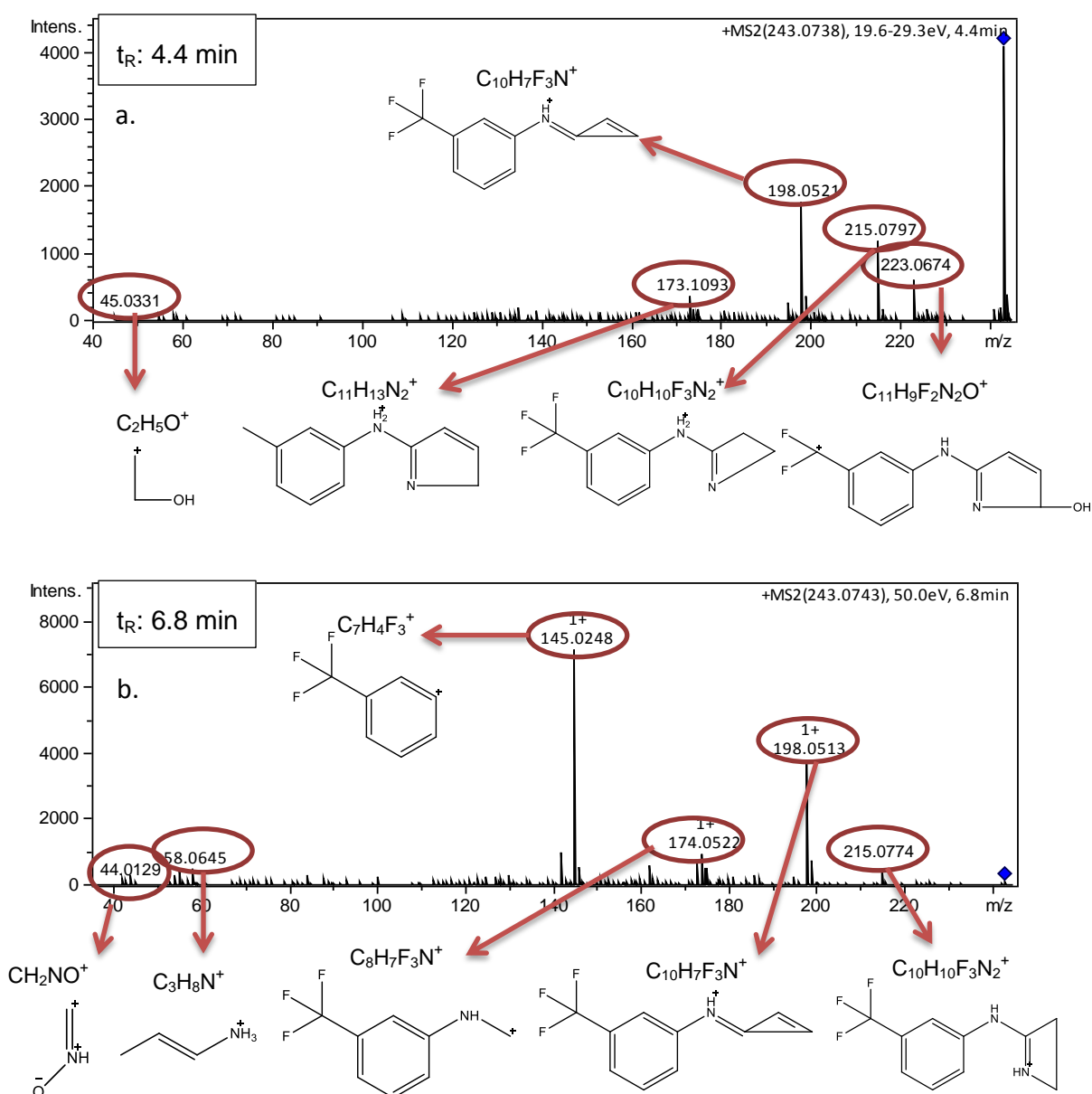


**Fig.51:** Analytical data for NA-242a, b in RP(+); MS/MS spectra showing the fragmentation and proposed fragments of (a) NA-242a and (b) NA-242b.

In RP(-), the MS spectra indicate the pseudo-molecular ion at  $m/z$  241.0591 for the TP eluted at 6.0 min and at  $m/z$  241.0587 for the TP eluted at 6.9 min. Both  $m/z$  adequately fit to the ion formula of  $C_{11}H_8F_3N_2O^-$ . The MS/MS spectrum for the first TP could not be acquired due to low intensity in the MS spectra. The fragmentation pattern (Fig. 52c) of the second eluted one, presents one fragment appeared at  $m/z$  145.0281 ( $C_7H_4F_3^-$ ) and the characteristic fragment of NA at  $m/z$  160.0367 ( $C_7H_5F_3N^-$ ).

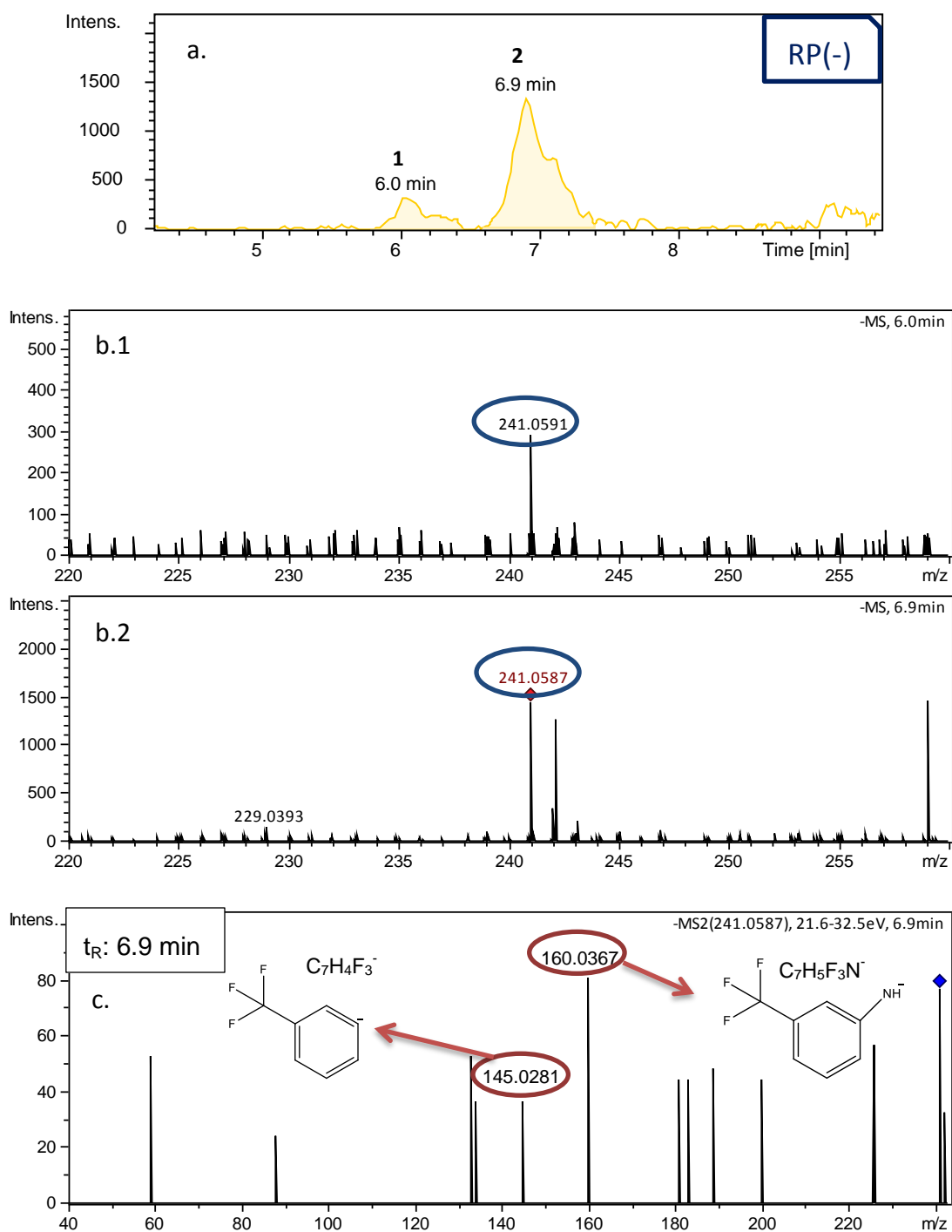


**Fig.52:** Analytical data for NA-242 in RP(-); (a) EIC of NA-242, (b) MS spectra and (c) MS/MS spectrum of NA-242 eluted at  $t_R$  6.9 min.

### 6.3.3.4 NA-243

NA-243 corresponds to two TPs eluted at  $t_R$  4.3 and 4.9 min in RP(-). The elemental formula ascribed to both of them is  $C_{11}H_8F_3NO_2$ . The proposed structures conform to the concurrent abstraction of  $CO_2$  group and HCN molecule from NA. Then, the subsequent formation of an aldehyde and either the N-oxidation of the aniline-like moiety or alternatively the formation of a C=O bond (ketone) is proposed for NA-243a. On the contrary, the formation of a carboxyl group is suggested for NA-243b.

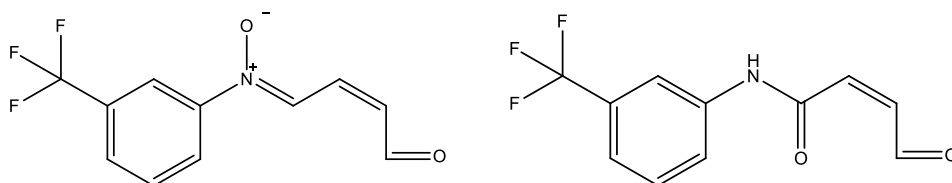


**Fig.53:** Proposed structures for NA-243a

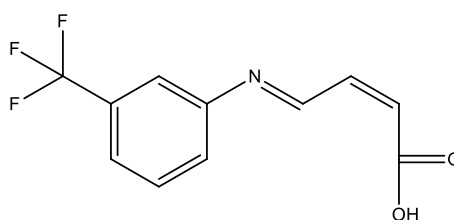


**Fig.54:** Proposed structure for NA-243b

The MS spectrum of the TP eluted at 4.3 min (Fig. 55b.1), NA-243a, points the pseudo-molecular ion  $[M-H]^-$  at  $m/z$  242.0431 ( $C_{11}H_7F_3NO_2^-$ ) which is in good fit with its theoretical mass (mass error of 1.5 ppm, 40.4 mSigma). Its fragmentation (Fig. 56a) depicts one neutral loss of a CO group, so  $m/z$  214.0495 ( $C_{10}H_7F_3NO^-$ ) was formed, indicating the presence of the aldehyde. Afterwards, a subsequent breakaway of an HF molecule produces the fragment at  $m/z$  194.0409 ( $C_{10}H_6F_2NO^-$ ). These data are not sufficient in order to reveal a unique structure for NA-243a and as a result its identification reaches the 3<sup>rd</sup> level.

The MS spectrum of NA-243b (Fig. 55b.2) shows its pseudo-molecular ion at  $m/z$  242.0435 ( $C_{11}H_7F_3NO_2^-$ ) with excellent mass accuracy and isotopic fitting (mass error of -0.5 ppm, 11.1 mSigma). The MS/MS spectrum (Fig. 56b) figures the characteristic fragment of NA at  $m/z$  160.0362 ( $C_7H_5F_3N^-$ ) and the

ion at  $m/z$  59.0147 ( $C_2H_3O_2^-$ ) which implies the presence of carboxyl group. Another one fragment is presented at  $m/z$  204.0301 ( $C_8H_5F_3NO_2^-$ ) produced by the loss of  $C_3H_2$  group. Thus, the identification confidence of this compound reaches the level 2b.

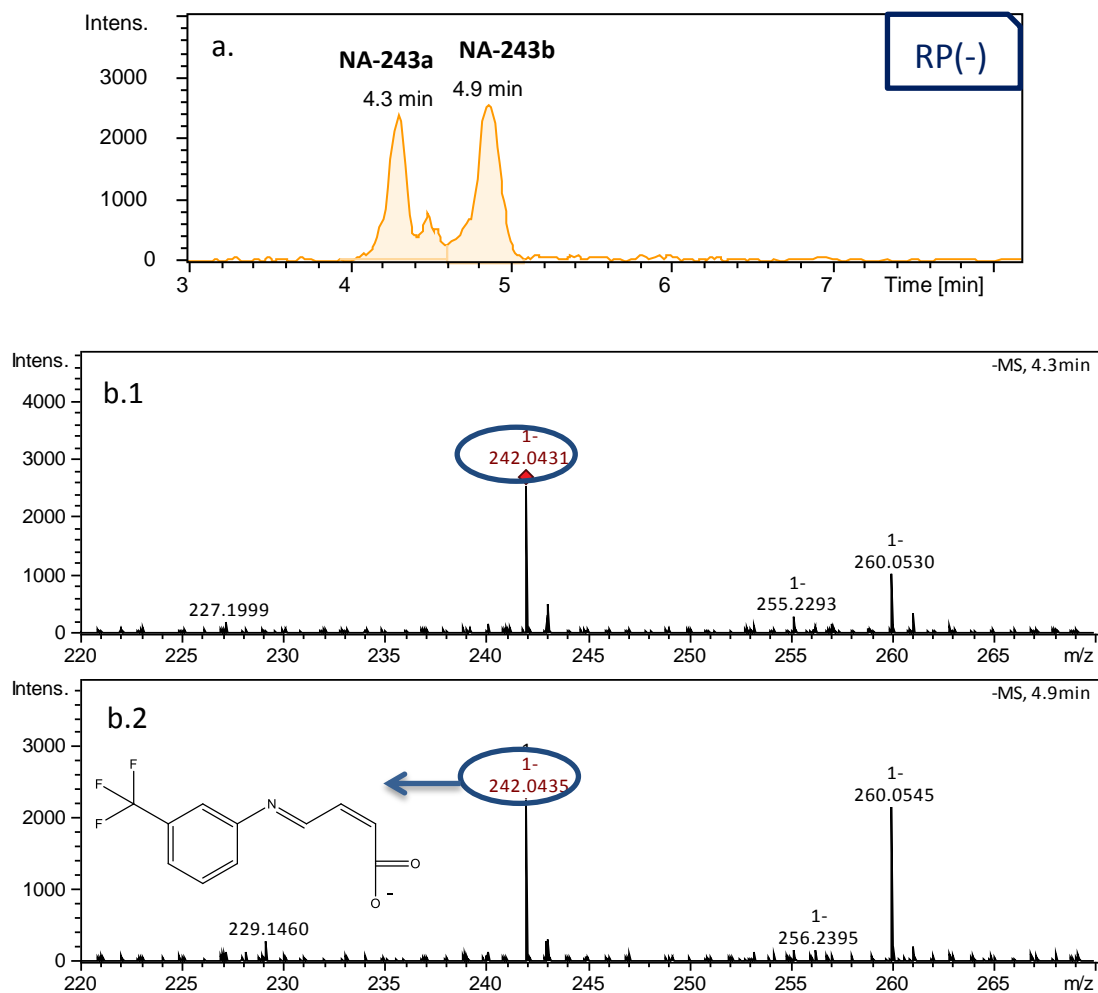


**Fig.55:** Analytical data for NA-243a, b in RP(-); (a) EIC of NA-243 and (b) MS spectra of: (1) NA-243a, (2) NA-243b.

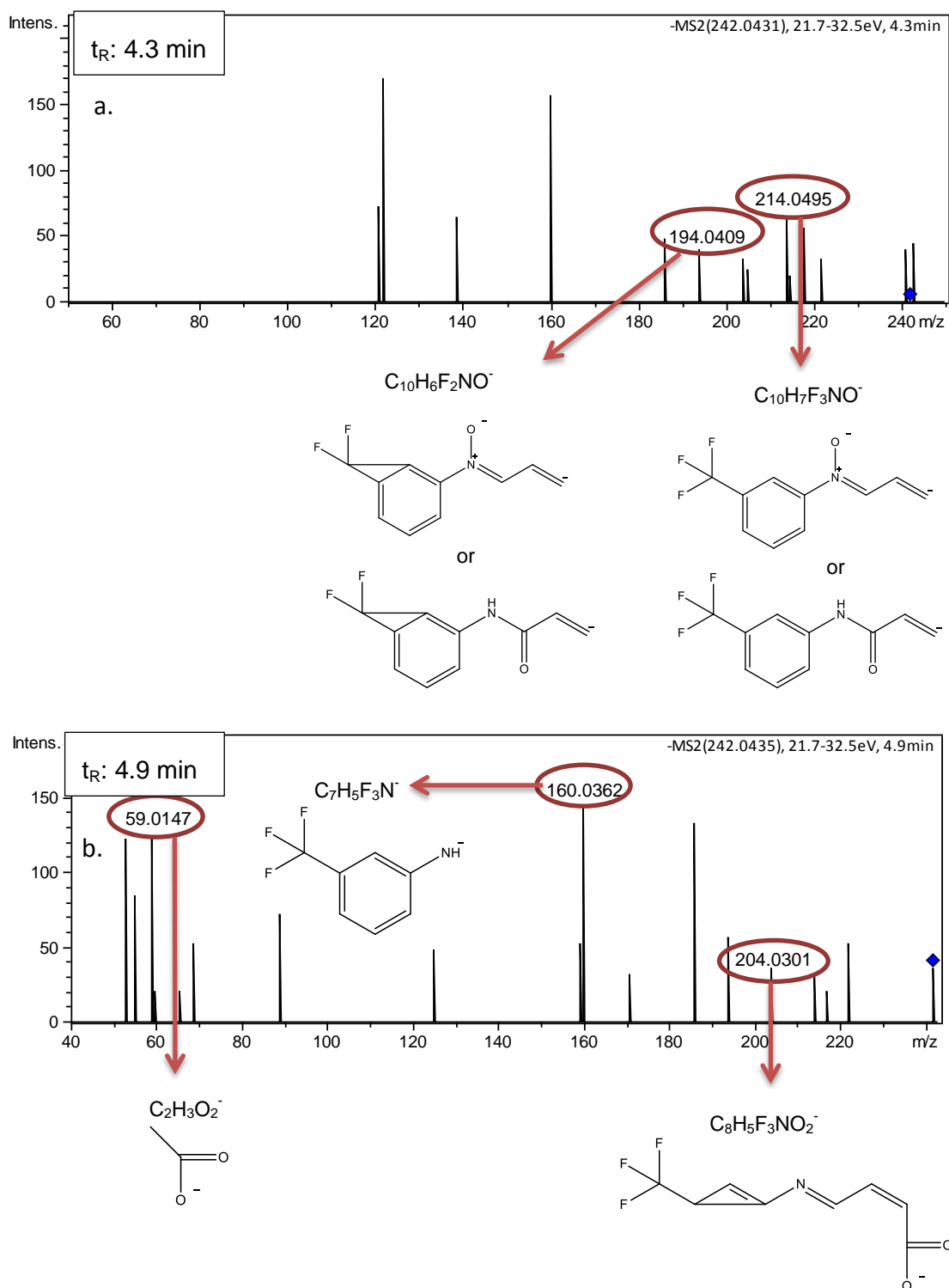


**Fig.56:** Analytical data for NA-243a, b in RP(-); MS/MS spectra showing the fragmentation and proposed fragments of (a) NA-243a and (b) NA-243b.

### 6.3.3.5 NA-232

At  $t_R$  8.2 min, the compound NA-232 is eluted in RP(-), which fits to the elemental formula  $C_9H_7F_3N_2O_2$ . The proposed structure suggests the abstraction of the  $CO_2$  group, the ozone attack on the  $C=C$  double bonds of the heterocyclic ring, through Criegee mechanism, and finally the formation of a hydroxylamine by N-oxidation.

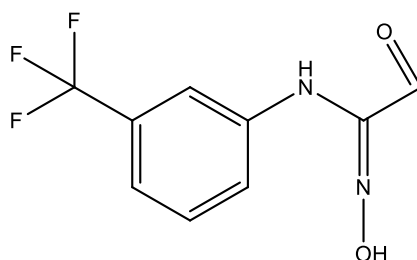


**Fig.57:** Proposed structure for NA-232.

This structure is supported clearly by the MS spectra (Fig. 58b) in which the pseudo-molecular ion is shown at  $m/z$  231.0385 ( $C_9H_6F_3N_2O_2^-$ ) in excellent fit with the theoretical mass (mass error of -0.7 ppm, 9.6 mSigma). Moreover, two in-source fragments can be observed. The first one at  $m/z$  203.0434 ( $C_8H_6F_3N_2O^-$ ) indicates the loss of a CO group which implies the presence of aldehyde group in the precursor ion, while the second one at  $m/z$  160.0372 ( $C_7H_5F_3N^-$ ) is produced by the cleavage of  $C_2HNO_2$  group verifying the presence of an hydroxylamine formed by oxidation of the nitrogen atom of the pyridine-like moiety of NA.

The MS/MS spectra (Fig. 58c) also depicts the ion formed by the critical loss of  $C_2HNO_2$  at  $m/z$  160.0376 ( $C_7H_5F_3N^-$ ) and the characteristic fragment of N-oxidation at  $m/z$  44.0141 ( $CH_2NO^-$ ). Furthermore, one more fragment ion is appeared at  $m/z$  121.0265 ( $C_5H_4F_3^-$ ).

According to the above mentioned data, the identification of NA-232 reaches the level 2b (probable structure).

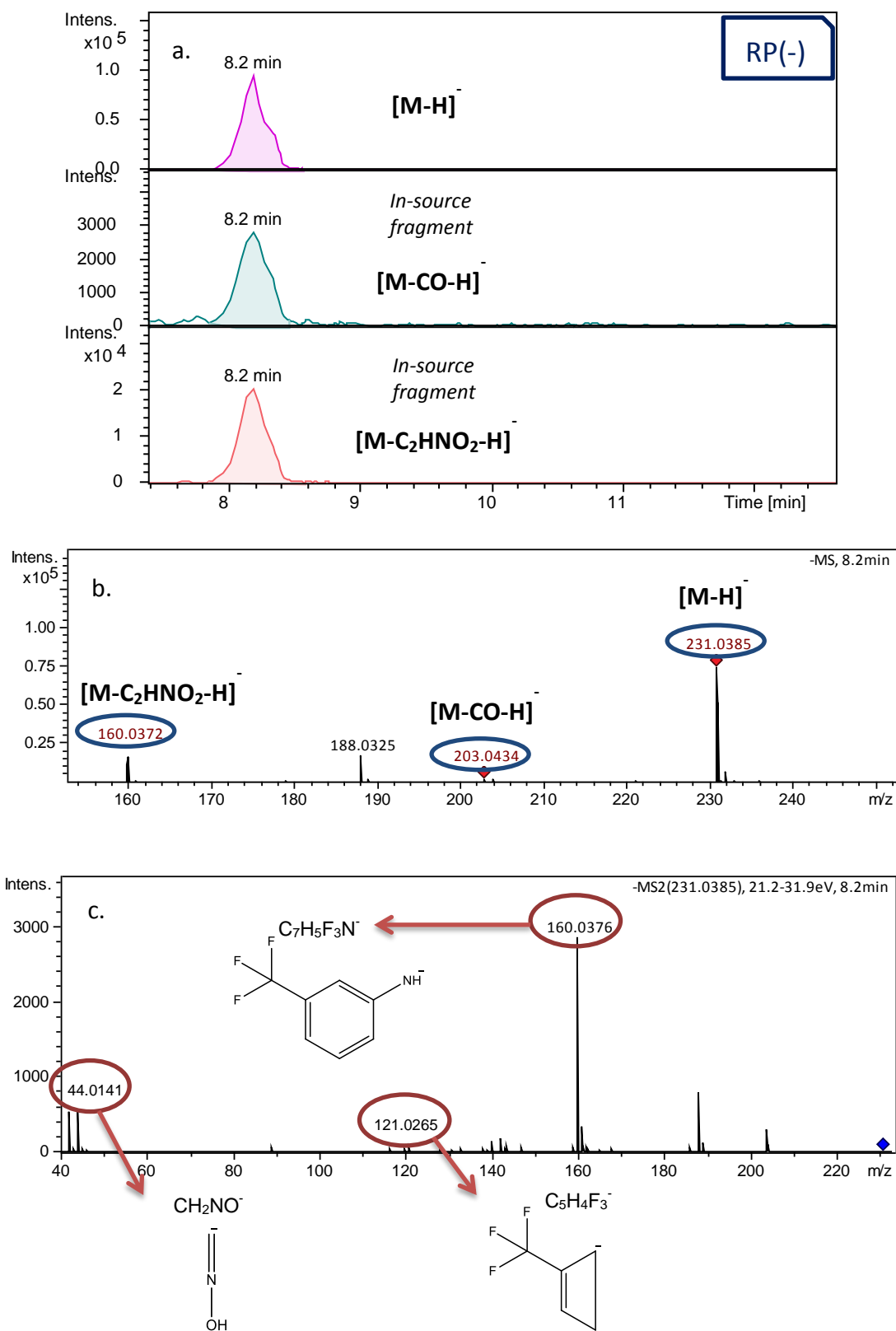


**Fig.58:** Analytical data for NA-232 in RP(-); (a) EICs of NA-232 and its in-source fragments, (b) MS and (c) MS/MS spectrum showing the fragmentation and proposed fragments of NA-232.

### 6.3.3.6 NA-228

This TP is detected at  $t_R$  3.0 min in RP(-) and can be attributed to the molecular formula  $C_9H_9FN_2O_4$ . The structure (Fig. 59) fitted in this compound presents the split of  $CO_2$  group and the loss of 3 carbon atoms due to the ring opening by the ozone attack on  $C=C$  double bonds in the active part of NA and simultaneously the loss of two fluoride atoms from its molecule. Then, the formation of a carboxyl group and two hydroxylamine groups in the remaining part of the molecule take place by oxidation.

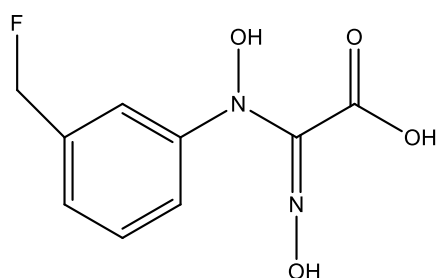


**Fig.59:** Proposed structure of NA-228.

The pseudo-molecular ion of this TP  $[M-H]^-$  is depicted in the MS spectrum (Fig. 60b) at  $m/z$  227.0472 ( $C_9H_8FN_2O_4^-$ ) and has excellent fit with the corresponding theoretical mass (mass error of -0.8 ppm, 29.3 mSigma). Moreover, an in-source fragment ion  $[M-CO_2-H]^-$  is observed at  $m/z$  183.0569 ( $C_8H_8FN_2O_2^-$ ). The proposed structure is supported by the MS/MS spectrum (Fig. 60c) in which the loss of  $CO_2$  is also detected at  $m/z$  183.0557 ( $C_8H_8FN_2O_2^-$ ) and the N-oxidation is justified by the aforementioned ion and the charged radical with  $m/z$  155.0593 ( $C_7H_9FNO_3^{\cdot-}$ ). Moreover, the presence of carboxyl group is insinuated by the fragment  $m/z$  59.0132 ( $C_2H_3O_2^-$ ). Therefore, the identification of this compound reaches the level 2b of confidence.

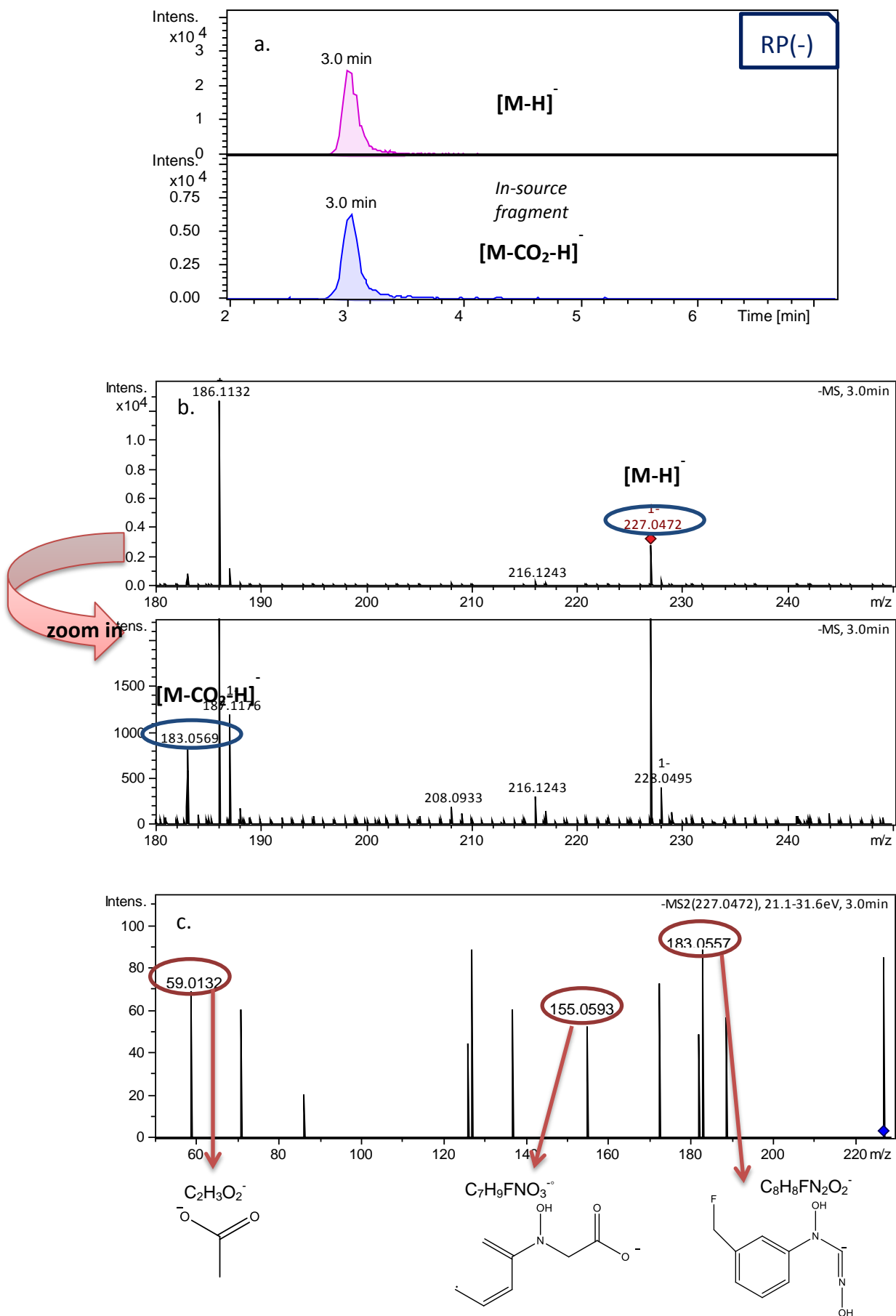


**Fig.60:** Analytical data for NA-228 in RP(-); (a) EIC of NA-228 and its in-source fragment, (b) MS and (c) MS/MS spectrum showing the fragmentation and proposed fragments of NA-228.

### 6.3.3.7 NA-204

NA-204a, b and c are three isomeric TPs detected at  $t_R$  2.9, 5.2 and 7.1 min, respectively, in RP(+). The elemental formula which is ascribed to all of them is  $C_8H_7F_3N_2O$  and their proposed structures arise from the concurrent abstraction of a  $CO_2$  group and a  $C_4H_2$  unit from the reactive part of NA molecule and the subsequent formation of a hydroxylamine or an aldehyde.

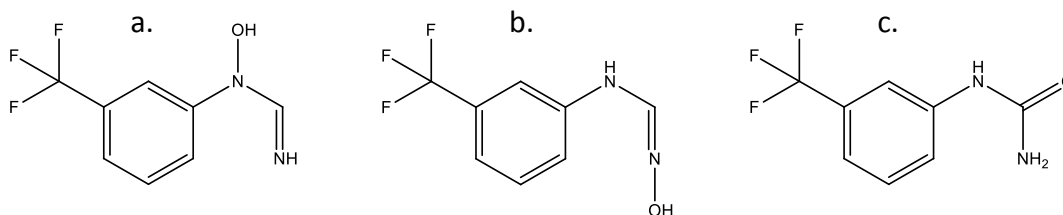


**Fig.61:** Proposed structures for NA-204a, NA-204b, NA-204c

In the case of NA-204a, the MS spectrum (Fig. 62b.1) shows the pseudo-molecular ion  $[M+H]^+$  at  $m/z$  205.0593 ( $C_8H_8F_3N_2O^+$ ) with excellent isotopic fitting (3.6 mSigma). Its MS/MS fragmentation (Fig. 63a) reveals firstly an initial loss of a  $H_2O$  molecule forming the fragment  $m/z$  187.0488 ( $C_8H_6F_3N_2^+$ ). The ion at  $m/z$  160.0560 ( $C_7H_8F_2NO^+$ ) is produced by the concomitant split of a fluoride atom and a CN group. This fragments is characteristic for this TP as it indicates the formation of the hydroxylamine in the N atom of aniline-like moiety. In addition the loss of the three fluoride atoms and the OH group forms the fragment ion at  $m/z$  131.0608 ( $C_8H_7N_2^+$ ).

The MS spectrum of NA-204b (Fig. 62b.2) depicts its ion  $[M+H]^+$ ,  $C_8H_8F_3N_2O^+$ , at  $m/z$  205.0592 (mass error of -4.4 ppm and good isotopic fitting 20.2 mSigma). Though MS/MS data could not be acquired, the fact that NA-204b is not detected in the ozonated samples from the experiments conducted at pH 4.0, evokes that the oxidation occurred in the nitrogen atom of the pyridine-like moiety of NA.

NA-204c pseudo-molecular ion  $[M+H]^+$ ,  $C_8H_8F_3N_2O^+$ , is detected at  $m/z$  205.0576 in the MS spectrum (Fig.62b.3). Its isotopic fitting is 15.7 mSigma. The MS/MS spectrum (Fig. 63b) indicates the concurrent cleavage of an HF and a  $NH_3$  molecule producing the fragment at  $m/z$  168.0268 ( $C_8H_4F_2NO^+$ ). Moreover, the characteristic fragment which reminds that the left part of NA

remains intact is detected as  $m/z$  162.0521 ( $C_7H_7F_3N^+$ ). A further cleavage of an HF molecule from 162 forms the ion at  $m/z$  142.0443 ( $C_7H_6F_2N^+$ ).

The identification of the compounds NA-204a and NA-204c reaches the level 2b of confidence.

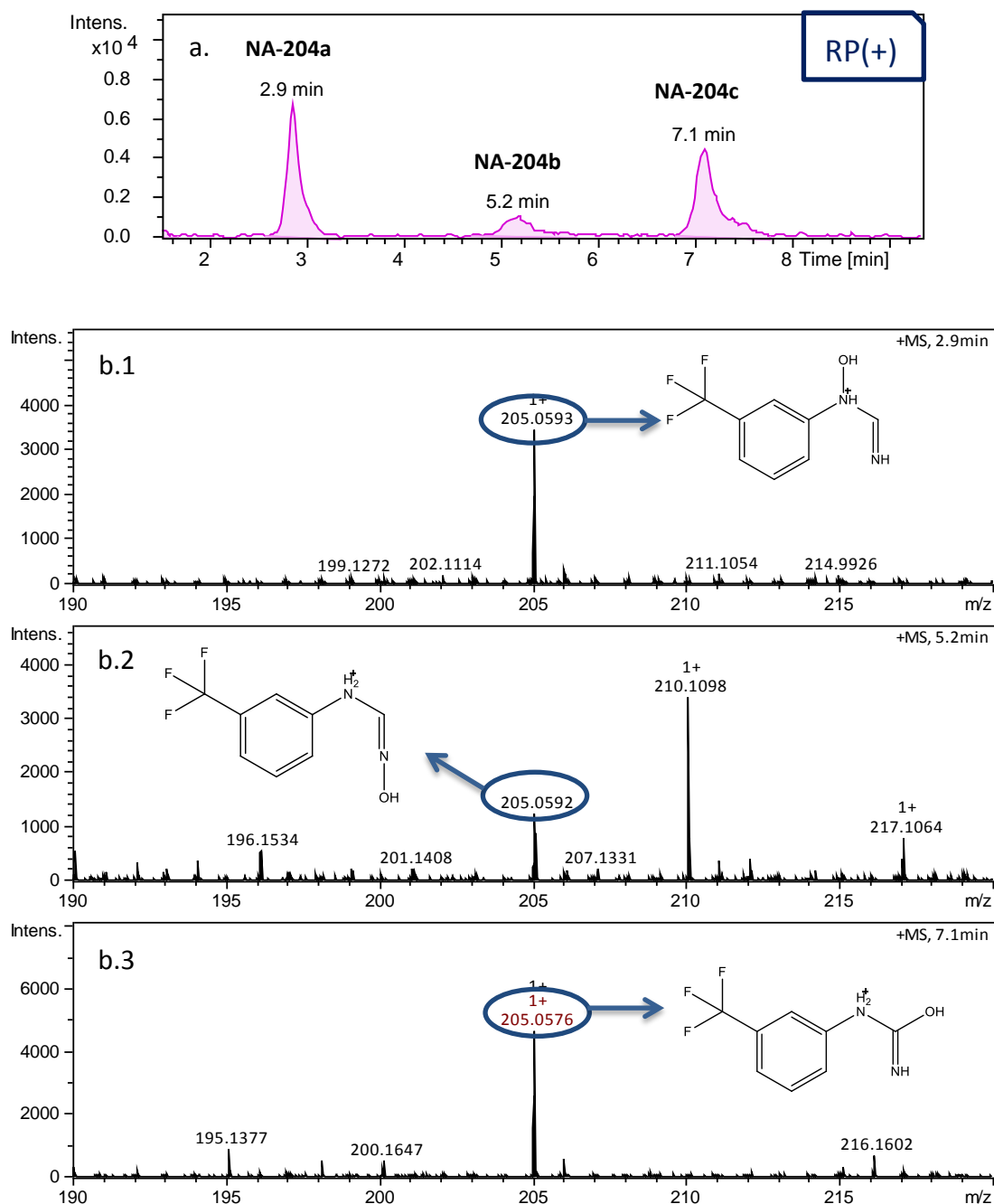


**Fig.62:** Analytical data for NA-204a, b and c in RP(+); (a) EIC of NA-204, (b) MS spectra of: (1) NA-204a, (2) NA-204b and (3) NA-204c.

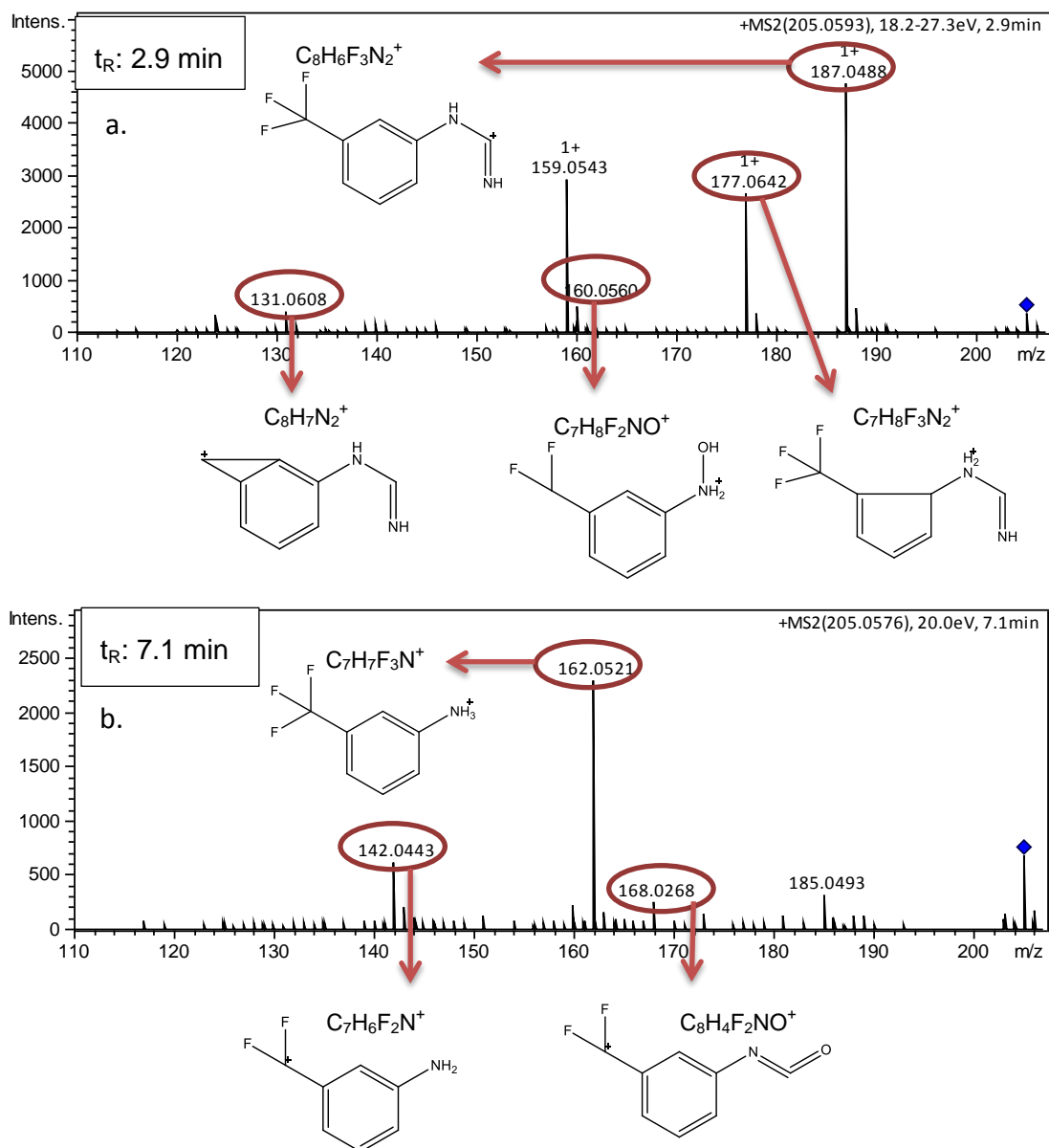


**Fig.63:** Analytical data for NA-204 in RP(+); MS/MS spectra showing the fragmentation and proposed fragments of (a) NA-204a and (b) NA-204c.

**Table 15:** Elemental composition of TPs, their adducts and fragment ions along with the measured m/z, the theoretical m/z and the mass error in ppm in RP(+), detected with non-target screening.

Compound	Ion formula	Theoretical m/z	Measured m/z	Mass error (ppm)	
<b>NA-272</b>	$C_{13}H_9N_2O_5^+$	273.0506	273.0501	1.8	
	Adduct	$C_{13}H_8KN_2O_5^+$	311.0065	311.0057	2.2
	Fragments	$C_{13}H_7N_2O_4^+$	255.0400	255.0395	2.3
		$C_{12}H_9N_2O_4^+$	245.0557	245.0557	-0.2
		$C_{13}H_5N_2O_3^+$	237.0295	237.0284	4.4
		$C_{12}H_7N_2O_3^+$	227.0451	227.0442	4.2
	$C_{12}H_7N_2O_2^+$	211.0502	211.0504	1.0	
	$C_{10}H_5N_2O_2^+$	185.0346	185.0327	10.2	
<b>NA-286</b>	Fragments	$C_{12}H_{10}F_3N_2O_3^+$	287.0638	287.0653	-5.1
		$C_{11}H_6F_3N_2O_2^+$	255.0376	255.0385	3.6
		$C_{10}H_6F_3N_2O^+$	227.0427	227.0424	-1.0
		$C_{10}H_6F_3N_2^+$	211.0478	211.0478	0.4
		$C_{11}H_8NO_2^+$	186.0550	186.0549	0.2
<b>NA-242a</b>	Fragments	$C_{11}H_{10}F_3N_2O^+$	243.0740	243.0738	-0.9
		$C_{11}H_9F_2N_2O^+$	223.0677	223.0674	1.7
		$C_{10}H_{10}F_3N_2^+$	215.0791	215.0797	-2.9
		$C_{10}H_7F_3N^+$	198.0525	198.0521	-2.1

Compound	Ion formula	Theoretical m/z	Measured m/z	Mass error (ppm)
	$C_{11}H_{13}N_2^+$	173.1073	173.1093	-11.5
	$C_2H_5O^+$	45.0335	45.0331	8.7
<b>NA-242b</b>	$C_{11}H_{10}F_3N_2O^+$	243.0740	243.0743	-1.5
Fragments	$C_{10}H_{10}F_3N_2^+$	215.0791	215.0774	7.9
	$C_{10}H_7F_3N^+$	198.0525	198.0513	-6.0
	$C_8H_7F_3N^+$	174.0525	174.0522	-1.9
	$C_7H_4F_3^+$	145.0260	145.0248	7.9
	$C_3H_8N^+$	58.0651	58.0645	10.5
	$CH_2NO^+$	44.0131	44.0129	4.3
<b>NA-204a</b>	$C_8H_8F_3N_2O^+$	205.0583	205.0593	4.4
Fragments	$C_8H_6F_3N_2^+$	187.0478	187.0488	5.5
	$C_7H_8F_2NO^+$	160.0568	160.0560	5.1
	$C_8H_7N_2^+$	131.0603	131.0608	-3.3
<b>NA-204b</b>	$C_8H_8F_3N_2O^+$	205.0583	205.0592	4.5
<b>NA-204c</b>	$C_8H_8F_3N_2O^+$	205.0583	205.0576	3.8
Fragments	$C_8H_4F_2NO^+$	168.0255	168.0268	-7.2
	$C_7H_7F_3N^+$	162.0525	162.0521	2.5
	$C_7H_6F_2N^+$	142.0463	142.0443	13.8

**Table 16:** Elemental composition of TPs, their in-source fragments and fragment ions along with the measured m/z, the theoretical m/z and the mass error in ppm in RP(-), detected with non-target screening.

Compound	Ion formula	Theoretical m/z	Measured m/z	Mass error (ppm)
<b>NA-272</b>	$C_{13}H_7N_2O_5^-$	271.0360	271.0357	1.4
Fragments	$C_{11}H_7N_2O^-$	183.0564	183.0553	-5.7
	$C_{10}H_7N_2^-$	155.0615	155.0599	9.8
<b>NA-286</b>	$C_{12}H_8F_3N_2O_3^-$	285.0493	285.0499	2.4
<b>NA-242, <math>t_R=6.0</math> min</b>	$C_{11}H_8F_3N_2O^-$	241.0594	241.0591	1.5
<b>NA-242, <math>t_R=6.9</math> min</b>	$C_{11}H_8F_3N_2O^-$	241.0594	241.0587	2.5
Fragments	$C_7H_5F_3N^-$	160.0380	160.0367	7.9
	$C_7H_4F_3^-$	145.0271	145.0281	-7.2
<b>NA-243a</b>	$C_{11}H_7F_3NO_2^-$	242.0434	242.0431	1.5
Fragments	$C_{10}H_7F_3NO^-$	214.0485	214.0495	-4.6
	$C_{10}H_6F_2NO^-$	194.0423	194.0409	7.2
<b>NA-243b</b>	$C_{11}H_7F_3NO_2^-$	242.0434	242.0435	-0.5
Fragments	$C_8H_5F_3NO_2^-$	204.0278	204.0301	-11.3
	$C_7H_5F_3N^-$	160.0380	160.0362	11
	$C_2H_3O_2^-$	59.0139	59.0147	-14.4
<b>NA-232</b>	$C_9H_6F_3N_2O_2^-$	231.0387	231.0385	-0.7
In- source fragments	$C_8H_6F_3N_2O^-$	203.0438	203.0434	1.8



## 6.4 Determination of 2-aminopyridine-3-carboxylic acid (NA-138) removal during ozonation

After the study of the removal and transformation of NA, the investigation of the fate of its most abundant TP during ozonation was followed. This process aimed at verifying the high reactivity of this part of the parent compound with ozone, since this TP was generated through the hydroxylation of the N atom connecting the two rings of the parent structure. Another critical point was to determine the ozone concentration which is required for the total removal of NA-138 by testing different initial concentrations in the experiments of pH 7.0 in the presence of scavenger. In preliminary experiments, the reaction of this TP with ozone is proven to be extremely fast, so only two samples have been withdrawn during the course of the ozonation experiments, in the 2<sup>nd</sup> and 10<sup>th</sup> min.

**Table 17:** NA-138 removal under various initial ozone concentrations in pH 7.0 in the presence of t-BuOH 50mM.

Time points (min)	% Removal			
	0.4 mg L <sup>-1</sup> O <sub>3</sub>	1.0 mg L <sup>-1</sup> O <sub>3</sub>	2.0 mg L <sup>-1</sup> O <sub>3</sub>	5.0 mg L <sup>-1</sup> O <sub>3</sub>
2	17.3	53.1	69.6	100.0
10	18.2	52.8	70.2	100.0

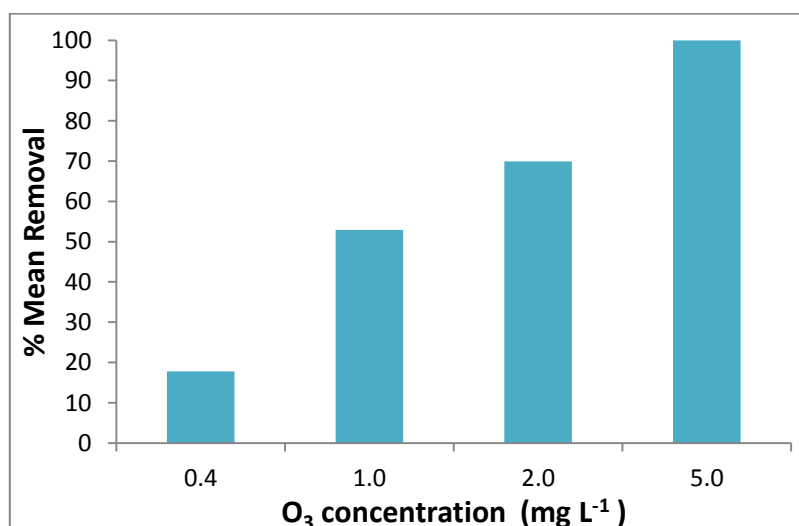


**Fig.65:** % NA-138 mean removal under various initial ozone concentrations in pH7.0 with scavenger ( $C_{o,NA-138} : 3.0 \text{ mg L}^{-1}$ ).

The removal of NA-138, shown in Figure 65, shows the same trend with NA. It is observed that the overall removal is directly correlated to the initial applied ozone concentration. More specifically, the application of  $2.0 \text{ mg L}^{-1} \text{ O}_3$  is adequate in order to eliminate 70% of the compound from the aqueous solution, while a concentration of  $5.0 \text{ mg L}^{-1}$  of  $\text{O}_3$  is capable of entirely eliminating NA-138 in the first minutes of the reaction.

- In addition, the removal of NA-138 in two different pH values (one acidic and one basic), was also studied, maintaining the ozone concentration constant at  $2.0 \text{ mg L}^{-1}$ . Two additional experiments with the following conditions were conducted: One at pH 4.0 without scavenger where a mean removal of 34% was achieved
- And one at pH 9.0 in the presence of scavenger where 28% of the tested compound was removed.

### 6.5 Identification of NA second generation-transformation products

Three transformation products of NA-138 were detected in RP(+) by suspect screening, while no additional TP were detected by non-target screening.

#### 6.5.1 NA'-98

NA'-98 is eluted at 1.4 min in RP(+) and fits to the molecular formula  $\text{C}_4\text{H}_6\text{N}_2\text{O}$ . The proposed structure, presented in Fig. 66, suggests the abstraction of the  $\text{CO}_2$  group from the parent compound, the elimination of one carbon atom and the formation of an aldehyde group through ring opening generated by the ozone attack.

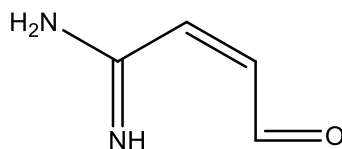


**Fig.66:** Proposed structure for NA'-98.

The MS spectrum (Fig. 67b) shows the pseudo-molecular ion  $[\text{M}+\text{H}]^+$ ,  $\text{C}_4\text{H}_7\text{N}_2\text{O}^+$ , at  $m/z$  99.0554 with excellent fit with its theoretical mass (mass error equal to 0.8 ppm) and very good isotopic fitting (6.2 mSigma) and its adduct ion  $[\text{M}+\text{K}]^+$ ,  $\text{C}_4\text{H}_6\text{KN}_2\text{O}^+$ , at  $m/z$  137.0118. The MS/MS spectrum (Fig. 67c) supports the proposed structure since an initial loss of a CO group

resulted in the formation of the fragment at  $m/z$  71.0599 ( $C_3H_7N_2^+$ ) and a further cleavage of a  $NH_3$  molecule producing the ion at  $m/z$  54.0338 ( $C_3H_4N^+$ ). The identification of this TP reaches the level 2b.

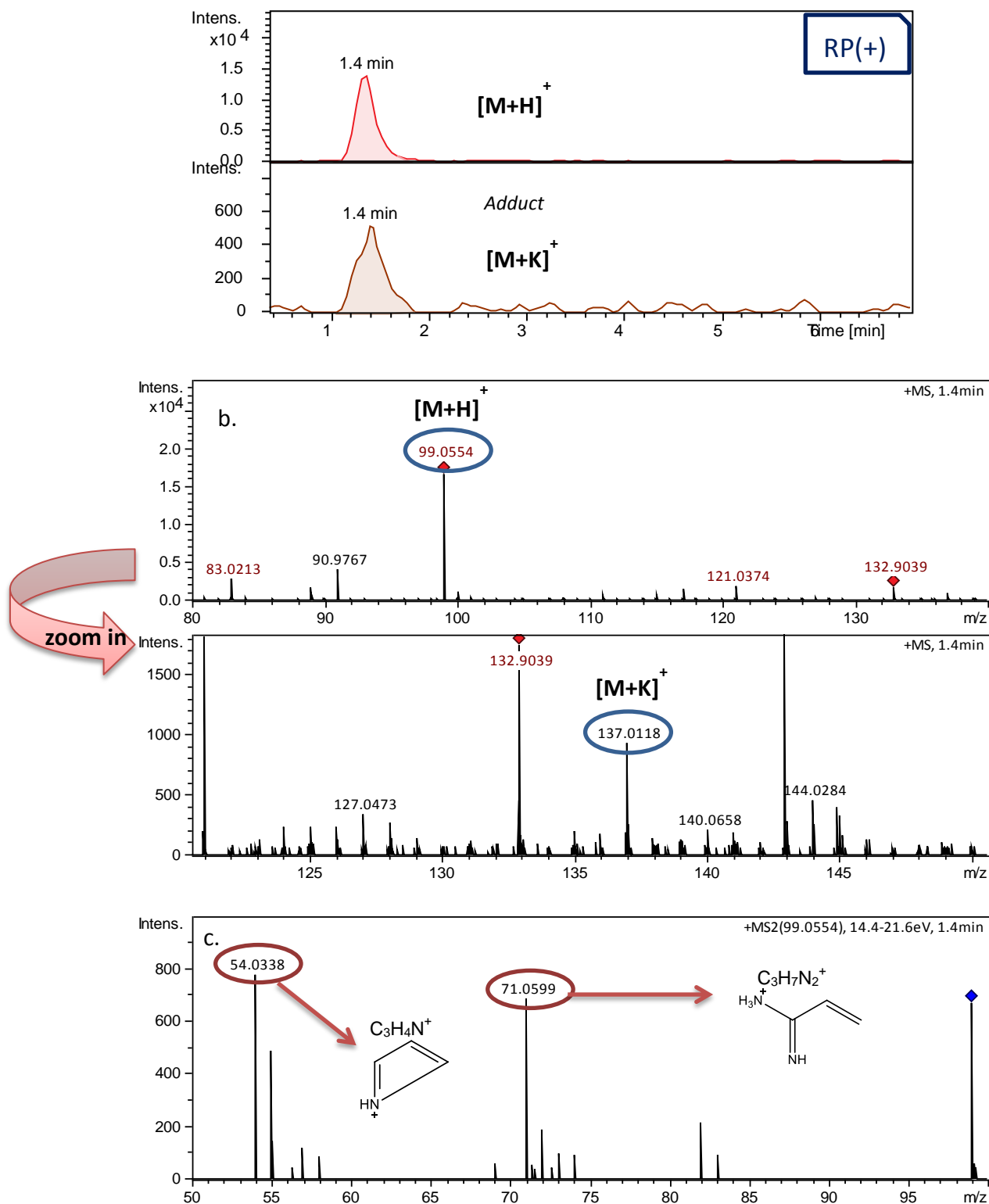


**Fig.67:** Analytical data for NA'-98 in RP(+); (a) EICs of NA'-98 and its adduct, (b) MS and (c) MS/MS spectrum showing the fragmentation and proposed fragments of NA'-98.

### 6.5.2 NA'-154

This TP of NA-138 is detected at 1.6 min in RP(+) and can be attributed to the elemental formula of  $C_6H_6N_2O_3$ , having one oxygen more than its parent compound and the same RDBE equal to 4.5. It is suggested to be the hydroxyl derivative of 2-aminopyridine-3-carboxylic acid.

The MS spectrum exhibits its pseudo-molecular ion  $[M+H]^+$  at  $m/z$  155.0442 ( $C_6H_7N_2O_3^+$ ) with a mass error of 5.3 ppm. No additional information was obtained by the MS/MS spectrum and as a result, the identification of this TP remains in level 4, where an unequivocal formula can be proposed. .

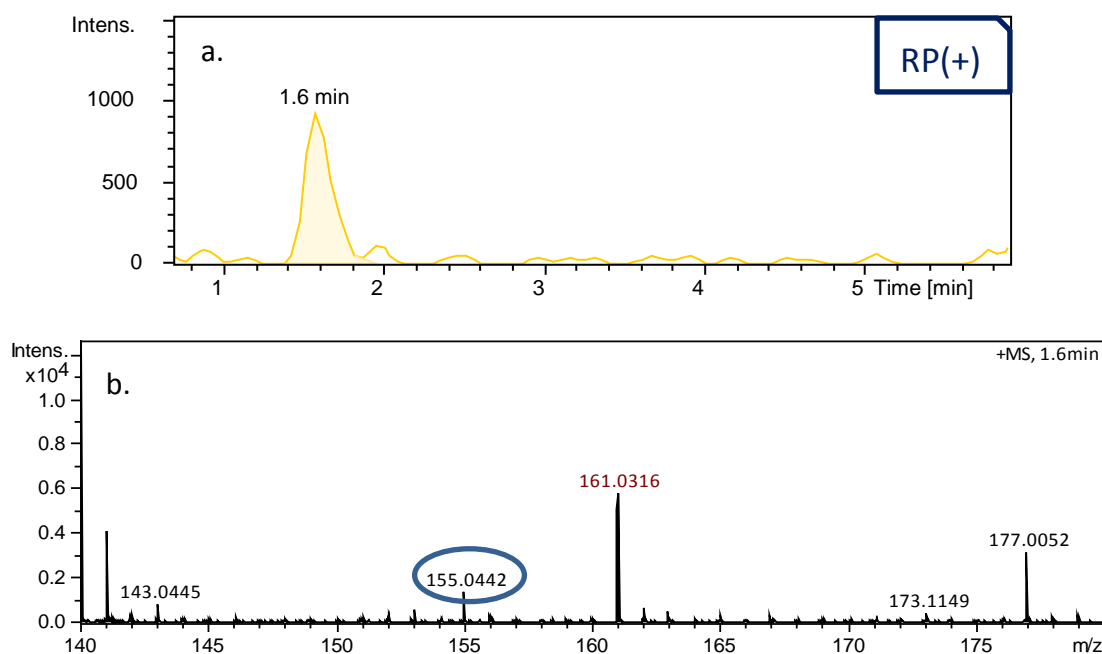


**Fig.68:** Analytical data for NA'-154 in RP(+); (a) EIC and (b) MS spectrum.

### 6.5.3 NA'-88

NA'-88 is eluted at 1.3 min in RP(+) and fits to the elemental formula of  $C_2H_4N_2O_2$ . The proposed formula implies the formation of a compound with two carbon atoms and either the formation of an aldehyde group and a hydroxylamine or the formation of carboxyl group. The MS spectrum shows the pseudo-molecular ion,  $C_2H_5N_2O_2^+$  at  $m/z$  89.0347 with low mass error (2 ppm), but no MS/MS spectrum information could be acquired due to the low mass of this TP.

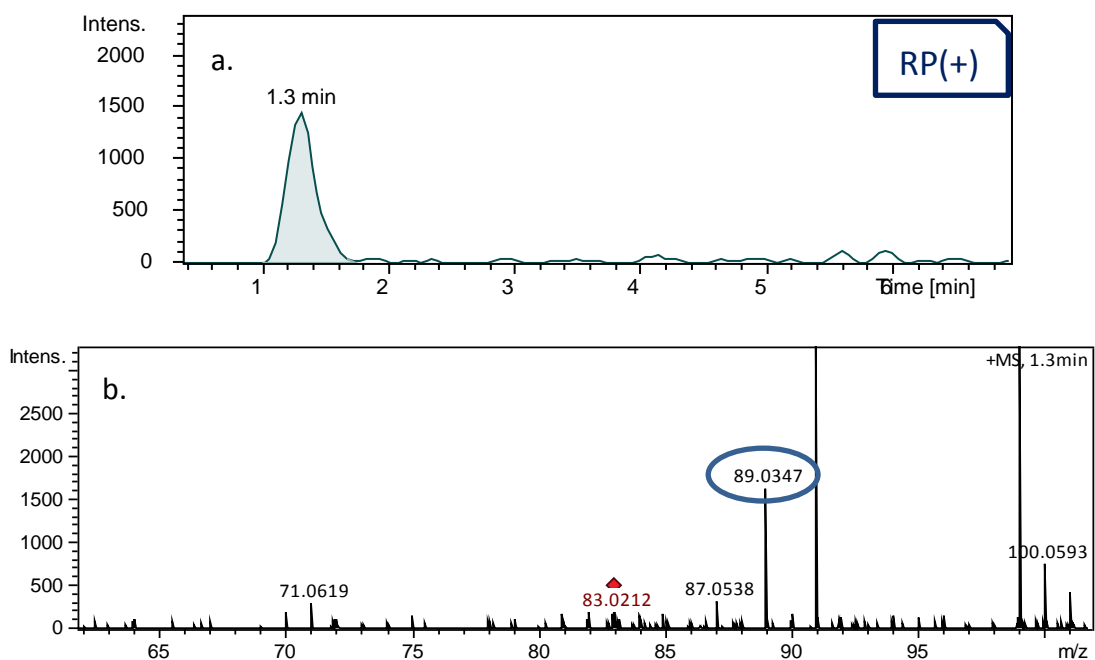


**Fig.69:** Analytical data for NA'-88 in RP(+); (a) EIC and (b) MS spectrum.

**Table 18:** Elemental composition of second generation TPs of NA, their adducts and fragment ions along with the measured m/z, the theoretical m/z and the mass error in ppm in RP(+), detected with suspect screening.

Compound	Ion formula	Theoretical m/z	Measured m/z	Mass error (ppm)
<b>NA'-98</b>	$C_4H_7N_2O^+$	99.0553	99.0554	0.8
Adduct	$C_4H_6KN_2O^+$	137.0112	137.0118	-4.2
Fragments	$C_3H_7N_2^+$	71.0604	71.0599	6.4
	$C_3H_4N^+$	54.0338	54.0338	1.4
<b>NA'-154</b>	$C_6H_7N_2O_3^+$	155.0451	155.0442	5.3
<b>NA'-88</b>	$C_2H_5N_2O_2^+$	89.0346	89.0347	2.0

## CHAPTER 7

### CONCLUSIONS-FUTURE PERSPECTIVES

Niflumic acid reaction with molecular ozone is extremely fast and is almost completed in most experimental conditions within the first minute. Initial ozone concentration and aqueous solution's pH are two essential parameters which influence the overall removal of NA. Higher percentages of removal were observed at high initial ozone concentration at neutral pH in the presence of scavenger. In addition, a total of 70% of removal was achieved at acidic pH in the presence of scavenger.

Parallel to the elimination of NA during ozonation, seventeen TPs were detected. All of them were detected in RP chromatographic system, nine of which were ionized in both PI and NI mode, while only five in NI and the rest of them only in PI.

The structure elucidation of the TPs shows that the oxidation occurred in the heterocyclic ring of the molecule, while the aniline-like part remain intact by ozone attack due to the presence of the three fluoride atoms, which act as electron withdrawing groups. The most abundant identified TP was 2-aminopyridine-3-carboxylic acid (NA-138) produced by the breakdown of parent compound structure during ozonation. This TP was confirmed through the analysis of the corresponding reference standard. A probable structure based on diagnostic evidence was proposed for the additional fifteen TPs, whereas only two candidate structures were assigned to the last one.

The high reactivity of the pyridine-like moiety of the parent compound with ozone was proven by the ozonation of its most abundant TP. 2-aminopyridine-3-carboxylic acid shows the same trend with NA. The application of  $5 \text{ mg L}^{-1}$   $\text{O}_3$  is adequate in order to eliminate completely this compound.

At the same time, during the elimination of NA-138, three second generation TPs were produced. All of them were detected in RP chromatographic system in PI mode. A probable structure based on diagnostic evidence was proposed for the one of them, while only an unequivocal formula was assigned to the other two.

Finally, as future perspectives can be proposed:

- the use of HILIC chromatographic system as a complementary technique for the identification of new, more polar TPs
- the application of screening of the identified TPs in order to investigate their presence in real wastewater samples treated with ozonation (full-scale system of Switzerland).

## ABBREVIATIONS AND ACRONYMS

**Table 19:** Abbreviations and acronyms

ACN	Acetonitrile
AOPs	Advanced Oxidation Processes
bbCID	broadband Collision-Induced Dissociation
BOD	Biological Oxygen Demand
CE	Collision Energy
Eawag-BBD PPS	Eawag Biocatalysis/Biodegradation Database Pathway Prediction System
ECs	Emerging Contaminants
EIC	Extracted Ion Chromatogram
EPs	Emerging Pollutants
ESI	ElectroSpray Ionization
FT-ICR	Fourier Transform-Ion Cyclotron Resonance
GC	Gas Chromatography
HPLC	High-Performance Liquid Chromatography
HR-MS	High Resolution Mass Spectrometry
LC	Liquid Chromatography
LC-HRMS	Liquid Chromatography coupled to High Resolution Mass Spectrometry
LC-QqQ MS/MS	Liquid Chromatography coupled with triple-Quadrupole Mass Spectrometry
LC-MS/MS	Liquid Chromatography tandem Mass Spectrometry
LC-QToF-MS	Liquid Chromatography–Quadrupole-Time-Of-Flight-Mass Spectrometry
MeOH	Methanol
MW	Molecular Weight

NA	Niflumic Acid
NI	Negative Ionization
NSAIDs	Nonsteroidal Anti-Inflammatory Drugs
PI	Positive Ionization
PPCPs	Pharmaceuticals and Personal-Care Products
QSRR	Quantitative Structure-Retention Relationship
RDBE	Ring Double Bond Equivalent
RP	Reversed Phase
RPLC	Reversed Phase Liquid Chromatography
SRM	Selected Reaction Monitoring
t-BuOH	tert-Butanol
ToF	Time-of-Flight
TP	Transformation Product
TrOCs	Trace Organic Compounds
UHPLC	UltraHigh-Performance Liquid Chromatography
UM-BBD PPS	University of Minnesota Biocatalysis/Biodegradation Database Pathway Prediction System
WWTP	WasteWater Treatment Plant

## REFERENCES

- [1] C. Miege, J. M. Choubert, L. Ribeiro, M. Eusebe, and M. Coquery, "Fate of pharmaceuticals and personal care products in wastewater treatment plants--conception of a database and first results," *Environmental Pollution*, vol. 157, pp. 1721-6, 2009.
- [2] R. Rosal, A. Rodriguez, J. A. Perdigon-Melon, A. Petre, E. Garcia-Calvo, M. J. Gomez, *et al.*, "Occurrence of emerging pollutants in urban wastewater and their removal through biological treatment followed by ozonation," *Water Research*, vol. 44, pp. 578-88, 2010.
- [3] K. Kummerer, "The presence of pharmaceuticals in the environment due to human use--present knowledge and future challenges," *Journal of Environmental Management*, vol. 90, pp. 2354-66, 2009.
- [4] A. Joss, S. Zabczynski, A. Göbel, B. Hoffmann, D. Löffler, C. S. McArdell, *et al.*, "Biological degradation of pharmaceuticals in municipal wastewater treatment: Proposing a classification scheme," *Water Research*, vol. 40, pp. 1686-1696, 2006.
- [5] D. W. Kolpin, E. T. Furlong, M. T. Meyer, E. M. Thurman, S. D. Zaugg, L. B. Barber, *et al.*, "Pharmaceuticals, hormones, and other organic wastewater contaminants in us streams, 1999-2000: a national reconnaissance," *Environmental Science and Technology*, vol. 36, pp. 1202-1211.
- [6] M. I. Farré, S. Pérez, L. Kantiani, and D. Barceló, "Fate and toxicity of emerging pollutants, their metabolites and transformation products in the aquatic environment," *TrAC Trends in Analytical Chemistry*, vol. 27, pp. 991-1007, 2008.
- [7] E. N. Evgenidou, I. K. Konstantinou, and D. A. Lambropoulou, "Occurrence and removal of transformation products of PPCPs and illicit drugs in wastewaters: A review," *Science of The Total Environment*, vol. 505, pp. 905-926, 2015.

- [8] K. H. Langford and K. V. Thomas, "Determination of pharmaceutical compounds in hospital effluents and their contribution to wastewater treatment works," *Environment International*, vol. 35, pp. 766-70, 2009.
- [9] B. J. Richardson M, "The Fate of Pharmaceutical Chemicals in The Aquatic Environment: review," *Journal of Pharmacy and Pharmacology*, vol. 37, pp. 1-12, 1985.
- [10] *Fate of Pharmaceuticals in The Environment and in Water Treatment Systems*. United States of America: CRC PRESS, 2008.
- [11] P. Guerra, M. Kim, A. Shah, M. Alaei, and S. A. Smyth, "Occurrence and fate of antibiotic, analgesic/anti-inflammatory, and antifungal compounds in five wastewater treatment processes," *Science of the Total Environment*, vol. 473-474, pp. 235-43, 2014.
- [12] A. Rodayan, P. A. Segura, and V. Yargeau, "Ozonation of wastewater: Removal and transformation products of drugs of abuse," *Science of The Total Environment*, vol. 487, pp. 763-770, 2014.
- [13] M. Pedrouzo, F. Borrull, E. Pocurull, and R. M. Marce, "Drugs of abuse and their metabolites in waste and surface waters by liquid chromatography-tandem mass spectrometry," *Journal of Separation Science*, vol. 34, pp. 1091-101, 2011.
- [14] T. M. Glenn, *Primary Treatment at Wastewater Treatment Plants*. United States of America: Lewis Publishers 1992.
- [15] S. R. Frank, *Handbook of Water and Wastewater Treatment Plant Operations*, Third ed.: CRC PRESS, 2014.
- [16] M. B. J. Van Metre P.C., Furlong E.T., "Urban Sprawl Leave Its PAH Signature," *Environmental Science and Technology*, vol. 34, pp. 4064-4070, 2000.
- [17] E. P. Agency, "Alternative Disinfectants and Oxidants Guidance Manual," EPA, Ed., ed. Washington, 1999a.
- [18] M. C. Nika, A. A. Bletsou, E. Koumaki, C. Noutsopoulos, D. Mamais, A. S. Stasinakis, *et al.*, "Chlorination of benzothiazoles and benzotriazoles

- and transformation products identification by LC-HR-MS/MS," *Journal of Hazardous Materials*, 2016.
- [19] M. W. Stewardship, "Chlorine and Alternative Disinfectants Guidance Manual," ed. Canada, 2005.
- [20] *Wastewater Technology Fact Sheet, Chlorine Disinfection*, 1999.
- [21] L. Meunier, S. Canonica, and U. von Gunten, "Implications of sequential use of UV and ozone for drinking water quality," *Water Research*, vol. 40, pp. 1864-76, 2006.
- [22] O. E. Legrini O., Braun A., , "Photochemical Processes for Water Treatment," *Chemical Reviews*, vol. 93, pp. 671-698, 1993.
- [23] R. Gehr, M. Wagner, P. Veerasubramanian, and P. Payment, "Disinfection efficiency of peracetic acid, UV and ozone after enhanced primary treatment of municipal wastewater," *Water Research*, vol. 37, pp. 4573-4586, 2003.
- [24] A. Hassen, M. Mahrouk, H. Ouzari, M. Cherif, A. Boudabous, and J. J. Damelincourt, "UV disinfection of treated wastewater in a large-scale pilot plant and inactivation of selected bacteria in a laboratory UV device," *Bioresource Technology*, vol. 74, pp. 141-150, 2000.
- [25] *Wastewater Technology Fact Sheet, Ozone Disinfection*, 1999.
- [26] F. J. Beltran, J. F. G. a-Araya, and P. M. Alvarez, "Sodium Dodecylbenzenesulfonate Removal from Water and Wastewater. 2.Kinetics of the Integrated Ozone-Activated Sludge System," *Industrial & Engineering Chemistry Research*, vol. 39, pp. 2221-2227, 2000.
- [27] Q. Dai, L. Chen, W. Chen, and J. Chen, "Degradation and kinetics of phenoxyacetic acid in aqueous solution by ozonation," *Separation and Purification Technology*, vol. 142, pp. 287-292, 2015.
- [28] P. R. Gogate and A. B. Pandit, "A review of imperative technologies for wastewater treatment I: oxidation technologies at ambient conditions," *Advances in Environmental Research*, vol. 8, pp. 501-551, 2004.

- [29] J. Hoigné and H. Bader, "The role of hydroxyl radical reactions in ozonation processes in aqueous solutions," *Water Research*, vol. 10, pp. 377-386, 1976.
- [30] C. v. Sonntag and U. v. Gunten, *Chemistry of Ozone in Water and Wastewater Treatment*. IWA Publishing, 2012.
- [31] D. Gerrity and S. Snyder, "Review of Ozone for Water Reuse Applications: Toxicity, Regulations, and Trace Organic Contaminant Oxidation," *Ozone: Science & Engineering*, vol. 33, pp. 253-266, 2011.
- [32] J. Lv, L. Wang, Y. Song, and Y. Li, "N-nitrosodimethylamine formation from ozonation of chlorpheniramine: Influencing factors and transformation mechanism," *Journal of Hazardous Materials*, vol. 299, pp. 584-594, 2015.
- [33] A. D. Coelho, C. Sans, S. Esplugas, and M. Dezotti, "Ozonation of NSAID: A Biodegradability and Toxicity Study," *Ozone: Science & Engineering*, vol. 32, pp. 91-98, 2010.
- [34] R. Andreozzi, V. Caprio, A. Insola, and R. Marotta, "Advanced oxidation processes (AOP) for water purification and recovery," *Catalysis Today*, vol. 53, pp. 51-59, 1999.
- [35] J. Hoigné and H. Bader, "Rate constants of reactions of ozone with organic and inorganic compounds in water—II," *Water Research*, vol. 17, pp. 185-194, 1983.
- [36] M. Cleuvers, "Mixture toxicity of the anti-inflammatory drugs diclofenac, ibuprofen, naproxen, and acetylsalicylic acid," *Ecotoxicology and Environmental Safety*, vol. 59, pp. 309-315, 2004.
- [37] B. L. Goodwin, *Handbook of Biotransformations of Aromatic Compounds*: CRC PRESS, 2005.
- [38] C. Hao, L. Lissemore, B. Nguyen, S. Kleywegt, P. Yang, and K. Solomon, "Determination of pharmaceuticals in environmental waters by liquid chromatography/electrospray ionization/tandem mass spectrometry," *Analytical and Bioanalytical Chemistry*, vol. 384, pp. 505-13, 2006.

- [39] A. A. Bletsou, J. Jeon, J. Hollender, E. Archontaki, and N. S. Thomaidis, "Targeted and non-targeted liquid chromatography-mass spectrometric workflows for identification of transformation products of emerging pollutants in the aquatic environment," *Trends in Analytical Chemistry*, vol. 66, pp. 32-44, 2015.
- [40] S. Pérez and D. Barceló, "Application of advanced MS techniques to analysis and identification of human and microbial metabolites of pharmaceuticals in the aquatic environment," *TrAC Trends in Analytical Chemistry*, vol. 26, pp. 494-514, 2007.
- [41] T. Kosjek and E. Heath, "Applications of mass spectrometry to identifying pharmaceutical transformation products in water treatment," *TrAC Trends in Analytical Chemistry*, vol. 27, pp. 807-820, 2008.
- [42] B. J. Vanderford, D. B. Mawhinney, F. L. Rosario-Ortiz, and F. a. S. A. Snyder, "Real-Time Detection And Identification Of Aqueous Chlorine Transformation Products Using QTOF MS," *Analytical Chemistry*, vol. 80, pp. 4193–4199, 2008.
- [43] M. Krauss, H. Singer, and J. Hollender, "LC-high resolution MS in environmental analysis: from target screening to the identification of unknowns," *Analytical and Bioanalytical Chemistry*, vol. 397, pp. 943-51, 2010.
- [44] F. Hernández, J. V. Sancho, M. Ibáñez, and S. Grimalt, "Investigation of pesticide metabolites in food and water by LC-TOF-MS," *TrAC Trends in Analytical Chemistry*, vol. 27, pp. 862-872, 2008.
- [45] M. J. Gomez, M. M. Gomez-Ramos, O. Malato, M. Mezcua, and A. R. Fernandez-Alba, "Rapid automated screening, identification and quantification of organic micro-contaminants and their main transformation products in wastewater and river waters using liquid chromatography-quadrupole-time-of-flight mass spectrometry with an accurate-mass database," *Journal of Chromatography A*, vol. 1217, pp. 7038-54, 2010.
- [46] A. C. Hogenboom, J. A. van Leerdam, and P. de Voogt, "Accurate mass screening and identification of emerging contaminants in environmental

- samples by liquid chromatography-hybrid linear ion trap Orbitrap mass spectrometry," *Journal of Chromatography A*, vol. 1216, pp. 510-9, 2009.
- [47] A. Agüera, M. J. Martínez Bueno, and A. R. Fernández-Alba, "New trends in the analytical determination of emerging contaminants and their transformation products in environmental waters," *Environmental Science and Pollution Research*, vol. 20, pp. 3496-3515, 2013.
- [48] K. F. Susane Kern, Heinz P. Singer, Rene P. Schwarzenbach, Juliane Hollender, "Identification of Transformation Products of Organic Contaminants in Natural Waters by Computer-Aided Prediction and High-Resolution Mass Spectrometry," *Environmental Science and Technology* vol. 43, pp. 7039-7046, 2009.
- [49] J. H. D. E. Helbling, H.-P. E. Kohler, K. Fenner, "Structure-based interpretation of biotransformation pathways of amide-containing compounds in sludge-seeded bioreactors," *Environmental Science and Technology*, vol. 44, pp. 6628-6635, 2010.
- [50] M. Ibanez, J. V. Sancho, O. J. Pozo, W. Niessen, and F. Hernandez, "Use of quadrupole time-of-flight mass spectrometry in the elucidation of unknown compounds present in environmental water," *Rapid Communications in Mass Spectrometry*, vol. 19, pp. 169-78, 2005.
- [51] H. P. S. Emma L. Schymanski, Philipp Longrée, Martin Loos, Matthias Ruff, Michael A. Stravs, Cristina Ripollés Vidal, and Juliane Hollender, "Strategies to Characterize Polar Organic Contamination in Wastewater: Exploring the Capability of High Resolution Mass Spectrometry," *Environmental Science and Technology*, vol. 48, pp. 1811-1818, 2014.
- [52] D. B. Yolanda Picó, "Transformation products of emerging contaminants in the environment and high-resolution mass spectrometry: a new horizon," *Analytical and Bioanalytical Chemistry*, vol. 407, pp. 6257-6273, 2015.
- [53] E. L. Schymanski, J. Jeon, R. Gulde, K. Fenner, M. Ruff, H. P. Singer, *et al.*, "Identifying small molecules via high resolution mass

spectrometry: communicating confidence," *Environmental Science and Technology*, vol. 48, pp. 2097-8, 2014.

- [54] M. Petrovic, M. J. de Alda, S. Diaz-Cruz, C. Postigo, J. Radjenovic, M. Gros, *et al.*, "Fate and removal of pharmaceuticals and illicit drugs in conventional and membrane bioreactor wastewater treatment plants and by riverbank filtration," *Philosophical Transactions. Series A, Mathematical, Physical, and Engineering Sciences*, vol. 367, pp. 3979-4003, 2009.
- [55] J. L. Santos, I. Aparicio, M. Callejon, and E. Alonso, "Occurrence of pharmaceutically active compounds during 1-year period in wastewaters from four wastewater treatment plants in Seville (Spain)," *Journal of Hazardous Materials*, vol. 164, pp. 1509-16, 2009.
- [56] R. Loos, R. Carvalho, D. C. Antonio, S. Comero, G. Locoro, S. Tavazzi, *et al.*, "EU-wide monitoring survey on emerging polar organic contaminants in wastewater treatment plant effluents," *Water Research*, vol. 47, pp. 6475-87, 2013.
- [57] N. K. Stamatis and I. K. Konstantinou, "Occurrence and removal of emerging pharmaceutical, personal care compounds and caffeine tracer in municipal sewage treatment plant in Western Greece," *Journal of Environmental Science and Health. Part. B, Pesticides, Food Contaminants, and Agricultural Wastes*, vol. 48, pp. 800-13, 2013.
- [58] S. K. Behera, H. W. Kim, J. E. Oh, and H. S. Park, "Occurrence and removal of antibiotics, hormones and several other pharmaceuticals in wastewater treatment plants of the largest industrial city of Korea," *Science of The Total Environment*, vol. 409, pp. 4351-60, 2011.
- [59] S. Zorita, L. Martensson, and L. Mathiasson, "Occurrence and removal of pharmaceuticals in a municipal sewage treatment system in the south of Sweden," *Science of The Total Environment*, vol. 407, pp. 2760-70, 2009.
- [60] B. Kasprzyk-Hordern, R. M. Dinsdale, and A. J. Guwy, "The removal of pharmaceuticals, personal care products, endocrine disruptors and illicit

- drugs during wastewater treatment and its impact on the quality of receiving waters," *Water Research*, vol. 43, pp. 363-80, 2009.
- [61] S. Terzic, I. Senta, M. Ahel, M. Gros, M. Petrovic, D. Barcelo, *et al.*, "Occurrence and fate of emerging wastewater contaminants in Western Balkan Region," *Science of The Total Environment*, vol. 399, pp. 66-77, 2008.
- [62] E. Gracia-Lor, J. V. Sancho, R. Serrano, and F. Hernandez, "Occurrence and removal of pharmaceuticals in wastewater treatment plants at the Spanish Mediterranean area of Valencia," *Chemosphere*, vol. 87, pp. 453-62, 2012.
- [63] C. P. Yu and K. H. Chu, "Occurrence of pharmaceuticals and personal care products along the West Prong Little Pigeon River in east Tennessee, USA," *Chemosphere*, vol. 75, pp. 1281-6, 2009.
- [64] V. G. Samaras, A. S. Stasinakis, D. Mamais, N. S. Thomaidis, and T. D. Lekkas, "Fate of selected pharmaceuticals and synthetic endocrine disrupting compounds during wastewater treatment and sludge anaerobic digestion," *Journal of Hazardous Materials*, vol. 244-245, pp. 259-67, 2013.
- [65] P. H. Roberts and P. Bersuder, "Analysis of OSPAR priority pharmaceuticals using high-performance liquid chromatography-electrospray ionisation tandem mass spectrometry," *Journal of Chromatography A*, vol. 1134, pp. 143-50, 2006.
- [66] A. S. Stasinakis, S. Mermigka, V. G. Samaras, E. Farmaki, and N. S. Thomaidis, "Occurrence of endocrine disrupters and selected pharmaceuticals in Aisonas River (Greece) and environmental risk assessment using hazard indexes," *Environmental Science and Pollution Research International*, vol. 19, pp. 1574-83, 2012.
- [67] M. E. Dasenaki and N. S. Thomaidis, "Multianalyte method for the determination of pharmaceuticals in wastewater samples using solid-phase extraction and liquid chromatography-tandem mass spectrometry," *Analytical and Bioanalytical Chemistry*, vol. 407, pp. 4229-45, 2015.

- [68] M. Ibanez, V. Borova, C. Boix, R. Aalizadeh, R. Bade, N. S. Thomaidis, *et al.*, "UHPLC-QTOF MS screening of pharmaceuticals and their metabolites in treated wastewater samples from Athens," *Journal of Hazardous Materials*, 2016.
- [69] P. Gago-Ferrero, V. Borova, M. E. Dasenaki, and S. Thomaidis Ni, "Simultaneous determination of 148 pharmaceuticals and illicit drugs in sewage sludge based on ultrasound-assisted extraction and liquid chromatography-tandem mass spectrometry," *Analytical and Bioanalytical Chemistry*, vol. 407, pp. 4287-97, 2015.
- [70] N. A. Alygizakis, P. Gago-Ferrero, V. L. Borova, A. Pavlidou, I. Hatzianestis, and N. S. Thomaidis, "Occurrence and spatial distribution of 158 pharmaceuticals, drugs of abuse and related metabolites in offshore seawater," *Science of The Total Environment*, vol. 541, pp. 1097-105, 2016.
- [71] D. Vogna, R. Marotta, A. Napolitano, R. Andreozzi, and M. d'Ischia, "Advanced oxidation of the pharmaceutical drug diclofenac with UV/H<sub>2</sub>O<sub>2</sub> and ozone," *Water Research*, vol. 38, pp. 414-22, 2004.
- [72] I. Michael, A. Achilleos, D. Lambropoulou, V. O. Torrens, S. Pérez, M. Petrović, *et al.*, "Proposed transformation pathway and evolution profile of diclofenac and ibuprofen transformation products during (sono)photocatalysis," *Applied Catalysis B: Environmental*, vol. 147, pp. 1015-1027, 2014.
- [73] H. H. Guoguang Liu, "Ozone-Oxidation Products of Ibuprofen and Toxicity Analysis in Simulated Drinking Water," *Journal of Drug Metabolism and Toxicology*, vol. 06, 2015.
- [74] F. Mendez-Arriaga, S. Esplugas, and J. Gimenez, "Degradation of the emerging contaminant ibuprofen in water by photo-Fenton," *Water Research*, vol. 44, pp. 589-95, 2010.
- [75] J. Madhavan, F. Grieser, and M. Ashokkumar, "Combined advanced oxidation processes for the synergistic degradation of ibuprofen in aqueous environments," *Journal of Hazardous Materials*, vol. 178, pp. 202-8, 2010.

- [76] H. Bader and J. Hoigné, "Determination of Ozone In Water By The Indigo Method: A Submitted Standard Method," *Ozone: Science & Engineering*, vol. 4, pp. 169-176, 1982.
- [77] H. Bader and J. Hoigné, "Determination of ozone in water by the indigo method," *Water Research*, vol. 15, pp. 449-456, 1981.
- [78] G. Gordon and B. Bubnis, "Residual Ozone Measurement: Indigo Sensitivity Coefficient Adjustment," *Ozone: Science & Engineering*, vol. 24, pp. 17-28, 2002.
- [79] Mynard Hamming and N. Foster, *Interpretation of Mass Spectra of Organic Compounds*. New York: Academic Press, 1972.
- [80] R. Aalizadeh, N. Thomaidis, A. Bletsou, and P. G. Ferrero, "Quantitative structure-retention relationships models to support suspect high resolution mass spectrometric screening of emerging contaminants in environmental samples Under Review."
- [81] M. Huber, S. Canonica, G.-Y.Park, and U. V. Gunten, "Oxidation of Pharmaceuticals During Ozonation and Advanced Oxidation Processes," *Environmental Science and Technology*, vol. 37, pp. 1016-1024, 2003.